Studies on RNF8, a ubiquitin ligase with a RING finger domain

Memòria per a optar al títol de Doctora en Biologia presentada per

Vanessa Plans Calafell

Sota la direcció del Dr Timothy M. Thomson[1]

i la tutela de la Dra Gemma Marfany

Bieni 2004-2005

Programa de doctorat del Department de Genètica

Facultat de Biologia

Universitat de Barcelona

[1] Departament de Biologia Molecular i Cel.lular. Institut de Biologia Molecular de Barcelona. Consell Superior d'Investigacions Científiques

La connaissance est une sphère dont la surface est l'inconnu.

ACKNOWLEDGEMENTS

Arribat a aquest punt després de molts esforços, alguns maltràngols però també moltes satisfaccions m'agradaria recordar a la gent que m'ha acompanyat en aquests cinc anys de la meva vida.

En primer lloc, et vull donar les gràcies a tu, Tim, per haver-me dirigit la tesi durant aquests anys i ensenyat gran part del que ara se. Quan faig balanç crec que a part de formar-me en gran varietat de tècniques també he après a tenir una opinió critica. Amb tu he aprendrès a obrir el meu espai de raonament, que ven segur em serà molt últil en el futur. En especial t'agraeixo el recolzament que m'has donat aquests últims mesos que han estat una mica complicats.

Gemma, et donc les gràcies per haver-me no només tutelat però també animat i ajudat a confeccionar aquesta feinada que és una memòria de tesi doctoral. Ja van dos cops que m'ajudes! Si t'en recordes vas rectififar un error burocràtic que em va permetre llicenciar al juny l'any que vaig marxar d'Erasmus!

També vull agrair a les noies del laboratori l'amistat que hem generat després de passar tantes hores juntes. Johanna, ja fa molts anys que ens coneixem i vam veure a la Cecile juntes! Marteta, hem parlat moltes hores fins les tantes i escoltat molta música... també en directe! Raquel o la computer woman gràcies per tots els pitis i els doowaps que t'he mangat. Teresa, o la fuccia girl espero que segueixis així d'organitzada fins que acabis la tesi, jo ho hagués agraït tant! Marta, espero que te hayas sentido a gusto trabajando conmigo y que tengas ganas de seguir este supercurro que queda detrás de mí. Juan y Andrés, gracias por haber traído un poco de variedad al lab y de haber sofocado tanta hormona femenina! Espero haver estat una bona companya també per vosaltres.

També vull recordar a tots els amics que he deixat a Vall d' Hebró, encara que no us vegi cada dia no m'oblido gens de vosaltres fins i tot els que ja no sou a Vall d' Hebró. Nour, siempre tan grande! Ester tenim una amistat molt còmplice,

oi? ¿Marianiquins cuando salimos a bailar Estopa? Us hi apunteu Anna, Roser, Jesús, Pep, Marta, Tomàs i companyia? Y aunque ahora hace mucho que no te veo, también me acuerdo de ti Víctor. I de la gent com el Bru que em van ajudar al principi d'aquest camí.

També li vull agrair el suport a les meves amigues del lycée per haver patit els meus eterns rotllos de tesi, els nervis... Ara és el moment de la part més maca i aquesta també la vull compartir amb vosaltres com tot, des de fa ara ja més de deu anys. María podrás venir desde Calais? A les demés us espero suposo que algun matí de juny a l'aula magna de Bio, i sinó dons a la Vireina, com sempre i fem un shawarma.

Finalment tan sols un record a la meva família i al Christian, al cap i a la fi sou els més importants. Aquest serà un any de celebracions! Es wird ein festliches Jahr werden, auch für dich!

Als meus pares

INDEX

Abbreviations

APC anaphase-promoting-complex/cyclosome

ATM Ataxia Telangiectasia Mutated

BIR Baculoviral IAP Repeat

bp base pairs

BSA Bovine Serum Albumin

CDK cyclin-dependent kinase

DUB Deubiquitylating enzyme

FHA Fork Head Associated

FBS Fetal Bovine Serum

GEF Guanidine-nucleotide Exchange Factor

GFP Green Fluorescent Protein

HECT Homologous to E6-AP Carboxy-Terminus

HRP Horseradish Peroxidase- conjugated

IAP Inhibitor of Apoptosis Proteins

KDa KiloDaltons

LB Luria Bertoni broth base

LCS Laser Scanning Cytometry

MEF Mouse Embryonic Fibroblast

MEN Mitotic Exit Network

NMR Nuclear Magnetic Resonance

NPC Nuclear Pore Complex

PBS Phosphate Buffer Saline

PBST Phospate Buffer Saline 0.1% Tween 20

PCR Polymerase Chain Reaction

PFA 4%Paraformaldehide in PBS

PML Promyelocytic Leukaemia

RING Really Interesting New Gene

RT Reverse Transcription

RTK Receptor Tyrosine Kinase

SCF Skp1-Cdc35/Cul1-Fbox protein

SDS-PAGE Sodium Dodecyl Sulphate Polyacrylamide Gel Electrophoresis

SIN Septation Initiation Network

siRNA Small Interfering RNA

SUMO Small Ubiquitin-related Modifier

TBS Tris Buffer Saline

TBST Tris Buffer Saline 0.1% Tween 20

TE Tris-EDTA

TGFβ Transforming growth factor β

TPR Tetratricopeptide Repeat

Ub Ubiquitin

UBC Ubiquitin Conjugating-domain

UBL Ubiquitin-Like Protein

UBP Ubiquitin Binding Protein

UBP Ubiquitin-specific Proteases

UCH Ubiquitin C-terminal Hydrolases

UIM Ubiquitin-Interacting Motif

INTRODUCTION

1. Ubiquitylation, overview

Ubiquitylation is a post-translational protein modification. Post-translational modifications introduce covalently linked moieties that modify the function of the target protein allowing the cell to generate signals in order to progress almost in every cellular pathway. For example, protein phosphorylation, one of the best understood modifications, can have several consequences for the modified protein. It can change protein stability, alter protein-protein interactions, imply a different subcellular localization or activate or inactivate a protein by allosteric changes (Johnson and Lewis, 2001). Post-translational modifications are extremely inter-dependent processes resulting in a proper protein function. Other posttranslational modifications such as ubiquitylation were thought to have more limited consequences on the fate of the substrate proteins. For many years it was seen as the main way the cell could target undesired proteins for degradation by the 26S proteasome. However, recent evidence suggests that signals generated by ubiquitylation can result in a wide variety of biochemical consequences for the target proteins, which may be at least as varied as phosphorylation. One of the mechanisms underlying this diversity is the fact that unique signals can be transmitted by means of different ubiquitin modifications (Fig. 1). Indeed, ubiquitylation regulates very different signaling pathways and biological processes such as endocytosis, vesicular traffic, DNA repair, transcription, protein quality control,

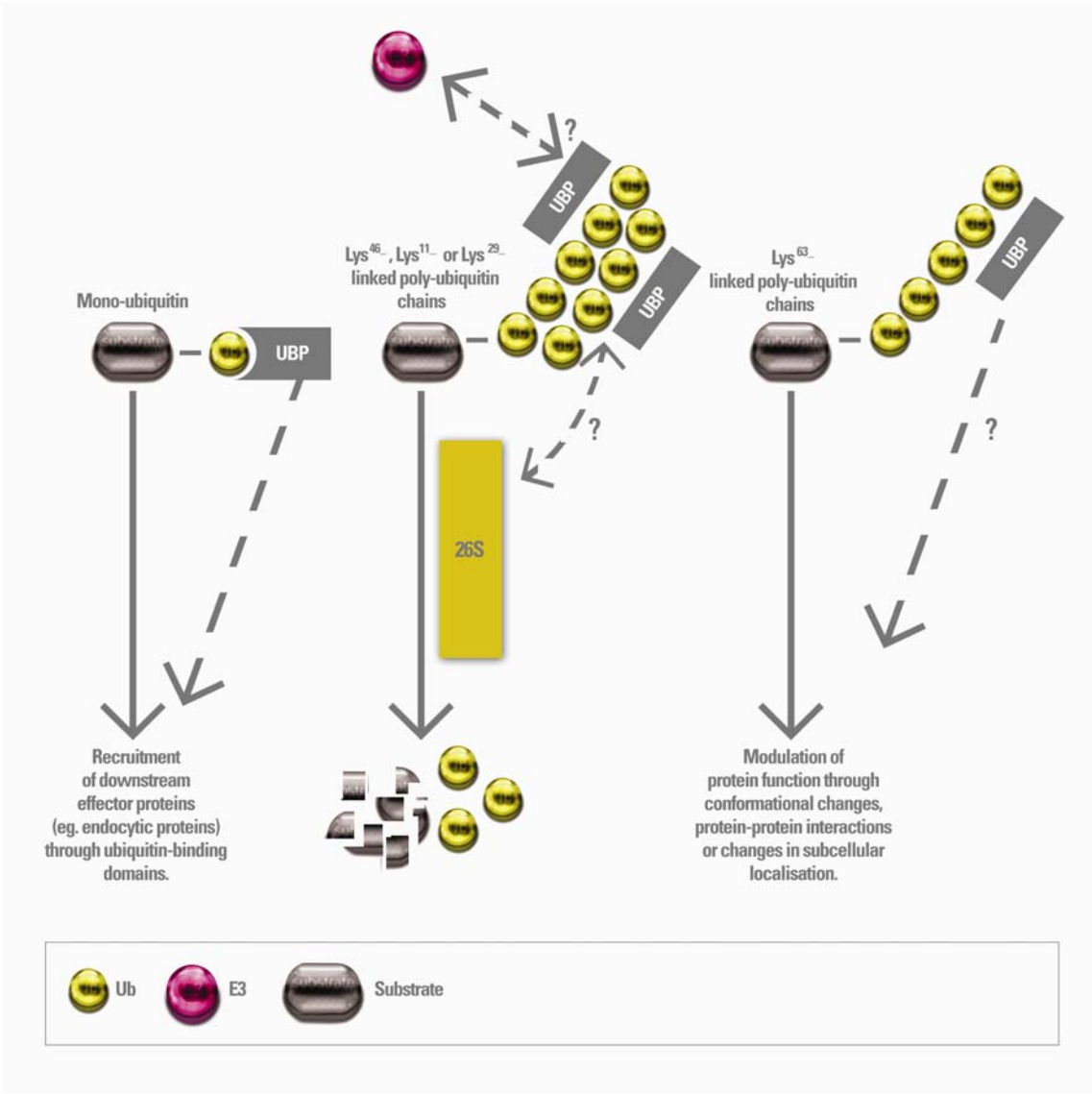

Fig 1. Ubiquitin modifications. The consequence of ubiquitylation is reliant on the type of ubiquitin modification. Monoubiquitylation mediates downstream signaling events. K48, K11 or K29 polyubiquitylation are recognized by 26S proteasome and therefore the so-modified protein is subject to degradation. It is possible that the ubiquitylation machinery is linked to the degrading one. K63 polyubiquitin chains are not recognized by the proteasome and seem to have functional consequences on the modified protein. Monoubiquitylated and polyubiquitylated proteins can be recognized by Ubiquitin Binding Proteins (UBP).

cell cycle, apoptosis, immune response, signal transduction or neuron degeneration (Hershko and Ciechanover, 1998; Hicke and Dunn, 2003; Jesenberger and Jentsch, 2002; Kloetzel, 2001; Muratani and Tansey, 2003; Reed, 2003). Schematically, three enzymes participate in ubiquitin conjugation: E1 or ubiquitin activating enzymes that activate ubiquitin in an ATP depending manner, E2 or ubiquitin conjugating enzymes that catalyze the ubiquitin transfer onto the substrate thanks to an E3 or ubiquitin ligase (Fig 3).

2. The discovery of ubiquitin

Goldstein and Dayhoff isolated a small protein around thirty years ago and called it ubiquitin. They thought it to be widespread in living cells although they identified it as a lymphocyte differentiation promoting factor (Goldstein et al., 1975). Two years later the non-histone component of the nuclear protein A24 was shown to be also ubiquitin, which indeed formed a covalent adduct with histone H2A (Hunt and Dayhoff, 1977). Ubiquitin is linked to histone H2A through an isopeptide bond between a lysine side chain ε-amino group of histone H2A and the glycine at the carboxyl terminus of ubiquitin (Goldknopf and Busch, 1977). It was thus established that ubiquitin could be conjugated to other proteins though covalent bonds.

The link between ubiquitin and protein degradation came quite immediately. Despite the understanding of protein synthesis, how proteins degrade into amino acids was a mystery. The lysosome system of mammalian cells was known to have this ability but it did not explain the rapid of some

proteins turnover and how lysosome-free cells such as rabbit reticulocytes could degrade proteins. Using the latter as a model, a soluble ATP-dependent proteolytic system was found (Etlinger and Goldberg, 1977). The fractionation of reticulocyte cytosol allowed purifying the APF-I factor which could be covalently conjugated to proteins in the presence of a second fraction (Ciechanover et al., 1980). APF-I was nothing but ubiquitin (Wilkinson et al., 1980).

3. Ubiquitin, the molecule

Ubiquitin is a highly conserved 76 amino acid protein (~8 kDa) found in all eukaryotes (Ozkaynak et al., 1984) (Fig 2). This heat-stable small molecule adopts a compact globular conformation with four strands of β-sheet and a single α-helix. The three C-terminal residues R-G-G are flexible and extend into the solvent, which makes the molecule very soluble. Ubiquitin has seven lysines that can potentially promote its conjugation to the substrate or to other ubiquitin moieties (Fig 2). It is chemically more complex than other post-translational modifications since it provides a molecular surface for protein-protein interactions. Owing to its intrinsic properties, ubiquitin has the potential to signal diverse outcomes.

Ubiquitin is synthesized in a variety of functionally distinct forms. One of these forms is a linear heat-to-tail polyubiquitin precursor, which needs specific enzymatic cleavage between the fused residues (Ozkaynak et al., 1984). As in many other precursors, the C-terminal glycine is here protected from exposure by an additional amino acid. In another precursor, ubiquitin is synthesized as an

N-terminal fused extension of two ribosomal proteins targeting them to the ribosome as a covalent chaperone. Once the ribosomal proteins are incorporated into the ribosomal complex, ubiquitin is cleaved and released (Redman and Burris, 1996) Redman 1994 corrections).

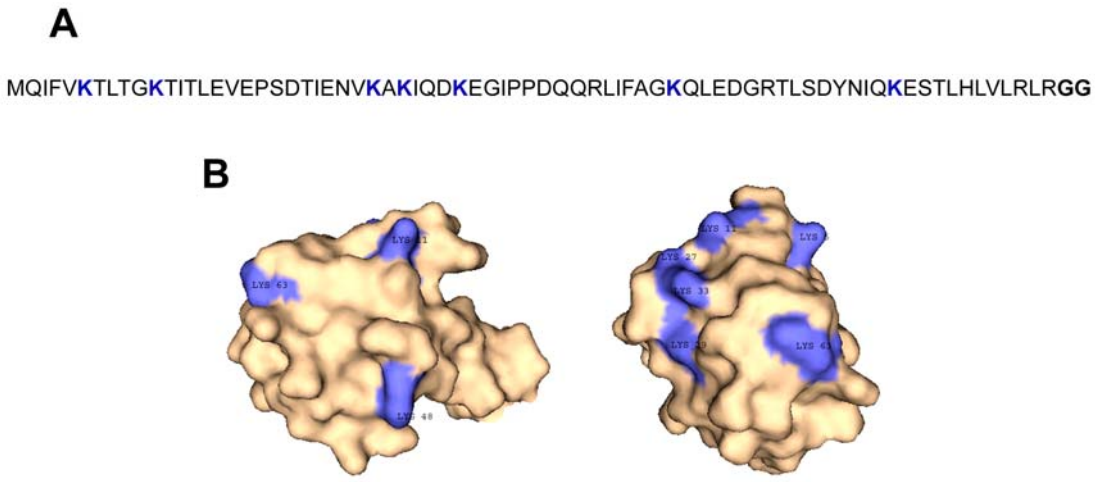

Fig 2. A. Primary structure of the ubiquitin molecule. The seven lysines are shown in blue and the terminal glycines in bold. **B**. Frontal and posterior view of a crystal structure of ubiquitin derived from the tetraubiquitin crystal, PDB: 1TBE, (Cook et al., 1994) lysines are also shown in blue.

4. Catalytic mechanisms of ubiquitylation and enzyme particularities

Ubiquitylation occurs in three distinct enzymatic steps catalyzed by (1) an E1 or ubiquitin-activating enzyme, (2) an E2 or ubiquitin-conjugating enzyme and (3) an E3 or ubiquitin ligase (Fig 3) (Hershko and Ciechanover, 1998; Pickart, 2001). Firstly, an E1 activates ubiquitin thanks to an adenylation of the C-terminus of ubiquitin, followed by the formation of a thiolester bond between its catalytic cysteine residue and the ubiquitin C-terminus (Haas and Rose,

1982; Haas et al., 1982). The non-covalent binding but adenylation of a second ubiquitin molecule is required in order to fully activate the E1. For this first step ATP is required. Secondly, the activated ubiquitin is transferred also by formation of a thiolester bond to the cysteine located in the active-site of an E2. Finally, ubiquitin is transferred from the E2 to the substrate in the presence of an E3. In this last step, the bond that links the ε-amino group of the substrate lysine and the C-terminal carboxylate of ubiquitin is an isopeptide bond. Not all E3's work in the same way. However, they all promote the transfer of ubiquitin from a thiolester-linkage on a E2 to an amide-linkage on either a substrate protein or another ubiquitin moiety (Hershko and Ciechanover, 1998). E3's are responsible for substrate specificity since they are responsible for recognizing the substrate proteins and tethering an E2 to its proximity (Glickman and Ciechanover, 2002; Hershko and Ciechanover, 1998; Pickart, 2001). At this point subcellular localization and temporal windows are important to regulate E3-substrate encounters.

The complexity of the ubiquitin system is built upon a pyramidal model such that one or few ubiquitin activating enzymes activate and transfer ubiquitin to a dozen or more ubiquitin conjugating enzymes, which in turn can use hundreds of different ubiquitin ligases for the modification of many substrates. Thus, Uba is the only type of E1 in eukaryotic cells, while there are between 10 and 30 different E2s (Glickman and Ciechanover, 2002; Pickart, 2001). Each E2 can interact with more than one E3, and the other way round (Plans et al, in press). The total number of E3 remains to be identified although it is already much larger than the E2 number (Glickman and Ciechanover, 2002), most likely several hundreds.

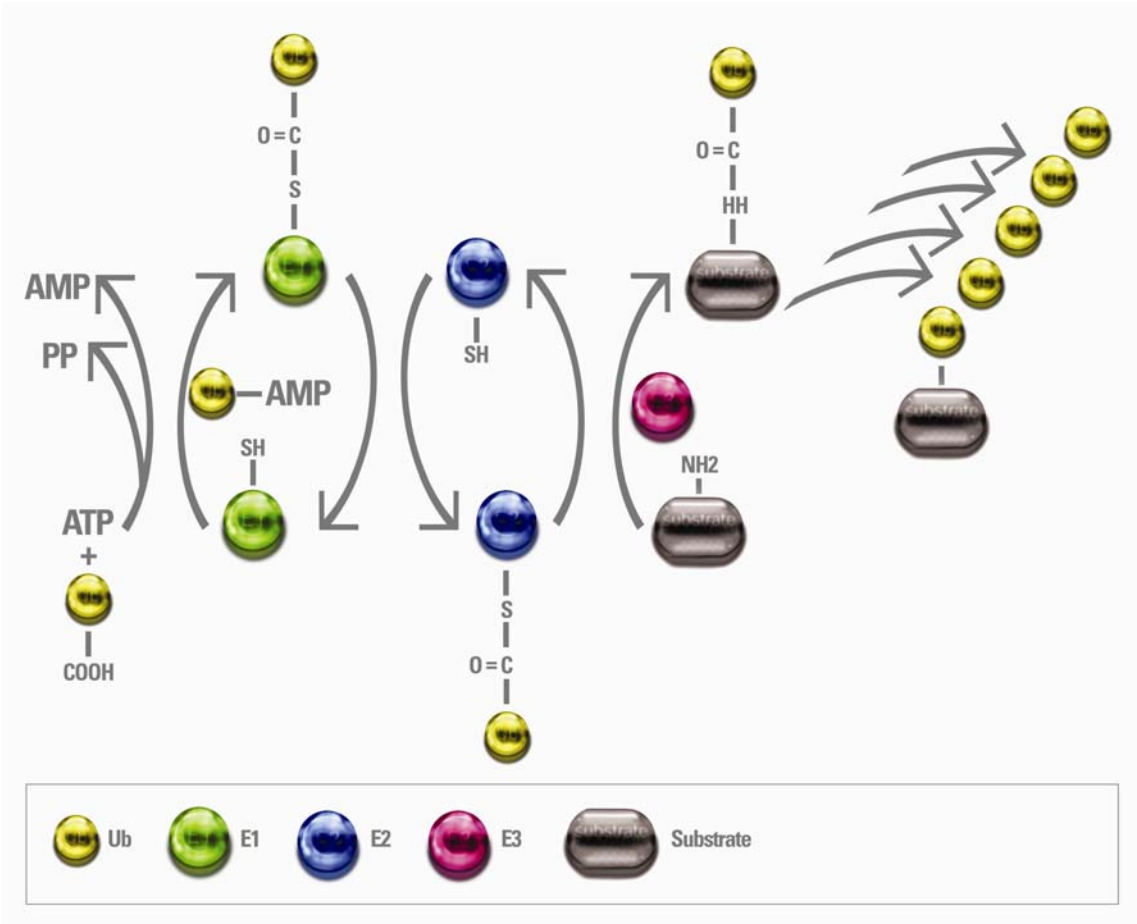

Fig 3. Ubiquitin conjugation. Ubiquitin (Ub) is conjugated to the substrate *via* three different enzymatic steps concerning the activities of E1 or ubiquitin activating enzyme, E2 or ubiquitin conjugating enzyme and E3 or ubiquitin ligase. The covalent anchoring of several ubiquitin moieties promotes polyubiquitylation. Such reaction can be reverted by deubiquitylating enzymes (DUB)

4. 1. E1 or ubiquitin-activating enzymes

Ubiquitin-activating enzymes are abundant proteins present both in the cytoplasm and the cell nucleus. The genes coding for E1's have been cloned in several organisms and in most of them, yeast and human for instance, a single E1 activates ubiquitin molecules to be transferred to the whole array of downstream conjugating enzymes (McGrath et al., 1991; Zacksenhaus and

Sheinin, 1990). Diubiquitin and higher chains can be activated by E1 as efficiently as ubiquitin to be transferred to an E2 (Chen and Pickart, 1990). Since no eukaryotic ubiquitin-activating enzyme (UBA1) has been crystallized so far, there is little molecular information about ubiquitin activation and transfer to an E2. Nevertheless, the co-crystal structures from two UBL-activating enzymes with the respective UBL, MoeB-MoaD and APPBP1-UBA3-NEDD8, provide an insight into the general mechanism for ubiquitin activation and transfer (Lake et al., 2001; Walden et al., 2003a; Walden et al., 2003b). The proteins MoeB-MoaD from molybdenum belong to the biosynthetic pathway of cofactors (Rajagopalan, 1997). MoeB shares homologies with UBA1 both in sequence and in its mechanism of action, and so does MoaD with ubiquitin (they both have two glycines at their C-terminus). More precisely, to activate MoaD, MoeB forms an acyl-adenylate intermediate, like E1 does with ubiquitin. The MoeB-MoaD crystal reveals the existence of a nucleotide binding pocket for ATP and a conserved aspartic acid residue that co-ordinates an Mg^{2+} ion. This ion is crucial for the MoaD nucleophilic attack on the α–phosphate of ATP (Lake et al., 2001). Interestingly, the interface between MoeB and MoaD is primarily mediated by hydrophobic interactions. Although the MoeB-MoaD crystal represents a good model for ubiquitin adenylation, it gives no clue about how the thioester link between the E1 catalytic cysteine and ubiquitin terminal glycine is formed. Instead of forming a thioester bond, there is a sulphurtransferase activity that converts the MoaD acyl-adenynalte to a thiocarboxylate.

As a second model, APPBP1-UBA3 forms a heterodimer whose activity consists in activating NEDD8, a UBL, for further conjugation. In other words,

APPBP1-UBA3 is the E1 for “neddylation”. The N-terminus of UBA1 is homologous to APPBP1 and its C-terminus to UBA3 (Osaka et al., 1998). In combination with the MoeB-MoaD structure, the APPBP1-UBA3 structure shows that the three functions of an E1 (adenylation, thioester bond formation and E2 binding) proceed in a coordinated “assembly line” fashion within a single groove where ATP and NEDD8/ubiquitin bind to two contiguous clefts (Passmore and Barford, 2004; Walden et al., 2003a). The crystal reveals an ubiquitin-like fold of UBA3 at a region which could be responsible for the binding of the E2. In addition, the distance between the adenylation site, where the C-terminus of NEDD8 is located, and the catalytic cysteine is 35 Å. Such a distance makes it necessary for NEDD8 to move from one active site to the other, maybe thanks to its flexibility or by conformational changes in the E1 (Walden et al., 2003a). Moreover, there is a conserved threonine residue which may be important for deprotonating both or any of the E1 and E2 catalytic cysteines (Walden et al., 2003b).

4. 2. E2 or ubiquitin-conjugating enzymes

Ubiquitin-conjugating enzymes are encoded by a gene family whose products share the UBC catalytical domain (Fig 4). This domain contains around 160 amino acids and includes a catalytic cysteine at the active site. Additional N- or C-terminal extensions provide to the different E2’s with special properties such as a particular subcellular localization (Jentsch, 1992). Thirteen different E2’s have been described in *S. cerevisiae* (Jensen et al., 1995) and

fewer than thirty in higher eukaryotes (Pickart, 2001). An E2 can interact with more than one E3: for example, UBC13 can interact with the E3's CHFR, RNF5, RNF8 or RAD5 (Bothos et al., 2003; Didier et al., 2003; Hoege et al., 2002)(Plans et al in press), while UBE2E2 can interact with ARA54, RNF8, CHFR, ZNRF2 and KF1 (Ito et al., 2001) (Plans et al in press) and UBC9, a SUMO-conjugating enzyme, with RAD5, RAD18, RanGAP (Bernier-Villamor et al., 2002; Hoege et al., 2002).

The UBC domain is well established as a central four stranded antiparallel β–sheet with four flanking α-helices (Pickart, 2001; VanDemark and Hill, 2002). The catalytic cysteine lies in a shallow groove on the long loop that connects S4 with H2 (Fig 4). It is in this shallow groove where the C-terminal tail of thioester-linked ubiquitin rests as show nuclear magnetic resonance (NMR) studies (Hamilton et al., 2001; Miura et al., 1999). Unfortunately, due to the instability of E2-ubiquitin thioester complexes, the mechanism of ubiquitin thioester bond formation and transfer to substrate are unknown. In addition, structural studies did not help to identify any obvious catalytic groups near the catalytic cysteine of E2s. So either ubiquitin is transferred spontaneously when the substrate and E2-ubiquitin thioester are correctly located or there are still catalytic groups to be identified in the E3 (Passmore and Barford, 2004).

However, a firmly conserved asparagine residue may play a catalytic role in isopeptide bond formation by stabilizing the oxyanion intermediate (Wu et al., 2003). More precisely, the E2 would suffer an allosteric activation due to a reorientation of a side chain implying a change of position for the asparagine. This asparagine would only be crucial when dealing with E2-substrate ubiquitin transfer and not for E1-E2 or E2-HECT/E3 transfer.

The recognition of the E3 by an E2 is mediated by only a few amino acids as shown in the two co-crystal structures between E6-AP and c-Cbl, two different types of E3, and the same E2, UbcH7 (Fig 6) (Huang et al., 1999; Zheng et al., 2000); UbcH7 interacts with a HECT domain on E6AP, while it interacts with a RING finger domain on c-Cbl. In both cases, the tips of the L1 and L2 loops of UbcH7 enter a hydrophobic groove on the E3, although the structural components that build the groove are completely unrelated in the two E3's (Zheng et al., 2000). Moreover, the fact that loop residues on several E2's that bind a given RING-E3 are event invariant (Zheng et al., 2000) and that single mutations on L2 can change the specificity of interaction between a given RING finger domain and a particular E2 (Martinez-Noel et al., 2001), suggests that the UBC loops are essential for determining E2-E3 recognition and specificity.

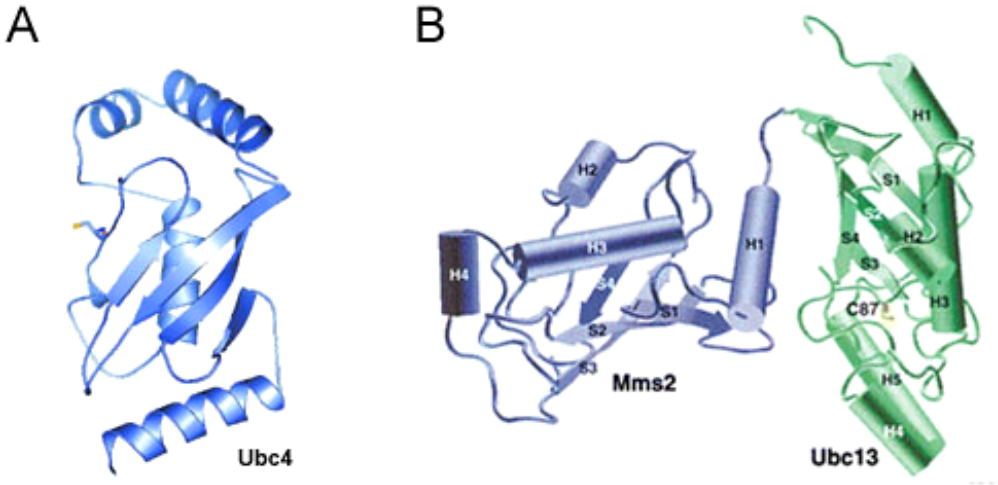

Fig 4. E2 ubiquitin conjugating enzymes contain the UBC domain. Crystal structure of Ubc4, PDB: 1QCQ (Cook et al., 1993), the catalytical cysteine is shown in orange. B Crystal structure of Ubc13-Mms2 hetererodimer, PDB: 1JAT, Mms2 in blue and Ubc13 in green (VanDemark et al., 2001).

Interestingly, UBC13-MMS2 does not need any E3 activity to synthesize in vitro K63-linked polyubiquitin chains (Hofmann and Pickart, 1999) demonstrating that the ability of conjugating K63-polyubiquitin chains resides in the E2 itself, which the crystal structure also supports (VanDemark et al., 2001). RanGAP is sumoylated by UBC9 also without any E3 activity (Bernier-Villamor et al., 2002). Taken together, this suggests that at least, if not all, part of the specificity for K63 ubiquitin chains is given by the E2 UBC13-MMS2 while specificity for sumoylation is provided by UBC9, in what may be a general property of ubiquitylation and similar reactions including canonical polyubiquitylation and monoubiquitylation.

4. 3. E3 or ubiquitin ligases

E3 ubiquitin ligases are responsible for direct or indirect substrate recognition, and thus they confer the substrate specificity in the ubiquitin system. Their role is to mediate the transfer of ubiquitin, provided by the E2, onto a substrate protein without discriminating if the E2 is loaded with one or more ubiquitins. There are basically two different types of E3: those that bear a HECT domain and those that carry a RING finger domain. Both of them interact efficiently with E2's, for example UbcH7 binds both E6-AP and Cbl (Huang et al., 1999; Zheng et al., 2000). These two types of E3 reflect not only a different structure but also different mechanisms, since HECT domain E3's bind ubiquitin through a thioester bond and contribute to the catalysis, while RING finger domain E3's do not. The number of E3's in a given organism remains still

unclear although it is certainly much larger than the number of E2's. Just by focusing on the RING finger domain, it is the fifteenth most common domain in the human proteome including more than 200 proteins containing one or more RING finger domains (Lander et al., 2001). Although it is possible that not all of them ligate ubiquitins, a random screen of six RING fingers has shown that all had the ability to catalyze the formation of polyubiquitin chains (Lorick et al., 1999). In addition, E3 seems to be the only component subject to regulation. Example

4. 3. 1. HECT domain ubiquitin ligases

Several proteins, such as human E6AP, Smurf1 and Smurf2, the mouse Nedd4 or yeast Rsp5, contain the ~350 amino acid HECT domain (Homologous to E6-AP Carboxy-Terminus) (Fig 5A). HECT domains form, like E2's and E1's, an intermediate thioester bond with ubiquitin via a catalytic cysteine residue (Huibregtse et al., 1995; Scheffner et al., 1995). This thioester bond is the donor for the final formation of an amide bond with the ε–amino group of a lysine on the substrate. The crystal structure of E6-AP with UbcH7 (Fig5A, (Huang et al., 1999)) shows that the E3 is arranged in two lobes (N and C) that form an L shape. UbcH7 binds to the N lobe conferring to the complex a final U form with the catalytic cysteines on opposed sides at a distance of 41Å. How ubiquitin is transferred from one cysteine to the other is unclear, considering the large distance between them. In another structure, the HECT domain of WWP1 adopts an inverted T shape because the C-lobe is located in the middle of the

N-lobe. The hinge loop that binds both lobes has to be flexible for proper ubiquitin conjugation (Verdecia et al., 2003b). Furthermore, in this WWP1 structure the distance between the two catalytic cysteines is only ~16 Å and there may be an amino acid in between the last five C-terminal residues which deprotonates either the HECT catalytic cysteine or the acceptor lysine of the substrate to form the isopeptide bond (Verdecia et al., 2003b).

4. 3. 2. RING domain ubiquitin ligases

The RING finger domain has received its name from the first protein on which this module was described (Really Interesting New Gene) (Borden and Freemont, 1996). Many more proteins bearing this domain have been described such as c-Cbl (Fig 5B), APC or SCF. E3's of this class promote ubiquitin transfer without forming a covalent intermediate with ubiquitin. They are dependent on an E2 activity for ubiquitin transfer (Lorick et al., 1999). Most likely, the ubiquitin transfer may happen spontaneously as soon as the extremely labile E2-ubiquitin thioester bond is presented to a substrate lysine in a favorable conformation (Borden, 2000; Pickart, 2001). The RING finger domain is organized as a loop-helix-loop and it coordinates two Zn^{2+} ions in a *cross-brace* organization thanks to eight conserved residues which are either cysteines or histidines (Borden, 2000). They can be classified as either RING-H2 or RING-HC depending on whether they contain a histidine of a cysteine at position 4 of the Zn-coordinating residues.

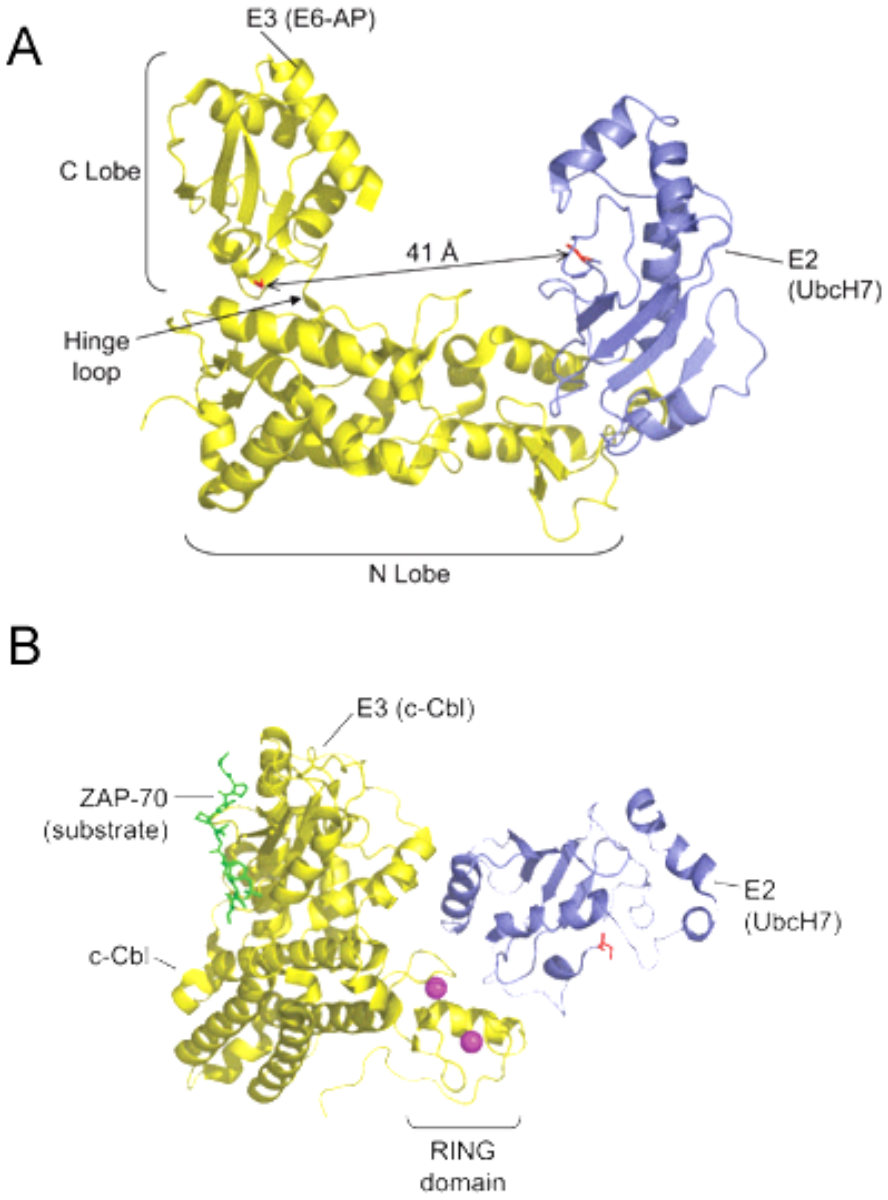

Fig 5. E3 ubiquitin ligases can contain either a HECT domain or a RING finger domain. A Structure of the E6-AP–UbcH7 complex, PDB: 1D5F, the HECT domain E3 is in yellow and the E2 in purple (Huang et al., 1999). B Structure of the UbcH7–c-Cbl, PDB: 1FBV, the RING domain E3 is in yellow and the E2 also in purple. Zinc ions are colored in magenta (Zheng et al., 2000).

Despite the fact that they were originally thought to participate in catalysis, RING finger domains only provide a scaffold in order to bring the ubiquitin-loaded E2 and the substrate into proximity (Passmore and Barford,

2004; Pickart, 2001). Although the RING finger domain directly interacts with the E2 (Fig 6B) (Zheng et al., 2002; Zheng et al., 2000), in the two existing crystal structures, UbcH7-c-Cbl and Cul1-Rbx1-Skp1-F-box, it is not located neighboring the catalytic cysteine and therefore is not expected to participate in the catalysis (VanDemark and Hill, 2002). In addition, since there are very few changes in the E2 structure when crystallized with a RING finger protein in comparison to the E2 alone (Zheng et al., 2000) it is not likely that the RING finger domain promotes allosteric changes in the E2. Furthermore, some E2's alone are able to conjugate polyubiquitin chains without any E3 (Hofmann and Pickart, 1999; Liu et al., 1996).

Some RING finger proteins function as multimeric complexes organized around a cullin domain to recruit together an E2 (Seol et al., 1999). APC is a good example, with more than thirteen different subunits among which APC2 is a cullin protein and APC11 a RING finger protein (Peters, 2002; Tang et al., 2001). Another example could be SCF which has event been crystallized: Cul1 provides the cullin domain while Rbx1 the RING finger domain (Zheng et al., 2002).

The RING finger domain is structurally related to another domain which adopts the same folding without coordinating any Zn^{2+} ion. This domain, called U-Box, is present in proteins such as Udf2a, CHIP and UIP5 and is stabilized by hydrogen bonds (Ohi et al., 2003). U-Box proteins are E3's or E4's that recognize unfolded proteins together with chaperones to target them to proteasome. For example, CHIP and Hsp70 recognize and ubiquitylate immature CFTR protein (mutated in cystic fibrosis) for degradation (Hatakeyama and Nakayama, 2003; Murata et al., 2001).

4. 4. E4 or ubiquitin-chain elongating enzyme

E4 ubiquitin-chain elongating enzymes are enzymes required in late steps of protein polyubiquitylation. They seem to recognize specifically ubiquitin linkages on ubiquitin chains, and can thus be considered as ubiquitin-dependent ubiquitin ligases which can not be activated by the substrate (Koegl et al., 1999). Udf2 catalyzes the formation of polyubiquitin chains together with a E1, an E2 and an E3 thanks to its U-box domain and it is implicated in cell survival under stressful conditions (Koegl et al., 1999).

4. 5. Deubiquitylating enzymes

Like many other protein modification systems, ubiquitylation is a reversible process, and there are ways to remove ubiquitin moieties from mistakenly ubiquitylated proteins or as a competitive process opposed to ubiquitylation. The enzymes responsible for this process are the deubiquitylating enzymes (DUB). There are at least 19 proteins in yeast and more than 90 DUBs have been identified in the human proteome (Baek, 2003; Wilkinson, 2000). Ubiquitin hydrolases are essential for ubiquitin biosynthesis since they release ubiquitin moieties before protein degradation by the proteasome. In general, they are thiolproteases that identify the C-terminal residue of ubiquitin and cleave it (Hochstrasser, 1996; Wilkinson, 1997). Ubiquitin hydrolases can be classified in two groups: UCH (Ubiquitin C-terminal Hydrolases) and UBP (Ubiquitin-specific Proteases). UCH are 25 KDa enzymes

involved in co-translational processing of pro-ubiquitin peptides and in the release of ubiquitin from adducts with small molecules such as amines and thiol groups (Wilkinson and Hochstrasser, 1998). Mutations in UCH family are associated with diseases: UCH-L1 I93M may be associated with Parkinson's disease (Leroy et al., 1998). BAP1 is another UCH associated with lung cancer which contains a 500 amino acid C-terminal domain that binds the RING finger domain of BRCA1, the breast cancer tumor suppressor (Jensen et al., 1998).

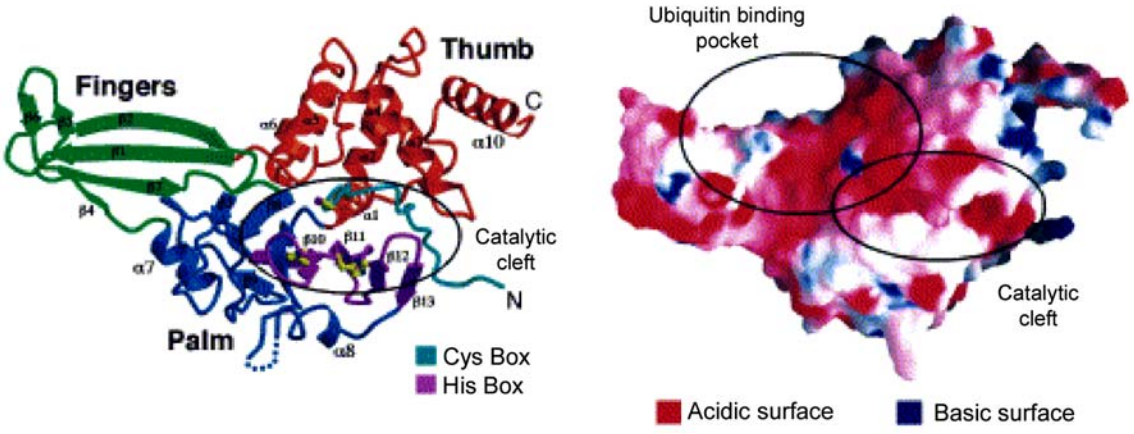

Fig 6. Ubiquitin-specific proteases (UBP) are deubiquitylating enzymes that contain a three-domain architecture comprising Fingers (in green), Palm (in blue) and Thumb (in red). Ubiquitin is specifically coordinated by the Fingers with its C terminus placed in the active site between the Palm and the Thumb. Structure of the HAUSP protein, PDB 1NBF, (Hu et al., 2002).

UBP are proteins from 50 to 350 KDa which contain a catalytic core of 350 amino acids with a variety of N-terminal or occasional C-terminal extensions. Thanks to those extensions the proteins are able to localize properly and to recognize their substrates. UBP can be either free or anchored

to the proteasome and they are responsible for the release of ubiquitin from conjugates. The crystal structure of HAUSP, a UBP that deubiquitylates and stabilizes p53, shows that the core of the protein binds ubiquitin aldehyde leading to a dramatic conformational change in the active site of the enzyme (Fig 6) (Hu et al., 2002). UBPs can regulate molecular pathways by stabilizing/destabilizing target proteins. For instance, when the UBP Ubp4 is mutated in yeast, the mating factor MATα2 fails to be degraded properly and the cells show impaired proteolysis in addition to DNA replication defects. This protein seems to remove polyubiquitin chains from the residual peptide that remains after proteasomal degradation of a polyubiquitylated substrate (Swaminathan et al., 1999). In *D. melanogaster*, deubiquitylation by FAT FACETS sends an inhibitory signal modulating the activity of the Ras/receptor tyrosine kinase pathway in order to limit the number of photoreceptors in a facet to eight (Huang et al., 1995; Wu et al., 1999). There is evidence that ubiquitin hydrolases can recognize particular types of G-K conjugates. For example, the tumor suppressor CYLD mutated in familial cylindromatosis enhances the activation of NFκB by deubiquitylating TRAF2 non K48-linked polyubiquitin chains and is probably the first UBP for K63-linked polyubiquitin chains (Kovalenko et al., 2003; Trompouki et al., 2003).

5. Modifications by ubiquitin

5. 1. Monoubiquitylation

Conjugation of proteins by a single ubiquitin moiety is a regulatory modification involved in diverse processes including transcription, endocytosis, histone function and membrane trafficking (Hicke, 2001; Hicke and Dunn, 2003; Katzmann et al., 2002; Muratani and Tansey, 2003). Monoubiquitylation of receptor tyrosine kinases or the N-terminal cytoplasmatic domain of other membrane proteins recruits proteins of the endocytic pathway signaling for endocytosis and targeting to the lysosome (Mosesson et al., 2003; Terrell et al., 1998). Endocytosis can occur by three distinct substrate ubiquitylations: monoubiquitylation, multiubiquitylation, which consists in multiple monoubiquitylations on the same substrate, or polyubiquitylation using lysine 63 on ubiquitin (see later) (Haglund et al., 2003). The single conjugated ubiquitin carries within its three-dimensional structure all the information necessary for regulating endocytosis both by modifying the activity of the protein transport machinery and by serving as a sorting signal attached to the transmembrane proteins to direct their movement between different cellular compartments (Hicke and Dunn, 2003; Shih et al., 2000). Ubiquitin serves as a signal for the entry of endocytic cargo into vesicles that will fuse to early endosomes which can either recycle the cargo back to the plasma membrane or fuse with lysosomes resulting in proteolysis. Signal-transducing receptors such as receptor tyrosine kinases (RTKs), immune receptors such as interleukin-2 receptor or transporters and channels such as glycine and AMPA glutamate

receptors are regulated by monoubiquitylation mainly by the E3's Cbl and Smurf 1/2 (Burbea et al., 2002; Büttner et al., 2001; Ebisawa et al., 2001; Joazeiro et al., 1999; Rocca et al., 2001; Shtiegman and Yarden, 2003). Several proteins involved in vesicular sorting signals and suspected to play a role as molecular adaptors to link ubiquitylated cargo to the clathrin-based endocytic machinery such as epsin, Hrs/Vps27 and STAM/Hse1 are both monoubiquitylated and carry one or more UIM's (Ubiquitin Interacting Motif) so that they can recognize monoubiquitylation of a given substrate as a signal (Hicke and Dunn, 2003; Hofmann and Falquet, 2001; Raiborg et al., 2002; Shekhtman and Cowburn, 2002). In other examples, transcriptional activation of histone H2B is regulated by a sequential attachment and removal of a ubiquitin molecule (Henry et al., 2003); and monoubiquitylation of the retroviral GAG protein is required for a late step in virus budding (Patnaik et al., 2000; Strack et al., 2000).

It is important to notice that a single ubiquitin conjugate is not sufficient for proteasome recognition (Thrower et al., 2000). Moreover, proteins bearing ubiquitin-interacting motifs (UIM), such as Hrs and those described above (Shekhtman and Cowburn, 2002), can also protect the monoubiquitin from elongation by binding and hiding the ubiquitin lysine residues, and therefore the modified protein from degradation by the proteasome.

5. 2. Canonical polyubiquitylation

Canonical polyubiquitylation consist in the attachment of a polyubiquitin chain where the moieties are linked to each other through isopeptide bonds

between G76 of the donor ubiquitin and K48 of the acceptor ubiquitin (Chau et al., 1989; Thrower et al., 2000). Canonical tetraubiquitin chains are sufficient for 26S proteasome recognition and degradation of the tagged protein (Thrower et al., 2000). The hydrophobic patch, which consists in L8-I44-V70 amino acids in the ubiquitin peptide, is critical for proteasome degradation even though mutations in these residues have little effect on the formation of polyubiquitin conjugates (Sloper-Mould et al., 2001). Canonical chains can be conjugated to substrates assembling unanchored chains thanks to substrate-specific conjugating enzymes using monoubiquitin as a chain initiator. Ubiquitin immunoblots of plant and animal extracts demonstrate the existence of significant levels of unanchored chains (Nocker and Vierstra, 1993; Spence et al., 2000a). However, there can be an initial ubiquitin conjugation by substrate-specific enzymes followed by an elongation by the same substrate-specific conjugating enzyme or by ubiquitin-specific enzymes (Koegl et al., 1999).

Such canonical polyubiquitin chains allow an irreversible and rapid control of protein abundance and it is often used when an on/off switch signal may be needed. Many cell cycle regulatory proteins undergo polyubiquitin conjugation and degradation by the proteasome in order to allow the irreversible progression from one stage to the other during cell cycle. Two multimeric E3 complexes play an essential role in proteolysis at two different cell cycle transitions: the anaphase-promoting-complex/cyclosome (APC) during G2-M and Skp1-Cdc35/Cul1-Fbox protein (SCF) during G1-S (Hershko and Ciechanover, 1998; Reed, 2003). APC regulates the exit from mitosis by targeting D-box or KEN box containing proteins for degradation. The recognition of the targets such as Securins, Plk1 or Cdc20 is mediated by the adaptor

proteins Cdc20 itself or Cdh1 (Pfleger and Kirschner, 2000; Shirayama et al., 1998; Visintin et al., 1997). SCF complexes ubiquitylate substrates thanks to the F-box adaptors that function as cellular receptors which recognize phosphorylated F-box motives present in several target proteins like Cyclin F, Skp2 or β-TrCP (Carrano et al., 1999; Kong et al., 2000; Margottin et al., 1998; Nakayama et al., 2000).

More than one chain is often conjugated to the substrate (Nakamura et al., 1994; Peng et al., 2003; Petroski and Deshaies, 2003). The reason for conjugating multiple ubiquitin chains on a substrate is not clear since a single chain is necessary and sufficient for the proper degradation of at least Sic1 and p21 (Bloom et al., 2003; Petroski and Deshaies, 2003). There are mechanisms to protect polyubiquitin chains from deubiquitylating enzymes (Hartmann-Petersen et al., 2003) or to coordinate polyubiquitylation with proteasome activities. As an example of this mechanism, some ubiquitin binding proteins also bind E3 and/or the proteasome, and so does Pus1 which binds an APC subunit in fission yeast and the proteasome (Kleijnen et al., 2000; Seeger et al., 2003).

Taken together, it seems as though protein degradation is extremely important for the cell and that evolution has selected different and complementing mechanisms to fulfill the cell requirements.

5. 3. K63 polyubiquitylation

K63 polyubiquitylation consist in ubiquitin chains built through isopeptide bonds between G76 of the donor ubiquitin and K63 of the acceptor ubiquitin. Such enzymatic reaction is thus far known to be mediated by a unique E2 conjugating enzyme formed by the catalytic subunit UBC13 and the regulatory subunit UEV1 or 2 (Hofmann and Pickart, 1999; VanDemark et al., 2001). Attachment of K63-linked chains to target proteins is important for signal transduction, DNA repair, stress response and endocytosis (Deng et al., 2000b; Galan and Haguenauer-Tsapis, 1997b; Hoege et al., 2002; Spence et al., 2000a). In response to the binding of the interleukin-1 molecule to its receptor, a set of adaptor proteins including MyD88 and IRAK bind to the receptor and recruit TRAF6 which is a RING finger domain protein. TRAF6 autocatalyses its K63 polyubiquitylation with the help of the Ub13-UEV1 heterodimer, and the K63-linked ubiquitin chains on TRAF6 are recognized specifically by TAB2 providing a scaffold to facilitate the activation of TAK1 kinase. TAK1 kinase initiates a phosphorylation cascade by phosphorylating IκB kinase, IKKβ, which in turn phosphorylates IκBα. Phosphorylated IκBα is targeted to the proteasome by canonical polyubiquitylation mediated by the SCF complex. NFκB, a heterodimer of P65 and P50, is thus free to enter the nucleus and activate gene expression (Kanayama et al., 2004; Sun et al., 2004; Wang et al., 2001b). In another example, DNA damage induces PCNA monoubiquitylation and nuclear import of UBC13/MMS2 heterodimer (MMS2 is the yeast homologue of UEV1). This heterodimer, together with RAD5, mediates K63 polyubiquitylation of PCNA, which then directly promotes DNA repair (Hoege et

al., 2002) (see sumoylation). In yeast, K63 polyubiquitylation of an uracil permease by Npi/Rsp5 strongly stimulates endocytosis of the protein reflected on the uracil uptake. In a UbK63R background the protein can still be monoubiquitylated but shows minimal endocytosis (Galan and Haguenauer-Tsapis, 1997b). K63-linked polyubiquitin chains have a more extended conformation, which is structural evidence to explain how such chains are not efficiently recognized by proteasome (Cook et al., 1992; Varadan et al., 2003; Varadan et al., 2002b).

5. 4. Polyubiquitylation using lysines other than K48 or K63

Ubiquitin has five other lysine residues and at least three of them (K6, K11, K29) can function as a linkage for polyubiquitin chains (Baboshina and Haas, 1996; Peng et al., 2003; Wu-Baer et al., 2003; You and Pickart, 2001). Although the molecular details of these forms of polyubiquitylation are still poorly understood, it seems that K11- and K29-linked polyubiquitin chains may target proteins for destruction (Baboshina and Haas, 1996; Johnson et al., 1995; Liu et al., 1996), while K6-linked polyubiquitin chains are disassembled by 26S proteasomes (Baboshina and Haas, 1996; Lam et al., 1997; Nishikawa et al., 2004). Interestingly, not even by means of extensive proteomics approaches have mixed chains been identified (Peng et al., 2003). This suggests that ubiquitin chains are not able to form branched structures composed of ubiquitin moieties attached through different lysines.

6. Ubiquitin-like proteins (UBL)

UBL constitute a family of small proteins which have structural similarities to ubiquitin and which can be covalently conjugated to a given substrate (Fig 7). Interestingly, UBL are not known to form polymers on a target protein even though they are also conjugated to a lysine residue. Moreover, their attachment has diverse consequences but in no case it implicates proteolysis.

Modifier	Activating enzyme	Conjugating enzyme	Processes regulated	Substrates	Fates
Ubiquitin	Uba1p	Ubc1-8p	DNA repair	PCNA	Regulation
		Ubc10-11p	Peroxisome biogenesis		"
		Ubc13-16p	Mito protein location		"
			DNA silencing		"
			DNA replication		"
			Tumor suppression	P53	proteolysis
			Transcription	IκBα, HIF-1	"
			Stress/protein damage	Damaged protein	"
			Receptor internalization	Surface receptor	"
			Protein processing	NFκB	"
Rub1p/ NEDD8	U1a1p, Uba2	Ubc12p	Ubiquitylation	Cdc53p	Ligase localization?
URCP			Interferon-induced		Cytoskeletal localization
SUMO/ Smt3p	Aos1p, Uba2p	Ubc9p	Nuclear transport	Ran GAP	Localization
			Nuclear dot formation	PML, Sp100	Subnuclear"
			Cytokinesis	Cdc3p	Bud neck "
			Transcription	IκBα, p53	Inh polyub
Apg12p	Apg7p	Apg10p	Autophagic vesicle		

Fig 7.Ubiquitin-like proteins. Modification by these small peptides is a targeting signal for several processes. Yeast proteins are indicated with the suffix p. The similarities between Apg12p and ubiquitin relay more on the enzymes involved in the conjugation than in the primary sequence of both peptides.

RUB1 is a yeast UBL which can modify CDC53/Cullin (Liakopoulos et al., 1998), a subunit of the SCF ubiquitin ligase complex. Although RUB1 does not modify CDC34 stability, it is likely that it may influence the activity of SCF or its specificity towards its different substrates. Conjugation of RUB1 requires ULA1/UBA3, that serves as a heterodimeric RUB1 activating enzyme, and UBC12, which is able to conjugate RUB1 (Liakopoulos et al., 1998). NEDD8 is the mammalian homologue of RUB1 which modifies Cul1, a step necessary for proper activation of the SCF complex (Jackson et al., 2000).

Agp12 is another yeast UBL involved in autophagy. In this process, Agp7 plays the role of an Agp12-activating enzyme, Agp10 of an Agp12-conjugating enzyme to finally conjugate Agp12 on the substrate: Agp5 (Mizushima et al., 1998).

Also in mammals, UCRP is a UBL interferon-inducible 15KDa protein which sequence consists in a double tandem repeat of ubiquitin. Proteins modified by UCRP seem to be targeted to the cytoskeleton (Loeb and Haas, 1994).

The best studied UBL is SUMO (Small Ubiquitin-related MOdifier). Many proteins are sumoylated by UBC9 and its homologs in many organisms from yeast to human beings (Schwarz et al., 1998). Even a SUMO-modification consensus site has been postulated, ψKxD/E, where ψ is a hydrophobic residue (Johnson and Blobel, 1999). For example, the conjugation of SUMO to histone H4 results in transcriptional repression, probably by recruitment of histone-deacetylases (Shiio and Eisenman, 2003). Sumoylation of RanGAP1 targets it to the NPC (Mahajan et al., 1997; Matunis et al., 1996), the mitotic spindle and kinetochores (Joseph et al., 2002), while sumoylation of PML targets it to

subnuclear foci called nuclear or PML bodies (Muller et al., 1998). A very interesting characteristic of SUMO is that it may be conjugated on the same lysine as ubiquitin in a mutually exclusive manner. Such a competitive modification permits a tight regulation of the modified protein. For instance, sumoylation of IκBα prevents its canonical polyubiquitylation, and hence it inhibits NFκB activation (Desterro et al., 1998); or sumoylation of PCNA stabilizes the protein during the S phase in order to replicate DNA (Hoege et al., 2002). PCNA is actually a very interesting and integrating example, since the protein can suffer monoubiquitylation, polyubiquitylation K63 and SUMOylation on the same lysine residue. PCNA, proliferating cell antigen, is a protein that associates with DNA as a homotrimer. During the S phase, it is SUMOylated on K164 in a reaction requiring several factors including the conjugating enzyme Ubc9. This inhibits PCNA's role in DNA repair and might promote some aspects of DNA replication. Upon DNA damage, PCNA is monoubiquitylated through the actions of Rad6 and Rad 18. A chain of K63-linked ubiquitin molecules is then assembled catalyzed by Ubc13/Mms2 and Rad5. This promotes PCNA's role in the postreplicative error-free DNA repair pathway. Rad5 and Rad18 are E3 ubiquitin ligases that bind to DNA and recruit the E2 Ubc13/Mms2 and Rad8, respectively (Hoege et al., 2002).

Despite their lack of polymerization, UBL's have provided important biochemical insights into ubiquitin attachment to target proteins since all are attached to a lysine side chain of the substrate through their C-terminal glycine residue to form an isopeptide linkage.

7. The problem of polyubiquitylation

When the ubiquitin machinery works to polyubiquitylate a substrate no matter on which lysine, as more ubiquitin moieties are added to the chain, the conjugating enzymes must separate progressively from the substrate. The problem consists in maintaining the substrate specificity considering the increasing distance between enzyme and substrate as polyubiquitin chains elongate. E4 enzymes could participate in the last steps but they do not explain how the chain specificity is preserved (Koegl et al., 1999). In contrast with E2's, there is no evidence of any E4 which would mediate a special type of polyubiquitylation. A second possibility relays on the multimeric complexes to which many RING finger proteins belong, that include E2's (Jackson et al., 2000; Varelas et al., 2003). The SCF E2, Cdc34p, forms multimers which are required for polyubiquitin formation. Due to multimerisation, different E2/E3 complexes could be involved in recognition and polyubiquitylation of the same or different substrates that are recognized by such complexes.

8. Ubiquitylation and cell cycle regulation

Ubiquitylation and degradation by the proteasome of the target proteins plays an essential role in the regulation of nearly all stages of the cell cycle and cell proliferation (Fig. 8). Ubiquitylation can both modulate biochemically the activity of a given protein and its subcellular localization (Liston et al., 2003; Margolis et al., 2003; Pray et al., 2002; Vogelstein et al.,

2000a).

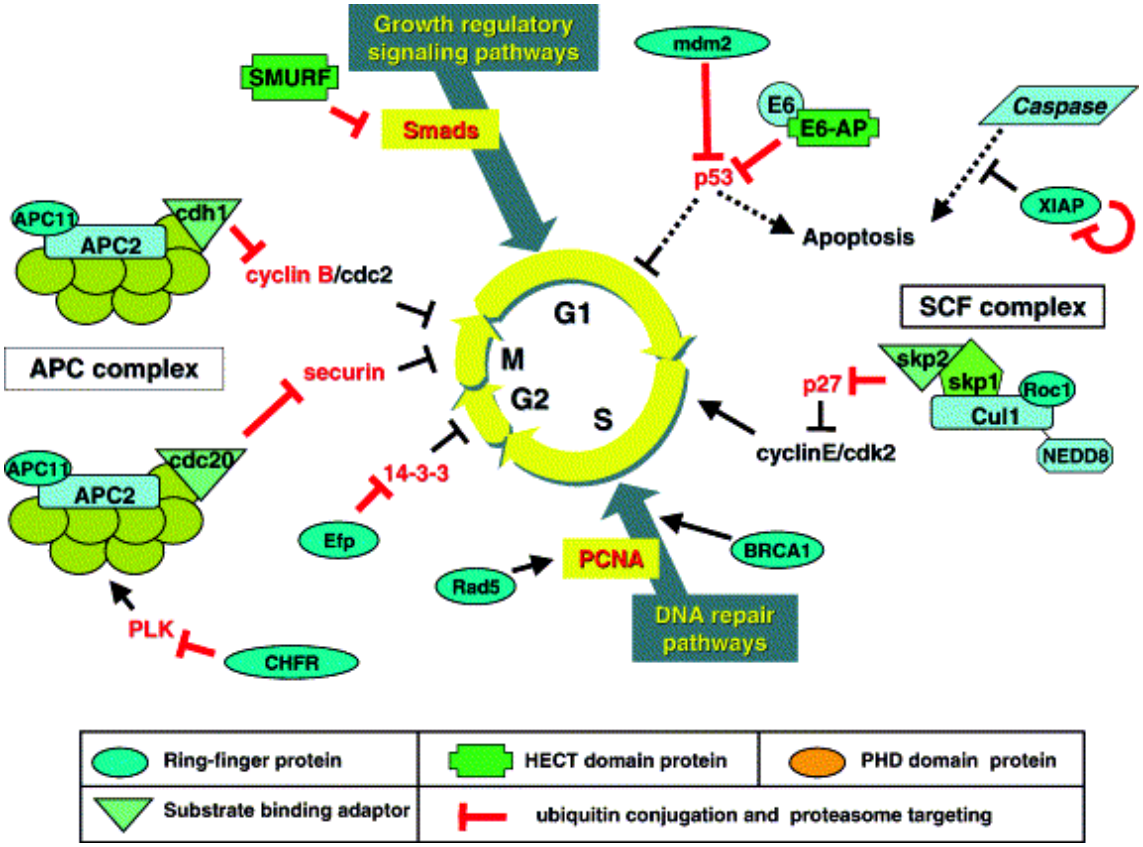

Fig 8. Regulation of the cell cycle, checkpoint activation apoptosis and growth signaling by means of ubiquitylation. Ubiquitylation of important regulators promoted by the activity of E3 or ubiquitin ligases, which contain a RING finger or a HECT domain, usually leads to the degradation of the substrate by 26S proteasome although it can also alter the subcellular localization or the activity of the substrate.

The multiprotein complex APC (anaphase promoting complex) regulates mitotic entry and exit by determining the levels of key proteins. The protein composition of the complex is described above (see RING domains ubiquitin ligases). The best characterized substrates of the APC are cyclin B and securin, which regulate the G2-M transition. Cyclin B is required for the activation of the cyclin-dependent kinase 1 (Cdk1) whose activity is critical for mitosis entry.

Securin regulates exit from mitosis by binding and inhibiting separase, which is an endoprotease responsible for the cleavage of the chromosome-tethering protein complex and cohesins, to allow sister chromatids separation when they are properly located. APC targets securin for destruction once the cell commits to enter anaphase. Other important substrates of APC are cyclin A, polo-like kinase 1, cdc 5, cdc 6 and KIP 1. The importance of ubiquitylation for the function of APC is reinforced by the fact that both Emi 1 and Mad2, two inhibitory proteins of the APC, seem to disrupt substrate presentation to the core complex by the adaptor proteins (see canonical polyubiquitylation).

The SCF complex regulates G1-S transition in a manner similar to APC (see RING domains ubiquitin ligases and canonical polyubiquitylation). Subunits of this complex recognize the substrates and bring them near the ubiquitin ligase for canonical polyubiquitylation. Thus, the negative regulator of the cell cycle progression p27 must be degraded in order to enter the S phase. Such degradation takes place when the F-box protein Skp-2 recognizes phosphorylated p27 and presents it for polyubiquitylation to SCF.

The tumor suppressor p53 can promote cell cycle arrest, DNA repair, apoptosis and cell senescence in response to DNA damage, cell cytoskeleton defects, ultraviolet light, stress, viral infection or oncogenic transformation by a number of proteins. MDM2 ubiquitin ligase is a key regulator of p53 by two distinct mechanisms: p53 transcriptional activity is inhibited directly by interaction with MDM2 which prevents the interaction of p53 with the transcriptional machinery; also, MDM2 is a ubiquitin ligase that supports conjugation of multiple monoubiquitins on p53, which promotes its nuclear export. Such monoubiquitins can be used as chain initiators to form canonical

polyubiquitin chains on p53 by an unidentified E3 thus targeting it to the proteasome. MDM2 ligase activity on p53 is tiny regulated by other proteins such as p14ARF. In addition to MDM2, p53 can be canonically polyubiquitylated by another E3, E6AP. This happens upon HPV infection in cervical carcinomas when E6 viral protein presents p53 to the cellular E6AP.

Transforming growth factor β (TGFβ) can arrest cell cycle by inhibiting G1 CDKs. TGFβ signals through two types of receptors and intracellular transducing molecules termed Smads which, once released from the plasma membrane, accumulate in the nucleus and after a double phosphorylation activate gene transcription. Canonical polyubiquitylation by HECT-domain Smurf1/2 on Smad proteins regulates its abundance and hence mediate the termination of TGFβ signaling.

The mitotic check point protein CHFR is a RING finger domain ubiquitin ligase that can block the cell cycle in metaphase. Plk1 is the substrate for this E3 and is target to the proteasome. Downregulation of Plk1 results in the inhibition of cyclin-dependent kinase 2 activation and mitotic entry. In contrast, the Efp RING finger domain E3 inhibits the 14-3-3σ inhibition of G2 by canonically polyubiquitylating the protein and targeting it for destruction.

Finally, it is worth mentioning the role of ubiquitylation in apoptosis through the protein family termed IAP (inhibitor of apoptosis proteins). IAP can block apoptosis by directly binding, through their BIR domain (baculoviral IAP repeat), caspase proteases which are effectors of the apoptotic response. Some IAPs like XIAP or c-IAP1/2 carry a RING finger domain and are indeed self ubiquitin ligases responsible for its own targeting to the proteasome resulting in an accomplishment of the apoptotic program and cell death.

9. Ubiquitylation and neurodegenerative diseases

Neurodegenerative diseases have been associated at different levels with the ubiquitin-proteasome system. Aberrant function of the latter can lead to a variety of disorders (Fig. 9) (Baek, 2003; Hardy, 1997; Layfield et al., 2001; Leroy et al., 1998; Steffan et al., 2004a).

Mutant gene product	Relationship to ubiquitylation	Disease
E6-AP	Ubiquitin ligase	Angelman's syndrome
Parkin	Ubiquitin ligase	Parkinson's disease (autosomal recessive juvenile)
PGP9.5	Deubiquitylating enzyme	Parkinson's disease (autosomal dominant)
Presenilin-1	Substrate	Alzheimer's disease (familial early onset)
Tau	Substrate	Fronto-temporal dementia
α-Synuclein	Substrate	Parkinson's disease (autosomal dominant)
Huntingtin	Substrate	Huntington's disease
Prp	Substrate	Prion disease
Ubiquitin	Cofactor	Alzheimer's disease (late-onset)

Fig. 9. Relationships between the ubiquitin system and Human neurodegenerative diseases.

Linkage and associative analysis of inheritable forms of neurodegenerative diseases reveal a striking involvement of the ubiquitin system in pathology. Notably, loss of function mutations in the Parkin gene, which codes for a RING finger ubiquitin ligase, cause the autosomal-recessive form of juvenile Parkinsonism. Normal Parkin protein seems to be involved in degrading misfolded proteins at the endoplasmatic reticulum. Interestingly, an autosomal dominant form of Parkinson's disease can be due to loss-of-function

mutations in the gene coding for the deubiquitylating enzyme PGP9.5. Although the human substrate of the enzyme is unknown, the *Drosophila* homologue UCH-D promotes IκBα deubiquitylation. More generally, PGP9.5 could be involved in processing ubiquitin precursors, and when mutated create a lack of free ubiquitin resulting in proteasome inhibition. Although the non-pathogenic substrate remains to be identified, it has been shown that mutations in E6-AP, a HECT domain ubiquitin ligase, cause Angelman's syndrome. This E3 polyubiquitylates p53 in the presence of the viral protein E6 (see Ubiquitylation and the cell cycle regulation).

Protein aggregation is a common feature of all chronic human neurodegenerative diseases such as amyloid plaques in Alzheimer's disease, cortical Lewy bodies in Dementia, or Lewy bodies or nuclear aggregates containing expanded Huntingtin in Huntington's disease. These protein inclusions are highly ubiquitylated and it remains unclear whether they create or protect from toxicity. The point is that several key proteins involved in disease are polyubiquitylated including α-synuclein, presenilins, prion proteins, Huntingtin (which is even sumoylated) and tau. At least for α-synuclein, it has been proved that A53T mutations results in a worst degradation by the ubiquitin proteasome system of the protein.

The ubiquitin-proteasome pathway could also explain he late onset of non-inheritable forms of neurodegenerative diseases. It has been reported that in ageing and Alzheimer's disease brains misreading in the ubiquitin precursor mRNA may result in a +1 frameshifted polyubiquitin peptide. The ensuing peptide consists in the first 75 amino acids of ubiquitin, lacks the essential glycine in position 76 and instead incorporates 20 non-sense amino acids. Such

Ubi+1 can be conjugated to other ubiquitins but fails to be removed by the isopeptidase-T deubiquitylating enzyme. Unanchored polyubiquitin chains usually play a role in inhibiting the proteasome, however an unanchored chain with ubiquitin+1 at the end would be indestructible and a strong inhibitor of the proteasome (Lam and Pickart, 2000). Disruption of the turnover of key regulatory proteins such as presenilin-1 could result in pathogenesis. This idea is supported by the fact that chemical proteasome inhibition in cultured cells result in a higher protein aggregate formation.

OBJECTIVES

- To identify molecular partners of the K63 ubiquitin conjugating enzyme UBC13 using the yeast two hybrid technique and confirm the interaction in mammalian cultured cells.

- To functionally study UCB interactions with RNF8 and determine if it has a ubiquitin ligase activity.

- To study the function of RNF8 in cellular processes, by means of over-expression and depletion by siRNA.

- To identify molecular partners of RNF8 that might help to understand the phenotype caused by RNF8 overexpression or knock-down.

MATERIALS AND METHODS

1. Yeast two-hybrid screening

Full-length cDNA for human UBC13 was generated by polymerase chain reaction (PCR) with specific primers carrying *Eco* RI and *Sal* I restriction sites using cDNA from the cell line HepG2 (table I), and cloned in frame with the Gal4 DNA-Biding domain in the pBD vector (Stratagene, La Jolla, CA). This construct was co-transfected by the lithium acetate method into the *S. cerevisiae* strain AH109 together with a human fetal brain cDNA library cloned in pACT2 (Clontech, Palo Alto, CA). Freshly prepared yeast competent cells were mixed with plasmid DNA together with herring testis carrier DNA and polyethyleneglicol-lithium acetate solution (40% polyethyleneglicol, 10 mM Tris, 1 mM EDTA and 100 mM lithium acetate) and incubated for 30 min at 30 ºC with shaking. Seven percent DMSO (Dimethyl sulphoxide) was added to the cells and followed by a 42 ºC heat-shock in a water bath. Cells were chilled on ice, centrifuged at 1000 g and resuspended in TE buffer (10 mM Tris-HCl pH 7.5, 1 mM EDTA) prior to plating in minimal media plates, thus testing for autoactivation of the HIS3, ADE2 and *LacZ* marker genes contained in the genome of the yeast strain AH109. Shuttle plasmids were isolated from yeast cells grown in minimal medium by phenol-chloroform extraction, rescued in *E. coli* and retransformed into AH109 with the bait plasmid. Inserts contained in pACT2 from confirmed interacting positives were analyzed by sequencing by the Sanger method. Screening efficiencies were calculated by plating 1/200 of

the total transformed yeast on Leu^- / Trp^- plates, thus assaying for the incorporation of pBD which confers triptophan auxotrophy and pACT2 which confers leucine auxotrophy, and counting the number of independent clones. Full-length cDNA's for human UBCH7, UBE2E2, CDC34 and UBCH6 were kindly provided by Dr. Ito from Gifu University School of Medicine, Japan, and generated as described in Ito et al 2001(Ito et al., 2001).

For the second yeast two hybrid screening of a cDNA fetal library, full-length cDNA for human RNF8 was generated together with two partial constructs containing only the FHA or the coiled-coil and the RING finger domains of RNF8 by polymerase chain reaction with primers carrying *Eco* RI and *Sal* I restriction sites, and using pHA-RNF8 as a template (Table I), and cloned in frame with the Gal4 DNA-Biding domain in the pBD vector. Only full-length RNF8 was used to screen the library as described above and after confirmation of interaction, pACT2 plasmids were retransformed into AH109 with the partial forms of RNF8 to determine the domain of interaction. Partial HERC1 WT and C4811A, full length HERC3 WT and C1018A cloned in frame with the Gal4 binding domain were gently provided by Dr. José Luis Rosa from the Universitat de Barcelona.

2. Generation of expression plasmid constructs, cloning and site-directed mutagenesis

Construct pFlag-UBC13 was generated by subcloning full-length UBC13 cDNA from pBD-UBC13 into the pFlag-CMV-6c vector (Sigma) with the original

restriction sites. pHA-RNF8 was generated by PCR with primers carrying *Eco* RI and *Xho* I sites using cDNA from the cell line IMR32 as a template and cloned into pACT2 (see Table I for primers). The resulting HA-tagged RNF8 cDNA was excised with *Bgl* II and *Xho* I, and subcloned into pcDNA3.1 (Invitrogen, Carlsbad, CA). To generate constructs for the expression of HA-tagged ubiquitin, cDNA for ubiquitin was amplified from Cos7-derived cDNA with primers carrying *Sal* I and *Not* I restriction sites (Table I), and the product cloned into pCMV-HA (Clontech). Construct pGFP-RNF8, for the expression of chimeric RNF8 bearing GFP at its amino terminus, was generated by PCR with primers containing sites for *Eco* RI and *Sal* I (Table I), and the product subcloned into pEGFP in frame with GFP (Clontech). Construct pHis$_6$-RNF8 was generated by inserting full-length RNF8 from pBD-RNF8 cDNA into the *Eco* RI and *Xho* I sites of pcDNA3.1HisC (Invitrogen). pFlag-HIP1 was kindly provided by Dr Michael Hayden from University of British Columbia, Vancouver, Canada.

Digested plasmids and inserts were purified from agarose gels using the Gel Extraction kit (Quiagen, Valencia CA, USA) and ligated with T4 ligase (Promega) in a 1:1 molar ratio between plasmid and insert. After ligation, all plasmids were transformed into *E. coli* DH5α by heat shock. Competent cells were thawed on ice, incubated with ligated plasmid-insert DNA for five minutes on ice followed by heat shock in a water bath at 42 ºC for 30 seg. Cells were chilled on ice and recovered with SOC medium at 37 ºC for 1 h in a shaker prior to plating on Luria Bertoni broth base (LB) agar plates with the appropriate antibiotic. Ampicillin was used at a final concentration of 50 μg/ml and kanamicin at 30 μg/ml. The detection of recombinant clones was assayed by

PCR with primers flanking the multiple cloning site of the vector and the colonies of interest were grown in LB liquid medium with the appropriate antibiotic at the same concentration as in agar plates. Cells were harvested by centrifugation and plasmidic preparations were preformed using either Wizard kit (Promega) for mini preparations and Quiagen endotoxine free plasmid kit for midi and maxi preparations (Quiagen). DNA concentration was calculated by absorbance at 260 nm. For use in mammalian cell transfection, plasmids were precipitated with cold ethanol and salts under sterile conditions.

For site-directed mutagenesis, the Quick Change procedure (Stratagene) was used. In a first step, the plasmid of interest was synthesized by the high fidelity polymerase Pfu with ~30-base pair-complementary oligonucleotides carrying the desired mutation at the center of the sequences. Secondly, the plasmid template was subject to *Dpn* I digestion for 1 h. Only plasmids of bacterial origin were restricted since *Dpn* I only cuts at methylated sites. After digestion, plasmids were transformed by heat shock (see above) into super competent 10^9-10^{10} / μg DH5α bacterial cells (Stratagene). Plasmids contained in the resulting transformants were isolated and sequenced to confirm the incorporation of the desired mutation. Constructs were then transfected into Cos 7 or HeLa cells and tested by Western blotting for expression of the mutated proteins.

Cysteine 403 of RNF8 was mutagenized to serine, using as templates pHA-RNF8, pHis_6-RNF8 and pGFP-RNF8 and the mutagenic oligonucleotides RNF8-C403S-Fw and Rev (Table I). For the generation of single and multiple-site ubiquitin mutants in which lysine residues at positions 29, 48 or 63 were mutagenized to arginine, the construct containing wild-type HA-tagged ubiquitin

was mutagenized at one of the positions, and subsequently mutagenized to a second. Primers are listed in Table I. Cysteine 87 of UBC13 was mutagenized to alanine using as template p-Flag-UBC13 and the four mutagenic oligonucleotides listed in table I at the same time.

Experiment	**Primers Fw and Rev**
pBD-UBC13	CCGGAATTCATGGCCGGGCTGC CGACGTCGACGATGCACACTTGATGATCG
pBD-RNF8	CCGGAATTCATGGGGGAGCCCGGCT CCGACGTCGACTCAGAACAATCTCTTTGCTTT
pBD-RNF8Δcoil/RING	CCGGAATTCATGGGGGAGCCCGGCT CCGACGTCGACATTCACAAGACACTTTATTTATTTT
pBD-RNF8ΔFHA	CCGGAATTCTCTGGTCAGCCAGTGAAATCA CCGACGTCGACTCAGAACAATCTCTTTGCTTT
Real time PCR S14	CAGGTCCAGGGGTCTTGGTC GGCAGACCGAGATGAATCCTCA
Real time PCR UBC13	GCTGCCATTGGGTATTCTTC ACCAGTTCCTGGCATCAAAG
Real time PCR RNF8	GAAGTTCCTGCTCCATTTGC GGTGACCATGTCCAGGATTC
Real time PCR KIAA0675	GCTCAGAAATTCCATGCTCA TGTATCAGATCTTGGGCAACTG
Real time PCR HIP1	CAAACGCCAAGAGATGGATT GCTCGTAGTGCTTTTTCCGAAGC
Realtime PCR Caspase-3	GAGGCCGACTTCTTGTATGC CGGTTAACCCGGGTAAGAAT
pACT2-RNF8	CCGGAATTCCGATGGGGGAGC CCGCTCGAGACTCAGAACAATCTCTT
pHA-Ubiquitin	GCGTCGACGATGCAGATTTTCGTGAAAACC TAGCGGCCGCTCAACCACCACGAAGTCTCAACA
pGFP-RNF8	CCGGAATTCCATGGGGGAGCCCGGCT CCGACGTCGACTCAGAACAATCTCTTTGCTTT

RNF8 C403S mutation	GAGAATGAGCTCCAATCTATTATTTGTTCAGAA TTCTGAACAATAATAGATTGGAGCTCATTCTC
Ubiquitin K29R mutation	AAAATGTAAAGGCCAGGATCCAGGATAAGG TCCTTATCCTGGATCCTGGCCTTTACATTT
Ubiquitin K48R mutation	TGATCTTTGCTGGCAGGCAGCTGGAAGATG CCATCTTCCAGCTGCCTGCCAGCAAAGATC
Ubiquitin K63R mutation	ACTACAATATTCAAAGGGAGTCTACTCTTC TGAAGAGTAGACTCCCTTTGAATATTGTAG
UBC13 C87A first step	CAAGTTGGGAAGAATATCTTTAGATATTTTGAAAG CTTTCAAAATATCTAAAGATATTCTTCCCACTTG
UBC13 C87A second step	CAAGTTGGGAAGAATAGCTTTAGATATTTTGAAAG CTTTCAAAATATCTAAAGCTATTCTTCCCAACTTG

Table I

3. Cell growth, transfection and drug treatments

HeLa and Cos7 cells were grown in Dulbecco's Modified Eagle's Medium (DMEM) (PAA Laboratories, Linz, Austria) supplemented with 10% heat-inactivated fetal bovine serum and antibiotics, penicillin (100 units/ml) and streptomycin (100 μg/ml), in an atmosphere of 5% CO_2. For inactivation of complement, fetal bovine serum was incubated for 1 h at 55 ºC, filtered through a 22 μm pore filter, aliquoted and stored at -20 ºC until used.

For transfection, cells were seeded on Petri dishes or sterile glass coverslips at 60 to 80% confluence and transfected the following day with the appropriate circular plasmids with cationic liposomes (Lipofectamine, Invitrogen) diluted in Optimem medium (Invitrogen) without fetal bovine serum. Cells were incubated in transfection medium for 5 h at 37ºC in an atmosphere of 5% CO_2 and the transfection medium replaced with fresh serum-containing DMEM to

allow the cells to recover. Cells were then either lysed or fixed at the times required by the experiment.

In some experiments, HeLa cells were treated with several drugs: etoposide (SIGMA) at 100, 25, 10, 1 or 0,1 μM, Cis-platinium 100 or 50 μM (SIGMA), thymidine 2 mM (SIGMA), nocodazole 0.1 μg/ml or 0.5 μg/ml (SIGMA) and taxol 10 μM (SIGMA) during 12 h or 24 h as indicated in the respective experiments. In other experiments, and prior to processing for immunocytochemistry, flow cytometry or cell sorting, cells were incubated with the caspase inhibitors Z-DVED (10 μM final concentration) or Z-VAD (30 μM) (Biomol, Plymouth Meeting, PA).

4. SiRNA synthesis and transfection

RNA duplexes for small interference RNAs were synthesized with the Silencer™ siRNA Construction Kit (Ambion Austin, Texas). Target sequences started with an AA dinucleotide and both *sense* and *antisense* sequences incorporated part of the T7 promoter region. Oligonucleotides corresponding to target sequences on RNF8 are listed in table II. Each siRNA name reflects the target exon on which its sequence is included. A “scrambled” oligonucleotide was also designed as a control. SiRNA oligonucleotide templates were hybridized with a T7 promoter-containing primer at 70 ºC for 5 min and filled with Klenow DNA polymerase for 30 min at 37 ºC. *Sense* and *antisense* double stranded DNA were transcripted separately by T7 RNA polymerase for 2 h at 37 ºC and then combined in a overnight incubation for RNA synthesis and duplex

formation. 5' overhanging leader sequences and DNA templates were digested by adding a single-strand specific ribonuclease and DNase was used to eliminate the template. Following digestion, double-stranded siRNA's were purified with a filter cartridge and quantified with a Nanodrop ND-1000 spectrophotometer.

Exon 2 Antisense	AATGGACAATTATGGACAACACCTGTCTC
Sense	AATGTTGTCCATAATTGTCCACCTGTCTC
Exon 3 Antisense	AATGCGGAGTATGAATATGAACCTGTCTC
Sense	AATTCATATTCATACTCCGCACCTGTCTC
Exon 3b Antisense	AAACATGAAGCCGTTATGAATCCTGTCTC
Sense	AAATTCATAACGGCTTCATGTCCTGTCTC
Exon 5 Antisense	AAATCGCCAGCAAGAAGGACTTCCTGTCTC
Sense	AAAAGTCCTTCTTGCTGCGATCCTGTCTC
Exon 7 Antisense	AATGAGAACAATTCGTCGTTCCCTGTCTC
Sense	AAGAACGACGAATTGTTCTCACCTGTCTC

Table II

SiRNAs were tested for specific RNF8 knock down by double transfection at 48 h intervals with Lipofectamine cationic liposomes (see above) in a range of concentrations. For further experiments final concentration of siRNA duplexes was 50 nM. Transfected HeLa cells were lysed 48 h after the second siRNA transfection in RIPA buffer (20 mM Tris, pH 7.2, 0.5% deoxycholate, 1% Triton X-100, 0.1% SDS, 150 mM NaCl, 1 mM EDTA with protease inhibitors, see co-immunoprecipitation for concentrations) and centrifuged at 13,000 rpm. Supernatants were quantified by the Bradford method (BioRad) and 20 μg of each sample were loaded on a SDS-PAGE gel

for Western blotting with anti-RNF8 and anti-β-tubulin for loading calibration (Fig 11A). In another experiment, transfected cells were prepared for fluorescent immunocytochemistry (see above) with anti-RNF8 and Hoechst dye for DNA visualization and analyzed with a confocal microscope (Fig 11B).

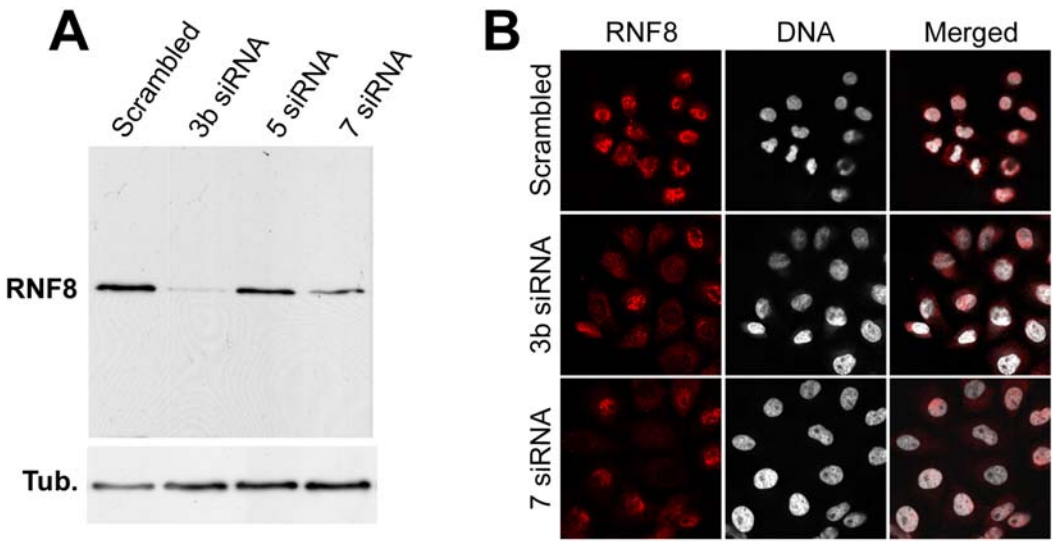

Fig. 11. Generation of small interfering RNA to knock down RNF8 expression. **A**, Western blot analysis of HeLa double transitory transfected with 50nM siRNA. siRNA treatments were performed in two rounds of transfection, separated by 48h. **B**, Immunocytochemistry analysis of double transfected HeLa cells with the corresponding siRNA. Nuclei were counterstained for DNA with Hoechst 33258.

5. Cell synchronization

Cells were arrested at the G_1-S boundary by double thymidine block (Sancho et al., 1998a). Preconfluent cells were incubated for 16 h with medium containing 2 mM thymidine, followed by a 9-h incubation with fresh medium

containing 24 µM deoxycytidine and a second incubation in medium with 2 mM thymidine for 16 h. Arrested cells were allowed to re-enter the cycle by washing away the blocking medium and incubating the cells with medium containing 24 µM deoxycytidine. At 1-h intervals, cells were washed with PBS and processed for further analysis.

6. Flow cytometry

The effects of GFP-tagged forms of RNF8, siRNA, as well as cell cycle arrest and progress after double thymidine block were monitored by flow cytometry analysis of propidium iodide-stained samples. For this, cells were harvested by trypsinization, washed twice with phosphate-buffered saline (PBS), resuspended in 1% bovine serum albumin in PBS 20 mM EDTA (BSA-PBS-EDTA), and fixed in 70% ethanol at -20 ºC for at least 1 h. Fixed cells were washed three times with 1% BSA-PBS-EDTA, incubated with RNase A (1 mg/ml; Promega, Madison, WI) at 37 ºC for 1 h, and stained with propidium iodide (0.1 mg/ml). DNA content was determined on as red fluorescence on a Coulter Epics XL flow cytometer (Coulter, Miami, FL). Single-fluorescence histograms were analyzed with Multicycle (Phoenix Flow System, San Diego, CA).

7. Laser Scan Cytometry (LSC)

For LSC analysis, cells grown on sterile glass coverslips were washed with PBS and fixed for 10 min. with ice-cold 4% PFA in PBS, incubated with 50 mM NH_4Cl for 30 min and permeabilized with blocking buffer (0.1 % saponine, 1% BSA in PBS) for 30 min. Cells were then incubated with RNase A (1 mg/ml in blocking buffer, Promega) at room temperature for 2h and stained with propidium iodide (0.1 mg/ml in blocking buffer). Coverslips were mounted in PBS:glicerol containing 0.1 mg/ml propidium iodide. DNA content was determined as red fluorescence on a Laser Scan Cytometer.

8. RNA extraction, Reverse transcription and Real-time RT-PCR

Total RNA was isolated from transfected or drug treated HeLa cells using the RNeasy kit (Quiagen). Cells were washed with PBS, scrapped in PBS with a cell scrapper, centrifuged and resuspended in guanidine isothiocyanate β-Mercaptoethanol buffer. Samples were homogenized, applied to RNeasy spin column for silica-gel binding, washed three times, and eluded in water. RNA was quantified in a spectrophotometer and 2 μg were used as template for reverse transcription with T4 enzyme (Invitrogene) with random hexamers to obtain cDNA.

Real time PCR was performed by SYBR Green incorporation to determine the expression levels of UBC13, RNF8, KIAA0675, GFP, Caspase-3 and HIP1 in fetal and adult human tissues or in HeLa cDNA's (see Table I for

primer sequences). Collections of human cDNAs were purchased from Clontech. Real-time PCR was performed on an ABI PRISM 7700 instrument (Applied Biosystems, Foster City, CA). Reaction conditions were 95 ºC for 15 min, 40 cycles of 95 ºC for 15 sec, 55 ºC for 30 sec and 72 ºC for 30 sec. All determinations were performed in triplicate. Since relative amplification efficiencies of target and reference samples were found to be approximately equal, the ΔΔCt method was applied to estimate relative transcript levels. Levels of ribosomal S14r amplification were used as an endogenous reference to normalize each sample value of Ct (threshold cycle) and the tissue which showed the lowest expression of the studied genes was used as calibrator for the rest of the tissues. The final results, expressed as n-fold differences in target gene expression were calculated as follows:

$$n_{TARGET}=2^{-[(Ct\ target-Ct\ reference)TISSUE-(Ct\ target-Ct\ reference)LOWEST\ TISSUE]}$$

9. Generation of antibodies

For the generation of polyclonal antibodies, two rabbits were immunized per peptide. Rabbits were inoculated twice, at 4-week intervals, with KLH-conjugated peptides together with Freud's adjuvant, bled and the resultant serum tested for reactivity with KLH-conjugated peptide and peptide free by ELISA assay. When reactivity was high, a third immunization was performed without Freud's adjuvant. Four weeks later, rabbits were bled out and final sera were retested for reactivity and specificity by ELISA and Western blotting.

The synthetic peptides used in our study corresponded to the following sequences: KNKELRTKRKC (RNF8, positions 146 through 155) and GIKAEPDESNARC (UBC13, positions 22 through 33). The reactivities of the final sera were titrated by ELISA (Fig. 10A), and tested for specificity by Western blotting (Fig. 10B).The antibodies were purified by affinity chromatography on the corresponding peptides immobilized on SulfoLink columns (Pierce, Rockford, IL), concentrated with a Centricon concentrator with a cut-off of 30,000 Daltons (Milipore Corporation, Bedford, MA, USA) and quantified both by Bradford's technique (BioRad) or by SDS-PAGE electrophoresis followed by Coomassie brilliant blue staining (Fig. 10D). Finally, the affinity-purified antibodies were tested again for activity by Western blotting on extracts from cells transfected with the appropriate constructs (Fig. 10B), and immunocytochemistry (Fig. 10C). After optimization, purified anti-RNF8 was used at 2.5 μg/ml and anti-UBC13 at 200 ng/ml for Western blotting and, for immunocytochemistry, anti-RNF8 was used at 50 μg/ml and anti-UBC13 at 0.1 μg/ml.

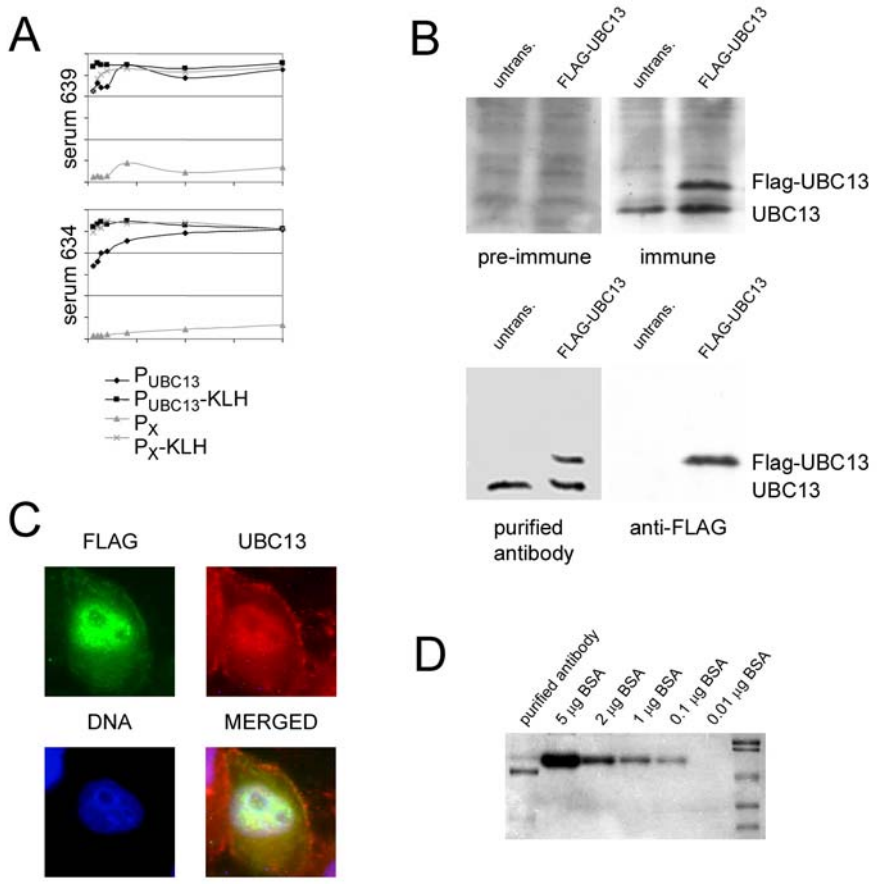

Fig. 10. Generation of rabbit polyclonal antibodies. **A**, ELISA assay using rabbit sera against specific and unspecific peptides. **B**, Western blotting with pre-immune and immune serum from rabbit 634, both endogenous and transfected UBC13 are detected. Western blotting with affinity purified anti-UBC13 and with anit-FLAG are also shown. **C,** Double fluorescent immunocytochemistry on FLAG-UBC13 transfected HeLa cells with anti-FLAG or anti-UBC13, DNA is stained with Hoescht 33258. **D**, SDS-PAGE electrophoresis followed by Coomassie brilliant blue staining of the affinity-purified antibody after concentration.

9. 1. ELISA

96-well Immunosorb plates (Costar) were coated with freshly prepared immunizing and control peptides diluted at 2 μg/ml in PBS pH 8.3 (Phosphate

Buffer Saline: 135.1 mM NaCl, 2.7 mM KCl, 10.4 mM NaH_2PO_4, 1.8 mM KH_2PO_4) overnight at room temperature. After three washes with PBS pH 8.3, the wells were blocked with blocking buffer containing 2% BSA (Bovine Serum Albumin) and 0.1% Tween-20 in PBS pH 8.3 (PBST) in a humid chamber for 2 h. After two more washes with PBST pH8.3, the wells were incubated with a dilution set ranging from 1/50 to 1/2000 of the immune or control rabbit sera in blocking buffer for 2 h. After three more washes the wells were incubated with horseradish peroxidase-conjugated goat-anti-rabbit IgG (Dako, Glostrup, Denmark) at 1/20,000 in blocking buffer for 2 h. After three washes with PBST pH 8.3 and one wash with PBS pH 8.3 the wells were incubated with OPD (SIGMA), a colorigenic substrate, for 30 min in the dark. 3 M HCl was used to stop the reaction and the plates were read at 492 nm in a plate spectrophotometer.

9. 2. Purification of antibodies by affinity chromatography

Peptides were freshly diluted at 5 mg/ml in PBS, and were immobilized on SulfoLink® Coupling Gel Columns for 15 min at room temperature by rocking and a further 30 min without shaking. Iodoacetyl groups on the SulfoLink® Coupling Gel reacts specifically with free sulfhydryls resulting in a covalent immobilization of peptides. All immunizing peptides were designed to contain one cysteine residue available for this reaction. To determine coupling efficiency to the column, both the original peptide solution and eluted solution were checked for 280 nm absorbance. When more than 70% of the peptide was

coupled, columns were blocked for 30 min with 0.05 M cysteine-containing blocking buffer, washed with PBS three times and incubated for 1 h with 1.5 ml of immune serum at room temperature. The column was washed twice with PBS and eluted with 100 mM glycine pH 2.8. 0.5 ml fractions were collected and immediately neutralized with 1 M Tris HCl pH 9. Elution of immunoglobulin molecules was monitorized by absorbance at 280 nm. The fractions with peack absorbance readings were pooled and dialyzed against phosphate-buffered saline (PBS) for 20 h at 4 ºC.

9. 3. Coomassie brilliant blue staining

Samples were prepared with Laemmli sample buffer (100 mM dithiothreitol, 50 mM TrisCl pH 6.8, 2% SDS, 0.1% bromophenol blue, and 10% glycerol), boiled for 5 min. and separated by SDS-polyacrylamide together with a rang of concentrations of bovine serum albumin (BSA). Gels were simultaneously fixed and stained with Coomassie Brilliant Blue (BioRad) diluted in methanol: glacial acetic acid (30:5) for at least 1 h at room temperature, and washed several times with a methanol:glacial acetic acid solution until bands could clearly been visualized.

10. Western blotting

Cells were washed with PBS, lysed in Laemmli sample buffer (100 mM dithiothreitol, 50 mM TrisCl pH 6.8, 2% SDS, 0.1% bromophenol blue, 10% glycerol), boiled for 5 min. and 100 μg of lysate, the protein concentration was determined using the Bradford reagent (BioRad), and samples were electrophoresed by SDS-PAGE (Running buffer contained 25 mM Tris, 190 mM glycine and 1% SDS). After electrophoresis, proteins were transferred electrophoretically onto PVDF membranes (transfer buffer 25 mM Tris, 190 mM glycine and 20% methanol) for 60 min. at 350 mA constant amperage at 4 ºC. Blots were washed, blocked with 5% defatted dry milk in TBST (10 mM Tris-HCl, pH 7.5, 150 mM NaCl, 0.1% Tween-20) or PBST (135.1 mM NaCl, 2.7 mM KCl, 10.4 mM NaH_2PO_4, 1.8 mM KH_2PO_4, and 0.1%Tween-20), incubated overnight with primary antibody diluted in blocking buffer at 4 ºC with shaking, washed in TBST or PBST three times for 10 min. and incubated for 1 h with horseradish peroxidase-conjugated secondary antibody diluted in blocking buffer. After final washes in TBST or PBST (three washes of 10 min.), membranes were incubated with a chemiluminescent substrate (Amersham), wrapped in plastic sheets and exposed to autoradiographic film. For sample normalization, tubulin or actin content was determined by incubating the membranes with a mouse monoclonal anti-β-tubulin antibody (Sigma) (working concentration 4 μg/ml) or goat-anti-actin (Santa Cruz) (working concentration 2 μg/ml). Relative protein mass was determined with the aid of pre-stained protein markers (BioRad, Hercules, CA), that were electrophoresed and transferred simultaneously with the samples. Anti-SUMO antibody was purchased from

Zymed Laboratories (San Francisco, CA) and used for Western blotting experiments at 1 μg/ml. Anti-caspase-8 was obtained from Pharmingen (San Diego, CA) (working concentration 0.5 μg/ml) and anti-caspase-3 from Cell Signaling (Beverly, MA) (working concentration 1/500 from the stock). Anti-cyclin B1 antibody was from Transduction Laboratories and used at 1 μg/ml. For the determination of PLK1 levels in cells transfected with wild-type and mutant GFP-RNF8, GFP-expressing living cells were sorted in a Cytomation MoFlo cell sorter (Fort Collins, CO). A threshold for GFP positivity was established using untransfected cells as a reference. Sorted GFP-positive cells were directly transferred to tubes containing culture medium, centrifuged, and the pellets lysed and boiled in Laemmli sample buffer. Western blotting of these samples was performed with an anti-PLK1 monoclonal antibody (Upstate, Waltham, MA) (working concentration 2 μg/ml) on extracts from 1.75 x 10^5 cells per condition (control or transfected cells), and further normalized by determining the expression levels of β-tubulin and UBC13 with the corresponding specific antibodies.

11. Immunocytochemistry

Cells grown on sterile glass coverslips were washed with PBS and fixed with cold 4% paraformaldehide in PBS (PFA), incubated with 50 mM NH_4Cl and permeabilized with blocking buffer (0.1 % saponine, 1% BSA and 1/40 normal goat serum). The fixed and permeabilized cells were incubated with primary antibodies for 2 hours at room temperature in a humid chamber, washed 3

times with PBS, and incubated for a further 1 hour with secondary antibody diluted in blocking buffer in a humid chamber protected from the light. Proteins carrying a Flag epitope were detected with a mouse anti-Flag M2 antibody (Sigma) at 20 μg/ml or rabbit anti-Flag polyclonal anti-body (Sigma) at the same concentration and anti-mouse FITC or TRITC antibodies (Sigma) diluted 1/400 or 1/200 from the stock solution. Proteins caring HA were detected with a rat anti-HA monoclonal antibody (Roche) at 2 μg/ml for 2 h followed by incubation with biotinilated anti-rat immunoglobulin antibody (Dako) at 1/400 from the stock solution for 45 min and streptavidin-ALEXA 488 (Molecular Probes, Eugene, OR) at 1/200 from the stock solution for 30 min. For the detection of β-tubulin, a mouse monoclonal antibody (Sigma) was used at 40 μg/ml, followed by incubation with goat anti-mouse IgG-FITC (Sigma) or anti-mouse Alexa 546 (Molecular Probes) at 1/300 from the stock solution. Anti-cyclin B1 antibody was from Transduction Laboratories and used at 2 μg/ml, anti-cyclin D1 from Santa Cruz Biotechnology (Santa Cruz, CA) at 5 μg/ml, and anti-PLK1 from Upstate at 20 μg/ml. Anti- PML and anti-PCNA were both purchase from Santa Cruz and both used at 2 μg/ml, followed by incubation with anti-mouse FITC. For the detection of endogenous RNF8 and UBC13, specific affinity-purified rabbit antibodies were used at 50 μg/ml and 0.1 μg/ml respectively, followed by incubation with goat anti-rabbit IgG-TRITC (Sigma) at 1/200 from the stock. Cell nuclei were stained either with Toto-3 iodide (Molecular Probes) at 1 μg/ml, incubated together with the secondary antibody for 1 h, or Hoechst 33258 (Sigma) at 5 μg/ml incubated for 10 min. diluted in blocking buffer after the secondary antibody. After processing, samples were mounted in Immuno-Fluore Mounting Medium (ICN, Costa Mesa, CA). Samples were observed in a

Leica DMLB fluorescent microscope (Wetzlar, Germany), and confocal images were captured in a Leica TCS 4D microscope.

For the determination of apoptotic cells based on morphologic criteria, cells were transfected with GFP-RNF8^{WT} or GFP-RNF8^{C403S}, and stained for DNA with Hoechst 33258. In some experiments, cells were also stained for either cyclin B1 or cyclin D1 as above, to detect cells in mitosis or in G1, respectively. Cells were considered apoptotic only if they showed clearly condensed or fragmented nuclei and had an irregular cellular outline. At least 200 cells were counted in 3 independent experiments. Untransfected (GFP-negative) cells in the same experiments were used as controls. For the evaluation of mitotic bridges, transfected cells were stained for DNA and β-tubulin, and the frequency of cells containing mitotic bridges was determined for GFP-positive and GFP-negative cells. Mitotic bridges were defined as morphologically detectable (visible by transmission microscopy) cytoplasmic bridges that spanned two cells, onto which tubulin-containing bundles converged from each of the two contiguous cells. For RNF8 localization in PML bodies, samples were stained with anti-RNF8 and anti-PML or anti-PCNA followed by confocal analysis.

12. Co-immunoprecipitation

Transfected cells were washed twice with PBS and lysed with cell lysis buffer (50 mM Tris HCl, pH 7.5, 100 mM NaCl, 1% Triton X-100 and protease inhibitors: 2 μg/ml aprotinin, 2 μg/ml leupeptin, 2 μg/ml pepstatin and 50 μg/ml

PMSF). Lysates were precleared for 30 min with Sepharose and incubated with matrix-bound anti-Flag antibody (Sigma) or Sepharose for 3 h at 4ºC. The matrix was washed 3 times with lysis buffer and the immune complexes eluted by boiling in Laemmli sample buffer. Samples were electrophoresed by SDS-PAGE, transferred to PVDF membranes and incubated sequentially with mouse anti-Flag M2 monoclonal antibody (Sigma) at 10 μg/ml and goat anti-mouse IgG-peroxidase (Dako) at a 1/2000 dilution, or rat anti-HA monoclonal antibody (Roche, Mannheim, Germany) at 200 ng/ml and goat anti-rat IgG-peroxidase (Dako) at a 1/2000, followed by ECL detection (Amersham).

For RNF8-HIP1 co-immunoprecipitations, phosphatase inhibitors were added to the lysis buffer (0.5 μM okadaic acid, sodium 100 μM ortovanadat, 10 mM β-glycerol phosphate and 25 mM sodium fluoride).

13. *In vivo* ubiquitylation assays

Cells co-transfected with constructs for the expression of His-tagged proteins and the wild-type or mutant ubiquitin constructs were washed twice with PBS and scraped in 6 M guanidine buffer at room temperature. Lysates were incubated in batch with ProBond matrix (Invitrogen) for 1 h at room temperature, transferred to a column and washed twice with denaturing binding buffer at pH 7.8, twice with denaturing wash buffer at pH 6.0 and twice with denaturing wash buffer at pH 5.3. Columns were eluted with 25 mM Tris-HCl, pH 7.5, and 200 mM imidazol. Eluted samples were boiled in Laemmli sample buffer, separated electrophoretically on SDS-PAGE, and transferred to PDVF

membranes. Membranes were processed as described earlier, blotted with anti-HA, and reactions detected by ECL chemiluminescent assays (Amersham).

1. First objective

To identify molecular partners of the K63 ubiquitin conjugating enzyme UBC13 using the yeast two hybrid technique and to confirm the interaction in mammalian cultured cells.

1.1. **Yeast two hybrid screening for UBC13 interaction partners**

After our laboratory discovered the UEV proteins (Sancho et al., 1998b), and the subsequent finding by the laboratory of Cecile Pickart of their role in conjugating K63-linked polyubiquitin chains (Hofmann and Pickart, 1999), we decided to search for molecular partners of UBC13 which is the catalytic subunit of the UBC13-UEV1A heterodimer responsible for K63-linked polyubiquitylation. This was done by a relatively unbiased approach by applying the yeast two hybrid technique (Fields and Song, 1989).

To generate a screening probe, UBC13 was cloned in frame with the Gal4 DNA binding domain and used as bait for a screening of a human fetal brain cDNA library into the AH109 yeast strain. Out of 1.5 x 10^6 independent clones screened, we confirmed interactions with UBC13 for 19 clones, corresponding to 3 distinct proteins (Figure 12A). Screenings of over 1 x 10^6 clones are considered sufficient for testing all the possible interacting proteins in the library (Yeast two hybrid protocol, Clontech).

The first interaction partner was UEV1 (16 clones), which thus provided a good control of the specificity of the interactions yielded by the screening. The second partner of interaction with UBC13 was a partial fragment of RNF8 (2 clones), a protein containing a RING finger domain. After we had performed our screening others have shown that this protein interacts with other E2's (Ito et al., 2001). The third interaction partner corresponded to a fragment of the KIAA0675 protein, which was later identified as hRUL138 and DZIP3 (Kreft and Nassal, 2003; Moore et al., 2003) and which also contains a RING finger

domain (one clone). Both RNF8 and hRUL138/DZIP3 interact with UBC13 through their RING finger domains since the library clones contained the whole RING and only part of the coiled-coil domain, consistent with the reported interactions of UBC13 with other proteins bearing RING finger domains such as TRAF2 and TRAF6 (Deng et al., 2000b), RNF5 (Didier et al., 2003) in humans and one yeast protein, Rad5p (Ulrich and Jentsch, 2000).

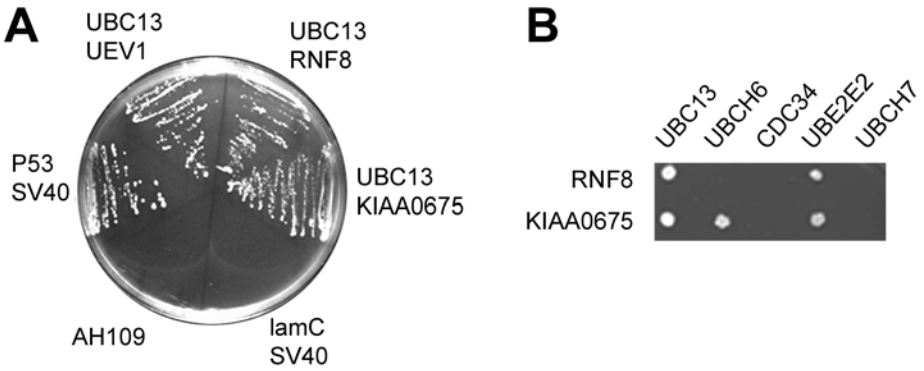

Fig 12. UBC13 interactors found by yeast two-hybrid assays. **A**. A human fetal brain cDNA library was screened for interactions with UBC13. Negative controls included the untransfected strain AH109 and cells co-transfected with laminin C and SV40 large T. As a positive control for interaction, cells were co-transfected with p53 and SV40 large T. The symbols for the interacting proteins are shown adjacent to each of the sectors of the plate. **B**. Yeast two-hybrid interactions of RNF8 and KIAA0675 with several E2 enzymes, as indicated.

As described in Introduction, RING finger domains define a distinct category of E3 ubiquitin ligases. These domains are organized in a loop-helix-loop structure which coordinates two Zn^{2+} ions in a *cross-brace* organization thanks to eight conserved residues which are either cysteines or histidines (Borden, 2000). They can be classified as either RING-H2 or RING-HC depending on whether they contain a histidine of a cysteine at position 4 of the

Zn-coordinating residues. Interestingly, RNF8 has a RING-HC while KIAA0675 has a RING-H2 configuration. Considering that they both have the ability to bind UBC13, it seems that one can not generalize whether UBC13 could interact with one RING finger protein or not only by looking at its RING structure.

1. 2. RNF8 related proteins

An analysis of the primary sequence of full-length RNF8 showed that, in addition to its RING finger domain, located at the carboxy terminus of the protein (positions 402-440), it contains a coiled-coiled region adjacent to the RING finger domain (positions 259-390) and a forkhead-associated (FHA) domain near its amino terminus (positions 45-109) (Fig. 13). FHA domains are structural motifs that recognize phosphopeptides in particular sequence contexts (Durocher et al., 2000; Liao et al., 1999). In addition to RNF8, only four other proteins contain a combination of a RING finger domain and a FHA domain (Fig. 13): In metazoans, CHFR, a mitotic checkpoint regulator (Kang et al., 2002; Seong et al., 2002); in budding yeast, ScDma1p and ScDma2p, both proteins involved in proper spindle positioning at mitosis probably by ensuring timely Mitotic Exit Network (MEN) activation in telophase (Fraschini et al., 2004); and in fission yeast, SpDma1p, a regulator of the septation initiation network (SIN) (Guertin et al., 2002b; Moore et al., 2003). Human RNF8 has orthologs in rodents, the amphibium *Xenopus laevis* and the fish *Danio rerio* (zebrafish), but no unambiguously conserved proteins are present in the insects *Drosophila melanogaster* and *Anopheles gambiae* or the nematode

Caenorhabditis elegans (Fig. 14). CHFR has recently been shown to interact with UBC13, and to function as a E3 ligase for the K63 polyubiquitylation of substrates, including itself (Bothos et al., 2003). However, the yeast proteins SpDma1p ScDma1p and ScDma2p have not been explored with regards to their possible interaction with UBC13, so far.

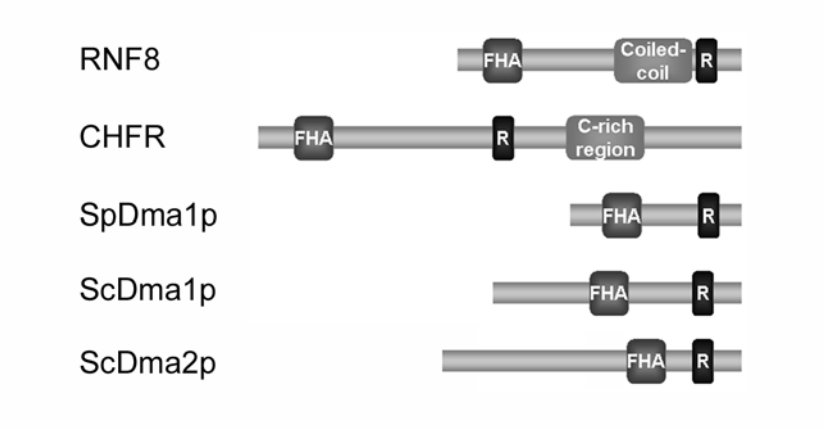

Fig 13 Schematic depiction of the domain architecture of proteins bearing one forkhead-associated (FHA) domain and a RING finger domain (R). RNF8 is one of these five proteins in all kingdoms, along with CHFR in metazoans, SpDma1p in *Schizosaccharomyces pombe* and ScDma1p and ScDma2p in *Saccharomyces cerevisiae*. RNF8 also contains a predicted coiled-coil region at the amino end of its RING finger domain. The yeast proteins SpDma1p and ScDma1/2p are not known to interact with UBC13. All predictions were performed on two domain prediction servers, SMART (http://smart.emblheidelberg. de/) and NCBI Conserved Domain Search (http://www.ncbi.nlm.nih.gov/Structure/cdd/wrpsb.cgi).

Fig. 14. ClustalW aligment of RNF8 orthologs from several organisms. Mm stands for *Mus musculus*, Rt for *Rattus norvegius*, Xl for *Xenopus laevis*, Dr *Danio rerio* and Hs for *Homo sapiens*.

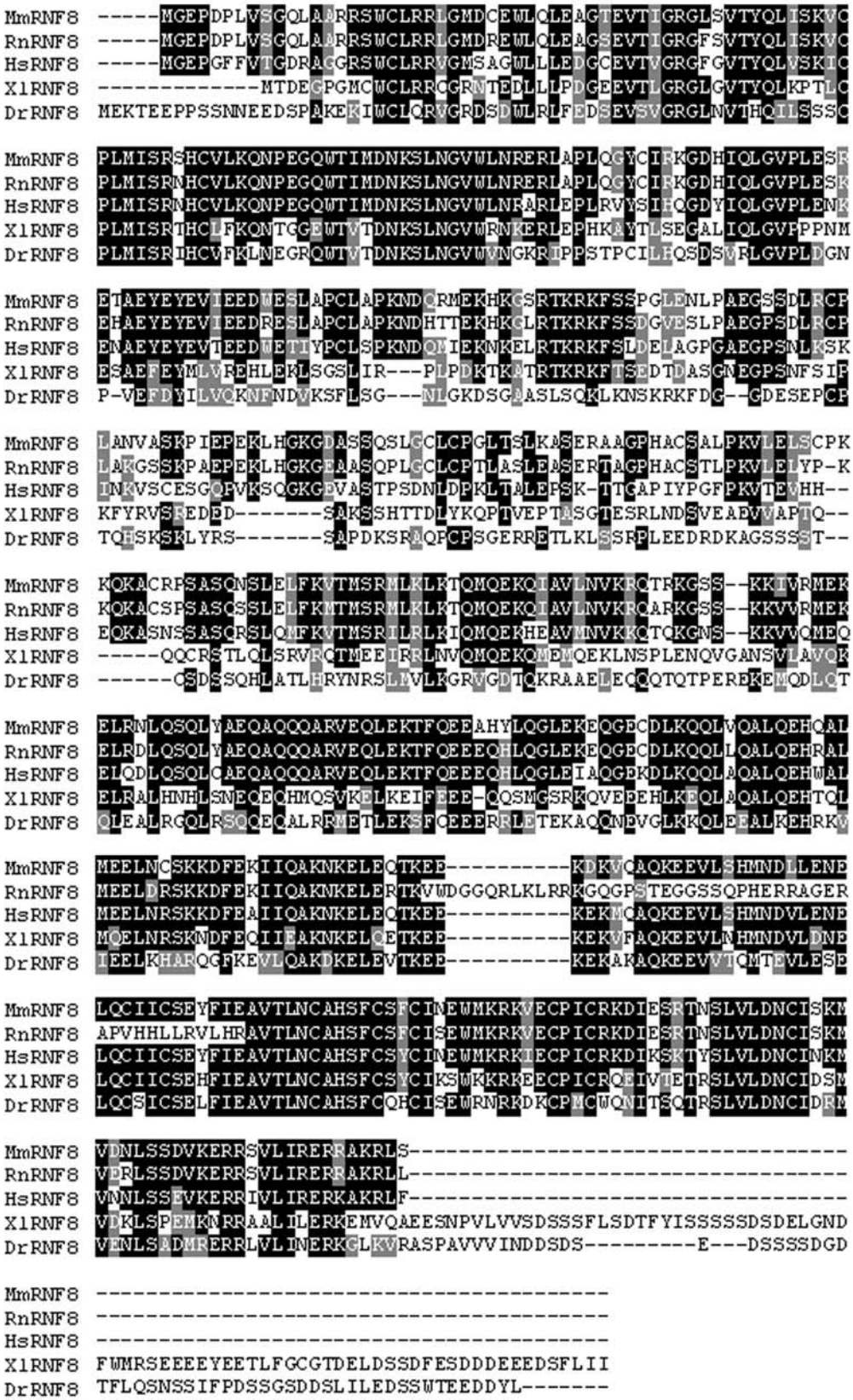
MmRNF8
RnRNF8
HsRNF8
XlRNF8
DrRNF8

1. 3. KIAA0675 related proteins

The second protein found to interact in the yeast two-hybrid screening with UBC13, KIAA0675, corresponds to a protein that has been designated as hRUL138 (Kreft and Nassal, 2003) or DZIP3 (Moore et al., 2003). This large protein has been recently reported to be cytoplasmically located, possibly in the endoplasmatic reticulum, to have a ubiquitin ligase activity and to bind to hepatitis B viral RNA (Kreft and Nassal, 2003) and, independently, to bind to DAZ, a protein that regulates germ cell development (Moore et al., 2003). KIAA0675 bears, in addition to a RING finger domain located near its carboxy terminus (residues 1148 to 1187), a region with a predicted coiled-coil structure (approximately from residues 784 to 905), and four tetratricopeptide repeats (one located approximately between positions 21 and 68, and two to three repeats predicted between positions 126 and 349), loosely conserved motifs that engage in protein-protein interactions (Das et al., 1998; Goebl and Yanagida, 1991; Lamb et al., 1995) (Fig 15A). The motif composition and architecture of KIAA0675 is very similar to that of a second protein known as TTC3 (Tsukahara et al., 1996) or DCRR1 (Eki et al., 1997), that bears tricopeptide repeats, coiled-coiled regions and a carboxy-terminal RING finger domain with in the same order as KIAA0675. The gene for TTC3 is located on chromosome 21q22.2, at the Down syndrome critical region 1. The gene for KIAA0657 is positioned on chromosome 3q13.13. The relationship between KIAA0675 and TTC3 is underlined by the fact that the RING finger protein domains on both proteins share a high degree of similarity to each other (Fig.

15B). Human KIAA0675 and TTC3 have homologues in rodents, but not in fish, insects or nematodes (Fig 16).

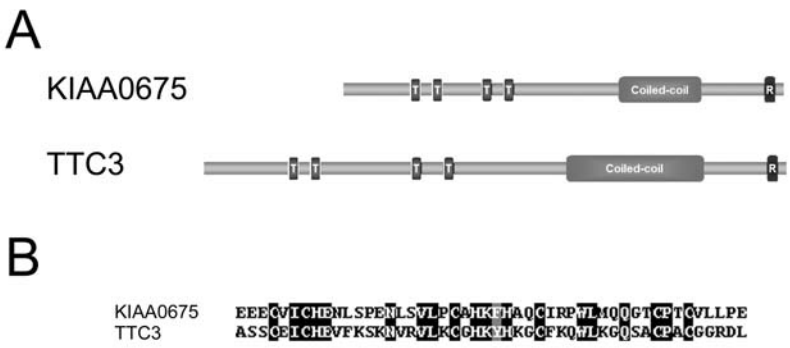

Fig. 15. A. Schematic depiction of the domain architecture of KIAA0675 and TTC3. KIAA0675 bears a carboxyterminally placed RING finger domain, several tetratricopeptide repeats (T) and a predicted coiled-coil region, like TTC3. All predictions were performed with two domain prediction servers, SMART (http://smart.emblheidelberg. de/) and NCBI Conserved Domain Search (http://www.ncbi.nlm.nih.gov/Structure/cdd/wrpsb.cgi). In the prediction of KIAA0675 tetratricopeptide repeats, prior alignments were performed with ClustalW and BLASTP with segments of TTC3 predicted to contain these motifs, and these subsequently used to search the motif databases in SMART and PFAM (http://pfam.wustl.edu/). **B**. Alignment of KIAA0675 and TTC3 RING finger domains.

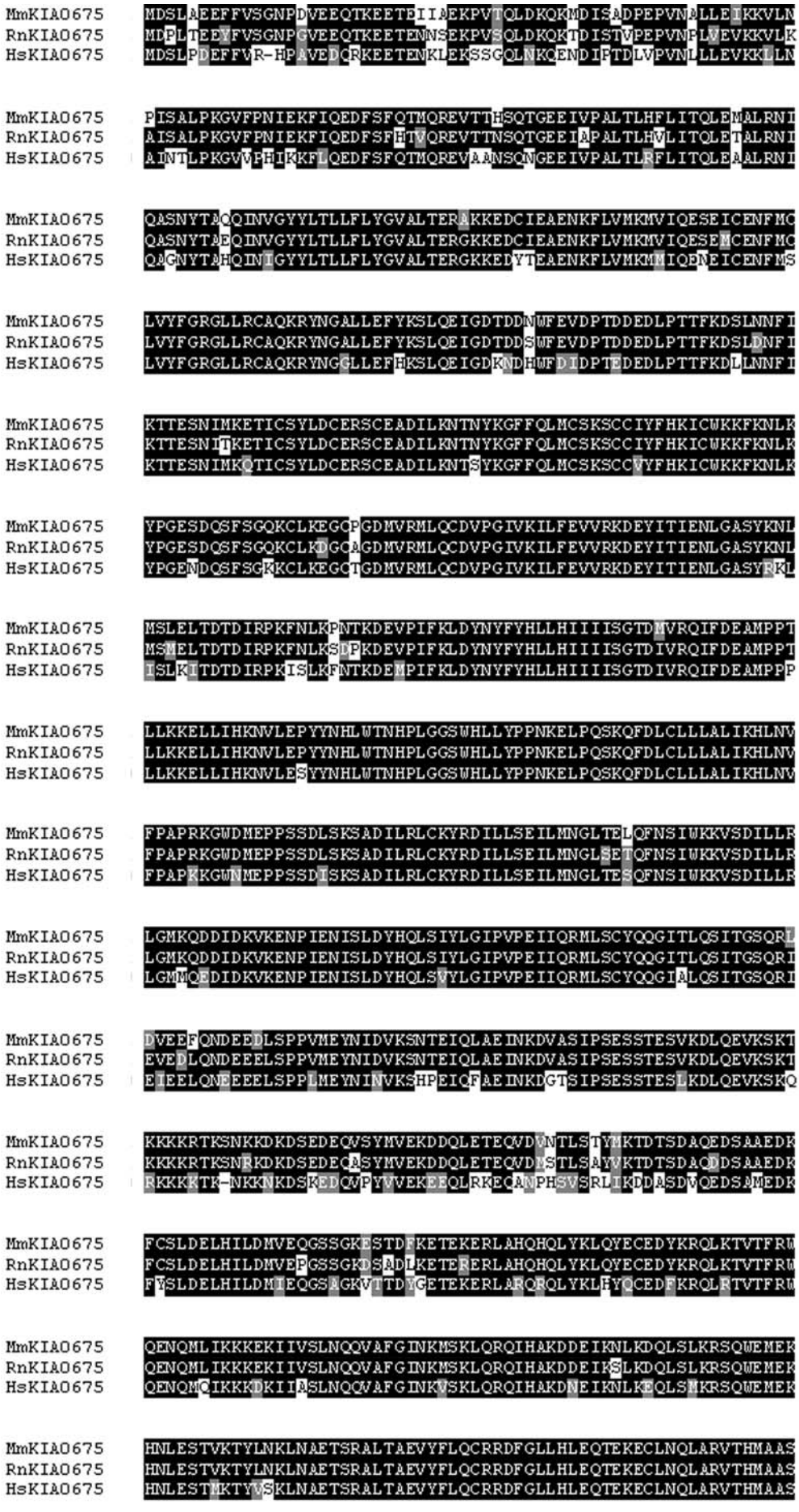
MmKIAO675
RnKIAO675
HsKIAO675

Fig. 16. ClustalW aligment of KIAA0675 homologues. Mm stands for Mus musculus, Rt for Rattus norvegius and Hs for Homo sapiens.

1. 4. Other E2's that interact with RNF8 and KIAA0675

Since RNF8 had been shown to recruit the ubiquitin conjugating enzyme UBE2E (Ito et al., 2001), we decided to test if KIAA0675 was also able to bind UBC other than UBC13 by yeast two hybrid assays (Fig 12B). Our experiments show that the RING finger domain from RNF8 interacts with UBC13 and UBE2E2, while the RING finger domain from KIAA0675 interacted with UBC13, UBE2E2 and UbcH6. It is likely that both RNF8 and KIAA0675 can function as E3's for the elongation of more than one class of polyubiquitin chains since they bind more than one UBC protein. Furthermore, but not unexpectedly, these experiments also show that a given E2 can interact with more than one RING finger domains, and, conversely, that a given RING finger domain has the capacity to interact with more than one E2. The two classes of interaction modules, RING finger domain and E2, show a pattern of mutual interactions that is specific for a particular interaction partner.

1. 5. Confirmation of the UBC13-RNF8 interaction in mammalian cells

We next proceeded to confirm the interaction of both RING finger proteins, RNF8 and KIAA0675, with UBC13 by means of co-

immunoprecipitation assays and subcellular colocalization in mammalian cells. Unfortunately, and despite several attempts, we were not able to express tagged forms of KIAA0675 protein in cultured mammalian cells and hence decided to focus on the characterization of the RNF8-UBC13 interaction.

RNF8 associated with UBC13 in mammalian cells *in vivo*, as shown by co-immunoprecipitation experiments in Cos-7 cells co-transfected with pHA-RNF8 and pFlag-UBC13 (Fig. 17A). This interaction required the integrity of the RING finger domain of RNF8, since a point mutation to alanine of the cysteine residue at position 403, one of the seven cysteines required for the coordination with Zn atoms in this class of RING finger domains (Borden and Freemont, 1996; Joazeiro and Weissman, 2000), resulted in a complete loss of the ability of RNF8 to bind to UBC13 (Fig. 17A). Work from others has also shown that the integrity of the RING finger domain of RNF8 is necessary for its interaction with E2's other than UBC13 (Ito et al., 2001). HA-tagged wild-type RNF8 was detected exclusively in the cell nucleus when analyzing cells in standard culture conditions (Fig. 17B). In contrast, the RING finger mutant form of RNF8 ($RNF8^{C403S}$) was seen in a cytoplasmic localization that excluded the nucleus in a variable proportion of transfected cells (Fig. 17B). Transfected UBC13 could be detected in several subcellular localizations, which included the cell nucleus, the plasma membrane and the cytoplasm (Fig. 17B). Upon co-transfection with HA-RNF8, the signal for nuclear localization of UBC13 was enhanced, with a corresponding decrease in the intensity of other subcellular localizations (Fig. 17C). This increase in the relative intensity of nuclear UBC13 was not seen when the co-transfection was done with the mutant $RNF8^{C403S}$. These observations suggest the occurrence of a nuclear retention of UBC13 in

association with high levels of RNF8, which is dependent on its interaction with the RING finger domain of the latter protein.

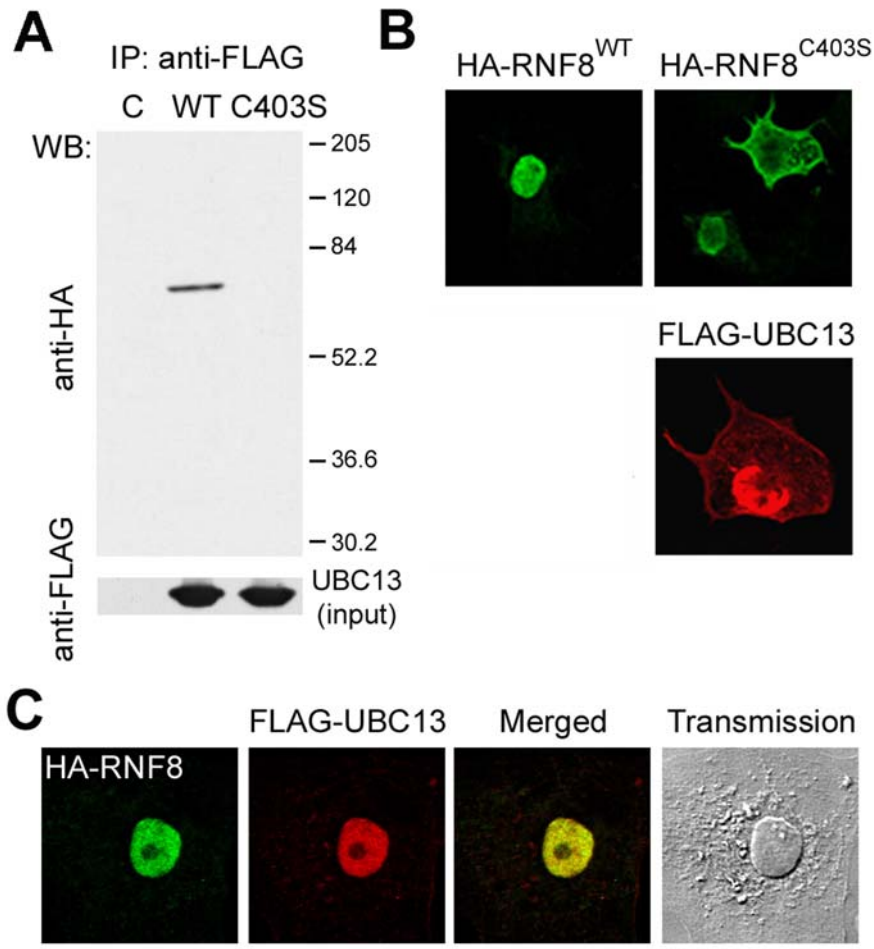

Fig. 17. Interaction between RNF8 and UBC13 in mammalian cells. **A**, UBC13 pulls down wild-type RNF8, but not a variant bearing a mutation on its RING finger domain (RNF8^{C403S}). Extracts of Cos-7 cells co-transfected with FLAG-UBC13 and either wild-type (WT) or mutant (C403S) HA-tagged RNF8 were immunoprecipitated with anti-FLAG and blotted with either anti-HA for the detection of HA-RNF8, or anti-FLAG to allow for comparison of input cotransfected FLAG-UBC13 (bottom). **B**, Subcellular localizations of wild-type and mutant (C403S) HA-RNF8 and of FLAG-UBC13 in transfected Cos-7 cells stained with anti-HA or anti-FLAG. **C**, Immunolocalization of co-transfected HA-RNF8 and FLAG-UBC13.

Although UBC13, RNF8 and KIAA0675 were already known proteins, there was little information in the literature about what can be called “general protein knowledge”. Under this name one can include data such as subcellular localization in different systems, gene expression, chromosomal mapping and so on. Therefore we decided to fulfill this “general knowledge” by generating our own data and thus fulfill our first objective. Such objective could be stated as follows: To examine the tissue range of expression of UBC13, RNF8 and KIAA0675 in human tissues, to study the subcellular localization and cell-cycle expression of endogenous UBC13 and RNF8, and analyze RNF8 expression under several drug treatments.

1. 6. Tissue expression of UBC13, RNF8 and KIAA0675

Real-time RT-PCR was performed to asses the levels of expression in human tissues of UBC13, RNF8 and KIAA0675. In general, RNF8 is widely expressed both in adult and fetal tissues. In human fetal tissues, expression of RNF8 transcripts is highest in brain, thymus and liver, while in adult tissues, expression is very high in brain, testis, and kidney and low in ovary and peripheral blood (Fig. 18). As reported by others (Kreft and Nassal, 2003), expression levels of KIAA0675 is generally low in all tissues tested, showing a tissue distribution that is similar to that of RNF8, with the highest levels in brain and thymus in fetal tissues, and in brain, testis and kidney in adult tissues (Fig. 18). UBC13 is expressed at high levels in a wide range of tissues. The highest levels of expression of UBC13 in fetal tissues are found in brain, thymus, skeletal muscle and spleen, and in testis and brain in adult tissues (Fig. 18).

Therefore, all three genes are co-expressed at significant levels in several tissues, notably brain and thymus in fetal tissues, and brain, testis and kidney in adult tissues.

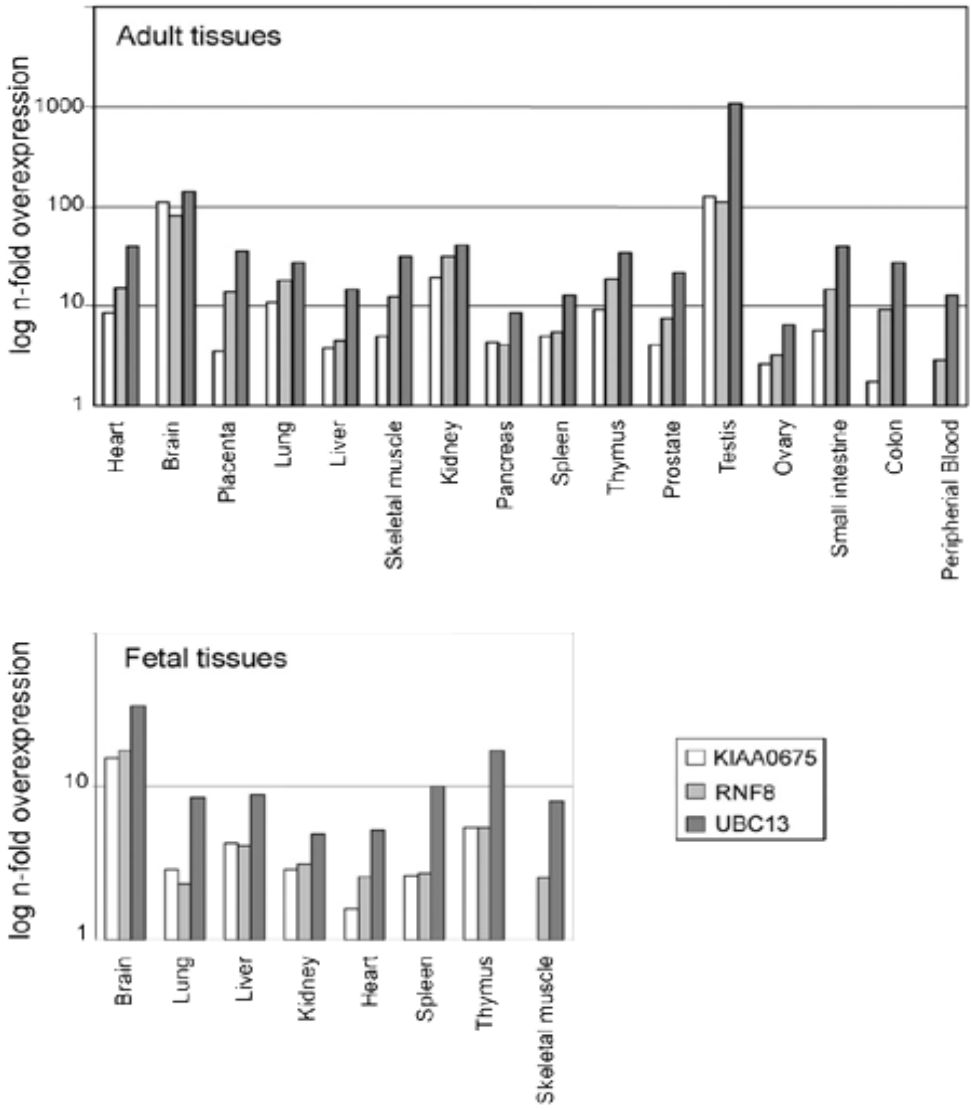

Figure 18. Relative expression levels of the genes for UBC13 and the UBC13-interacting proteins RNF8 and KIAA0675 in normal human adult and fetal tissues, determined by real-time RT-PCR. cDNA collections from adult or fetal tissues were used as templates in Sybr-Green PCR reactions with specific primers, and the C_T levels were determined in real time on a ABI 7700 instrument (see Materials and Methods). C_T values were normalized in each case against values obtained for the reference gene S14r, and then further normalized against the tissue with the lowest expression levels in each set, adult or fetal.

1. 7. Subcellular localization of endogenous RNF8 and UBC13

In cultured cells, endogenous RNF8 was visualized by immunocytochemistry with our affinity-purified antibody specific for RNF8. As with transfected RNF8, the endogenous protein localizes mainly in the cell nucleus. The endogenous protein showed a dotted pattern (Fig 19A) that is reminiscent to the patterns seen for other proteins present in Promyelocytic Leukaemia (PML) nuclear bodies, although PML nuclear bodies show perhaps a smaller number of dots. These discrete nuclear structures are organized by the sumoylated tumor suppressor PML (Ishov et al., 1999; Salomoni and Pandolfi, 2002; Zohong et al., 2000). Several of its components are also sumoylated including Daxx, involved in transcriptional regulation and apoptosis (Li et al., 2000a; Yang et al., 1997), p53, which localizes in this structures after DNA damage for DNA repair, cell cycle arrest or apoptosis (Carbone et al., 2002; Guo et al., 2000; Rodriguez et al., 1999; Vogelstein et al., 2000b), and CBP, a regulator of transcription (Girdwood et al., 2003). Double fluorescent staining for RNF8 and either PML or PCNA, showed a limited overlap of RNF8 with PML or PCNA, a situation that did not change in different stages of the cell cycle (not shown). However, under DNA damage conditions such as exposure to UV light, etoposide or cis-platinium (Fig 19D), the colocalization of both proteins subtly increased especially in the conditions that had the strongest inducing activity of RNF8 levels (see below). Although PML does not localize to all PML nuclear bodies the partial colocalization of both proteins was too weak to confirm RNF8 localization in those structures.

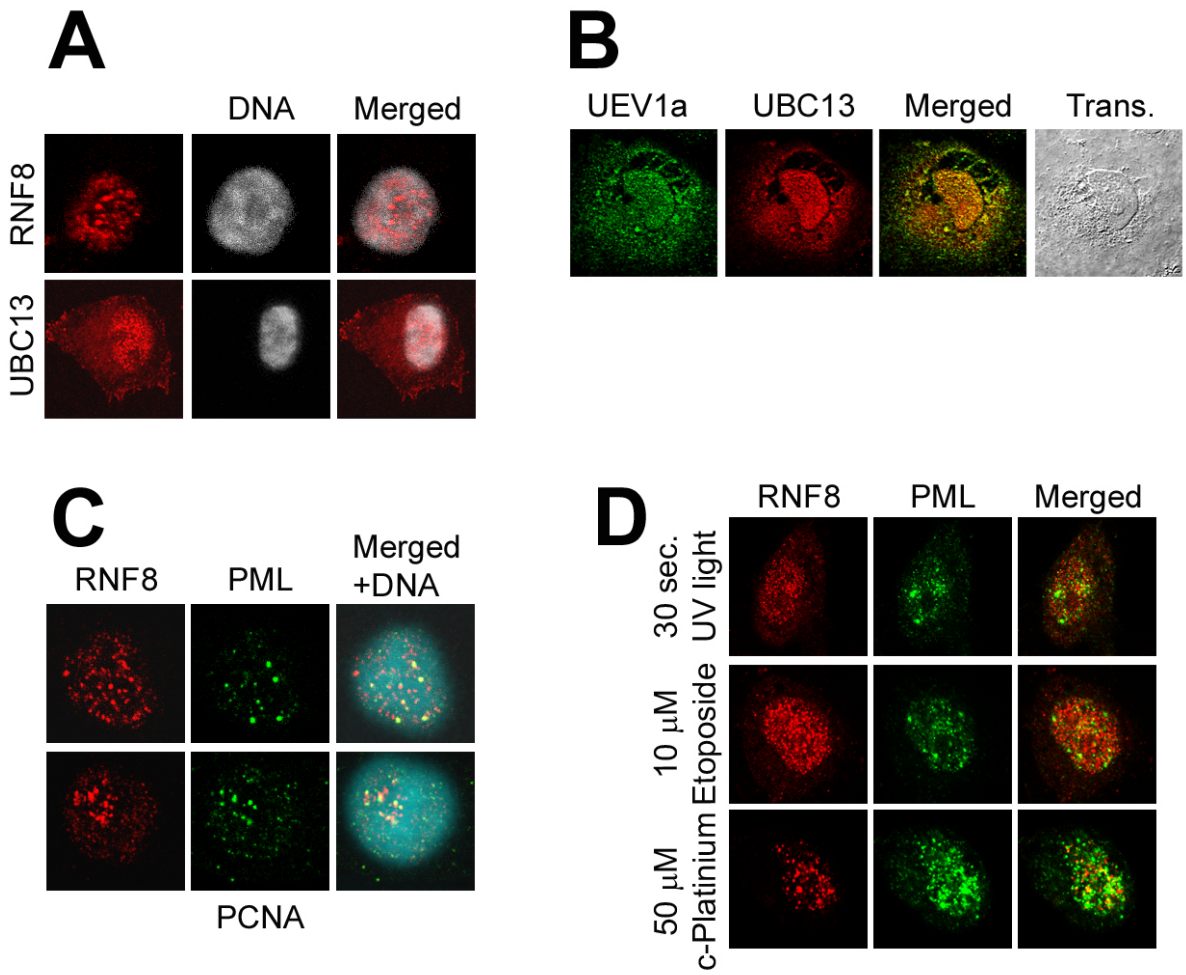

Fig. 19. **A**, Endogenous RNF8 localizes in the cell nucleus with a dotted pattern (top panel). HeLa cells were seeded on glass coverships and RNF8 was detected by immunocytochemistry with specific polyclonal antibodies. DNA was stained with Hoechst 33258. Endogenous UBC13 localizes in the cell nucleus but also in the cytoplasm and in the plasma membrane (down). HeLa cells were treated like above and UBC13 was detected with specific polyclonal antibodies. **B**, Immunolocalization of co-transfected HA-UEV1a and FLAG-UBC13 in Cos 7 cells, the two members of the heterodimer show a good overlap in the signals. **C**, Endogenous RNF8 presents a partial overlap with PML and PCNA in the cell nucleus. RNF8, PML or PCNA were detected immunocytochemicaly with specific antibodies and DNA was visualized by Hoechst staining. **D**, Endogenous RNF8 and PML visualized like in C. HeLa cells were treated with several DNA-damage inducing stimuli such as 30 seconds of UV light, 10 μM Etoposide and 50 μM Cis-Platinium. All images were captured using a confocal microscope.

Endogenous UBC13, also detected with our affinity-purified antibody, was present in several subcellular localizations including the nucleus, the plasma membrane and the cytoplasm (Fig 19A), and so did the transfected protein. The latter localizations would be consistent with UEV1 localizations (Fig 19B) (Thomson et al., 2000) and with the known function of the heterodimeric E2 formed by UBC13 and UEV in signal transduction from cytokine receptors (Deng et al., 2000a; Habelhah et al., 2004; Wang et al., 2001a) and in the regulation of cortical cytoskeletal dynamics and cell motility (Didier et al., 2003).

1. 8. Cell cycle dependent turnover of RNF8

The similarities of RNF8 with CHFR, whose levels are regulated in different phases of the cell cycle (Chaturvedi et al., 2002), and the fact that the levels of endogenous RNF8 oscillated between different cells led us to study possible variations in its expression during the cell division cycle. HeLa cells were synchronized by double thymidine block, released from the block, and analyzed at 1-h intervals for the expression of endogenous RNF8 by immunocytochemistry and Western blotting (Fig. 20). Samples were analyzed in parallel by flow cytometry, to monitor for the enrichment of cells in a given phase of the cell cycle (Fig. 20A). Cells arrested at the G_1-S boundary expressed detectable levels of RNF8, that increased in intensity during the S phase (3 to 4.5 h after release), and continued to rise until the end of the G_2 phase (4.5 – 5 h), until the signal for RNF8 abruptly decreased at approximately 6 h after release from the thymidine block, which corresponds to mitosis (Fig. 20B). RNF8 showed a nuclear localization in G_1 and S, whereas during

prophase, concomitant with nuclear envelope breakdown, RNF8 localized throughout the cell, with a dotted staining pattern (Fig. 20C). The protein was basely detectable in anaphase. In telophase, and coincident with the reestablishment of the nuclear envelope RNF8 localized again in the nucleus and also as discrete dotted patterns in the cytoplasm and plasma membrane. In late telophase, RNF8 localized intensely in the midbody of the tubulin bridge that will be abscised in cytokinesis. After mitosis and during early G_1, expression of RNF8 was reinstated, with a gradual increase in signal upon entering a new cycle (Fig. 20C). It is also important to remark that even though endogenous RNF8 localizes in the cell nucleus, it is usually excluded from chromatin containing regions which show a stronger staining with DNA dyes. In other words, RNF8 does not seem to associate with condensed chromosomes.

Interestingly, while RNF8 was present during S and early G_2 mostly in its usual 55 kDa form, several discrete high-molecular weight forms of RNF8 increased their levels during a very narrow window during mitosis, before a rapid decline in levels of the protein (Fig. 20B). This suggests the occurrence of a covalent modification of RNF8 that takes place immediately preceding the degradation of the protein at the initiation of anaphase. The ladder-like pattern of discrete bands that differ in size by approximately 7-8 kDa, or multiples, with the neighboring bands (Fig. 20B) suggesting that the covalent modification of RNF8 is related to ubiquitylation. Treatment of cells with nocodazole or taxol resulted in increased levels of the higher molecular weight forms of RNF8, supporting that accumulation of covalently modified forms of the protein is associated with mitosis (Fig. 20B).

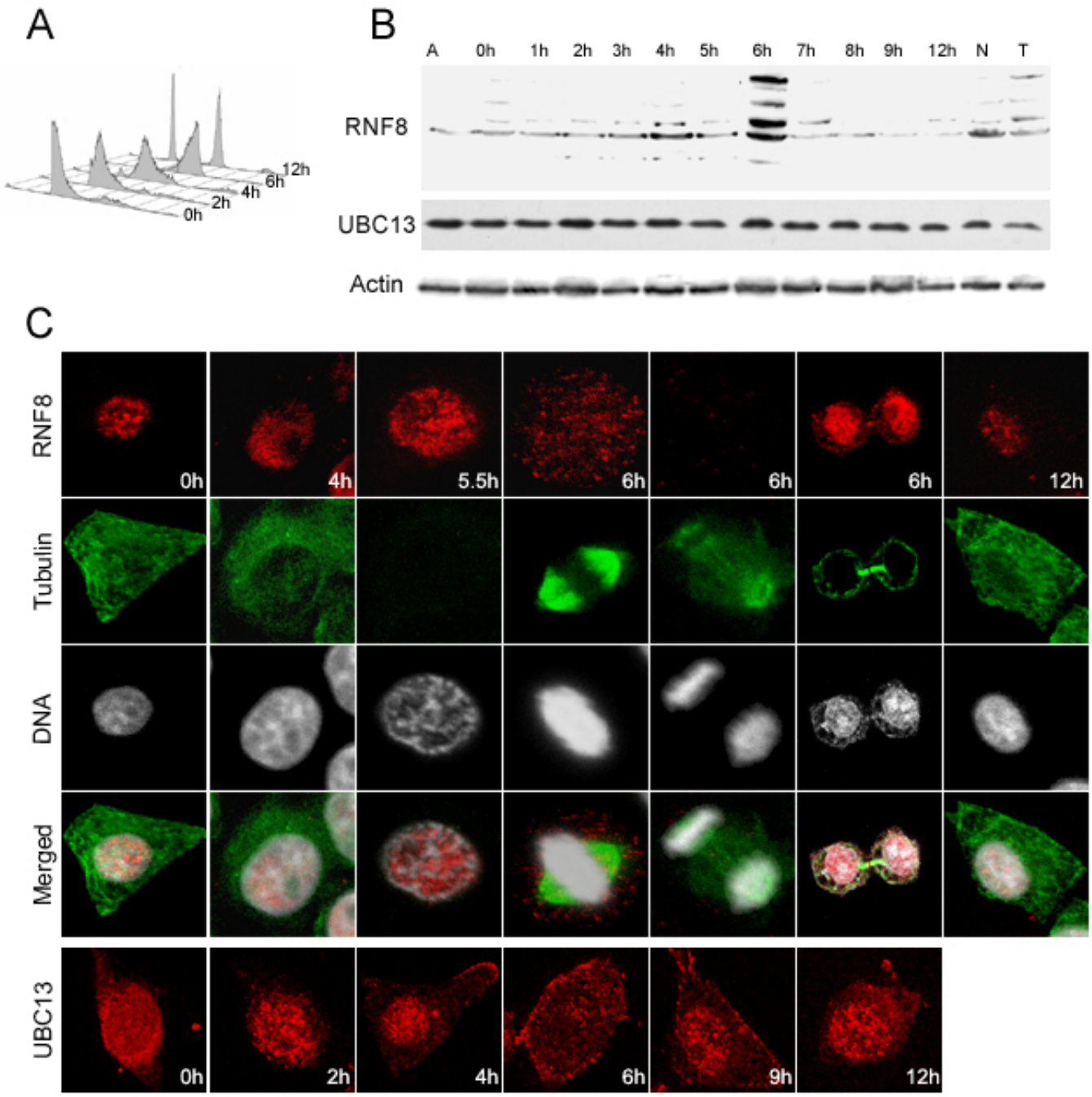

Fig. 20. Cell-cycle dependent modulation of expression of endogenous RNF8. **A**, HeLa cells were synchronized at G1-S by double thymidine block, released from the block and analyzed for flow cytometry at different times after the release. **B**, Cell-cycle dependent turnover of endogenous RNF8 shown by Western blotting with a rabbit antibody specific RNF8 on cell lysates obtained at different times after release from double thymidine block. Middle panel, the same extracts analyzed for UBC13 levels and bottom panel with actin for normalization. *A* stands for asynchronously growing cells, *N* for cells treated for

16 h with nocodazole (0.1 μM), and *T* for cells treated for 16 h with taxol (10 μM). **C**, Cell cycle-dependent associated changes in the expression of endogenous RNF8 shown by immunocytochemical detection with an antibody to RNF8 on HeLa cells fixed at different times after release from double thymidine block. The preparations were stained for RNF8, for β-tubulin with a mouse monoclonal antibody, and for DNA with Hoechst 33258, and analyzed under a Leitz confocal microscope. Cell cycle associated modulation of subcellular localization of endogenous UBC13, shown by immunocytochemistry of HeLa cells with a specific rabbit anti-UBC13 antibody.

In contrast to the cell cycle-dependent modulation in the levels of RNF8 protein, UBC13 levels did not show significant oscillations in association with the cell cycle phases (Fig. 20B). The subcellular localization of UBC13, however, presented subtle variations during the cell cycle (Fig. 20C). The signal for nuclear UBC13 was noticeably stronger during the S phase and mitosis, with a very weak localization elsewhere in the cells. During the G_1 phase there was an increased localization of UBC13 in the cytoplasm and the plasma membrane.

1. 9. RNF8 levels under mitotic arrest inducing drugs

To confirm that endogenous RNF8 is more abundant during mitosis, cells were seeded and treated with nocodazole and taxol in order to induce mitotic arrest, and cell lysates were analyzed by Western blotting with anti-RNF8 (Fig. 20B). Both nocodazole and taxol treatments enhanced the protein expression in comparison with levels of the asynchronous cells.

These data indicate that RNF8 is a protein with a cell-cycle regulated localization and expression, that accumulates in mitosis, more specifically before metaphase, and whose levels are modulated by drugs that activate the mitotic checkpoint. Together, these observations strongly suggest a role of RNF8 in the cell cycle.

2. Second objective

To functionally study UCB interactions with RNF8 and determine if it has a ubiquitin ligase activity.

2. 1. **RNF8 ubiquitin ligase activity**

RNF8 is a RING finger domain protein that interacts with at least two different ubiquitin conjugating enzymes, namely UBE2E2 and UBC13. UBC13 is known to promote K63-linked polyubiquitin chains (Hofmann and Pickart, 1999) while there is no evidence about what kind of polyubiquitin chains promote UBE2E2. In addition, many E3 ligases support self ubiquitylation (Kang et al., 2002; Kreft and Nassal, 2003). Taking both facts in consideration, we decided to test whether RNF8 has a self-ubiquitin ligase activity *in vivo*, and the type of polyubiquitin chains involved.

Therefore, we generated a set of constructs for the expression of HA-tagged wild type and mutant ubiquitin, yielding the mutant constructs UbK48,63R, UbK29,63R and UbK29,48R, each carrying two lysine to arginine mutations at the indicated positions. These positions correspond to the lysine residues on ubiquitin that appear to be predominantly used for the formation of polyubiquitin chains *in vivo* (Pickart, 2001). Consequently, the ubiquitin molecules expressed by transfection of these constructs have only one of these three lysine residues available for isopeptide bond formation during elongation of polyubiquitin chains, at positions 29, 48 and 63, respectively. These constructs were cotransfected in Cos-7 cells either with $pHis_{6}$-$RNF8^{WT}$ or the RING-dead mutant construct $pHis_{6}$-$RNF8^{C403S}$. Extracts from transfected cells were enriched for histidine-tagged proteins by affinity chromatography on Ni-derivatized beads, and the eluted proteins analyzed for modification by the co-transfected ubiquitins by Western blotting with anti-HA antibodies. These

experiments showed that wild-type RNF8, bearing a functional RING finger domain, can be modified by all three mutant ubiquitins, implying the formation of polyubiquitin chains that use predominantly the lysines at positions 29, 48 and 63 (Fig. 21A). In contrast, the mutant RNF8^{C403S}, in which the RING finger is no longer functional and fails to interact with UBC13 (Fig. 17A) or other E2's (Ito et al., 2001), fails to be modified by UbK29,63R and UbK29,48R but is still modified by UbK48,63R (Fig. 21A). We conclude from these observations that RNF8 functions as a self ubiquitin ligase for polyubiquitylation through lysines 48 and 63 of ubiquitin, probably mediated by UBE2E2 and UBC13, respectively. On the other hand, our experiments show that polyubiquitylation of RNF8 with K29-type polyubiquitin chains does not require its own functional RING finger domain, suggesting that this modification of RNF8 is mediated by a different E3, rather than by itself.

To further confirm tat K63-based polyubiquitylation of RNF8 depends on UBC13, a UBC13 dominant negative variant was generated by mutating its catalytic cysteine into alanine (C87A) (Sun et al., 2004) and used for in vivo ubiquitylation assays on RNF8 with UbK29, 48R. Co-transfection of RNF8 with UBC13C87A inhibited its K63 polyubiquitylation, consistent with the fact that such polyubiquitylation is mediated by the interaction and catalytic activity of UBC13 (Fig. 21B). As expected, the RING-dead variant of RNF8 remained unmodified with K63-lincked polyubiquitin chains when cotransfected with dominant negative UBC13.

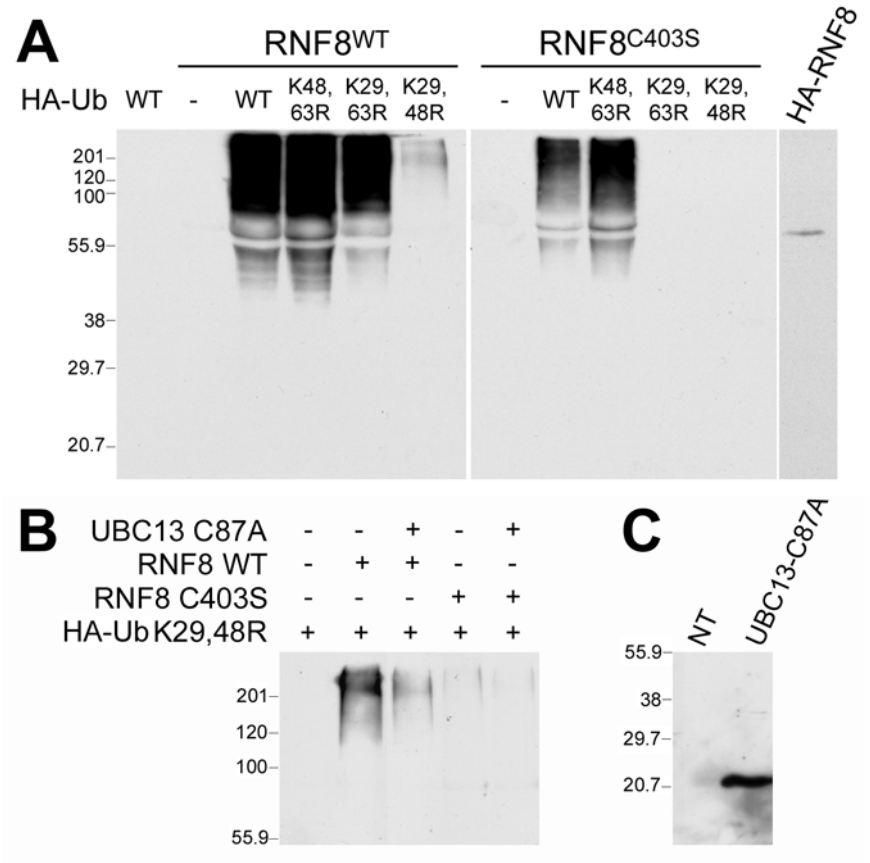

Fig. 21. **A**, *In vivo* ubiquitin-ligase activity of RNF8 with specificity for different classes of polyubiquitin chains. Extracts of Cos 7 cells co-transfected with wild type or RING finger mutant His6-RNF8 and HA-tagged ubiquitin variants were enriched for polyhistidine-containing proteins by Ni affinity chromatography, and analyzed for ubiquitylation of RNF8 by Western blotting with anti-HA antibodies. One lane (HA-RNF8) was run in parallel and blotted with anti-HA, to show the size of the unmodified transfected HA-tagged RNF8. **B**, UBC13 dominant negative inhibits RNF8 K-63 polyubiquitylation. Extracts from Cos 7cells transfected with wild type or RING finger mutant His6-RNF8, UBC13 C87A and HA-ubiquitin K29, 48R were enriched for polyhistidine-containing proteins by Ni affinity chromatography, and analyzed for ubiquitylation of RNF8 by Western blotting with anti-HA antibodies. **C**, expression of UBC13 dominant negative. Cos 7 cells were transfected with Flag tagged form of UBC13 C87A and protein extracts were analyzed by Western blot with M2 anti-Flag monoclonal antibody to test the correct expression of the mutant.

2. 2. RNF8 can be sumoylated

The partial co-localization of RNF8 to PML bodies (page 87) prompted us to determine if RNF8, in addition to be a substrate for polyubiquitylation, was modified by the ubiquitin-like polypeptide SUMO. Cos-7 cells were transfected either with $pHis_6$-$RNF8^{WT}$ or empty vector and cell extracts were also enriched for histidine-tagged proteins by affinity chromatography on Ni-derivatized beads under denaturing conditions, and the eluted proteins examined for modification by endogenous SUMO by Western blotting with anti-SUMO antibodies. This experiment showed that wild-type RNF8 was indeed sumoylated (Fig. 22A).Contrary to ubiquitylation, sumoylation occurs on lysine residues within consensus sequences. When analyzing RNF8 primary sequence, two potential sumoylation sites were identified that fit the sumoylation consensus ψKxD/E, where ψ is a hydrophobic residue (Johnson and Blobel, 1999). These sites correspond to the sequences GKGE and EKHE at positions 190 and 264 of RNF8 (Fig. 22B). The GKGE site shows a very high similarity to the two sumoylation sites on p53 while the EKHE site is similar to the sumoylation site at position 155 of PML (Fig. 22C). To demonstrate that these predicted lysines are the sites of sumoylation of RNF8, further experiments need to be undertaken. For example, the $pHis_6$-$RNF8^{WT}$ construct could be mutated at the lysines in positions 191 and 265 to arginine and the resulting mutants tested by the same *in vivo* sumoylating assay as above.

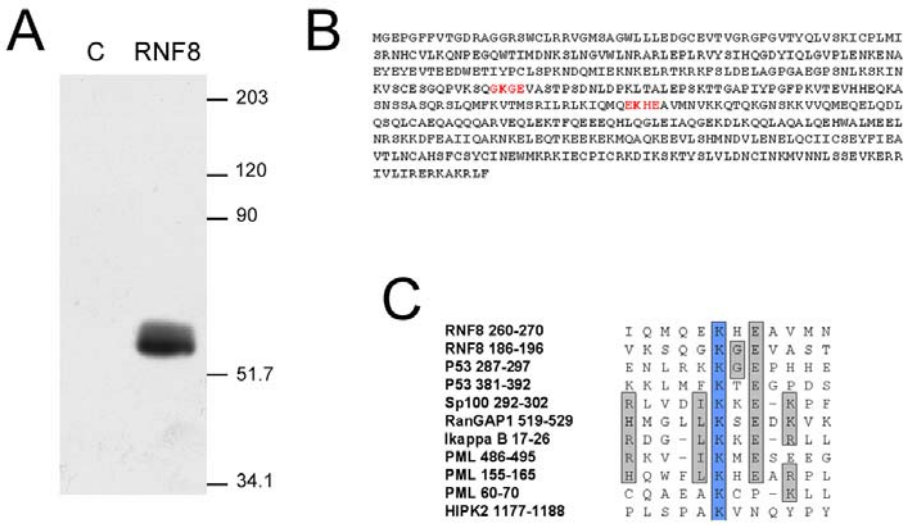

Fig. 22. *In vivo* sumoylation of RNF8. **A**. Extracts of HeLa cells co-transfected with wild-type His6-RNF8 or empty vector were enriched for polyhistidine-containing proteins by Ni affinity chromatography, and analyzed for sumoylation of RNF8 by Western blotting with anti-SUMO antibodies. **B**. RNF8 amino acid sequence showing putative sumoylation sites. **C**. Comparison of known consensus SUMO-1 conjugation sites with potential SUMO-1 conjugation sites of RNF8 at lysine 191 and 265. Blue boxes show sites of conjugation at lysine residues, grey boxes indicate identities or similarities between the residues (Kwek et al., 2001).

3. Third objective

To study the function of RNF8 in cellular processes, by means of over-expression and depletion by siRNA.

.

After analyzing the interactions of RNF8 with E2's and having analyzed its modification by polyubiquitin chains and by SUMO, and also having studied its cell cycle dependent turnover and subcellular localization, we decided to study the involvement of RNF8 in specific cellular processes by means of over expression or knock-down the protein in mammalian cells.

3. 1. Effects of the overexpression of RNF8 in the cell cycle

Since we have found an association of the levels of endogenous RNF8 with specific stages of the cell cycle it was interesting to study the possible functional consequences of its overexpression in the distribution of cells along the cell cycle. Green fluorescent protein forms of wild-type and RING-dead ($RNF8^{C403S}$) of RNF8 were transfected into HeLa cells, and cell cycle distribution analyzed by flow cytometry at 28 and 33h post-transfection. As controls, analyses were performed on untransfected cells in the same experiments. Exogenous expression of GFP-$RNF8^{WT}$ induced an increase in the population of cells with G_1 DNA content, and a reduction in the S phase and G_2-M populations relative to that of the control untransfected cells of the same experiment (Fig. 23A, B). These effects were attenuated when the RING-dead mutant $RNF8^{C403S}$ was transfected (Fig. 23A, B). This suggests that overexpression of RNF8 induces a delay in G_1.

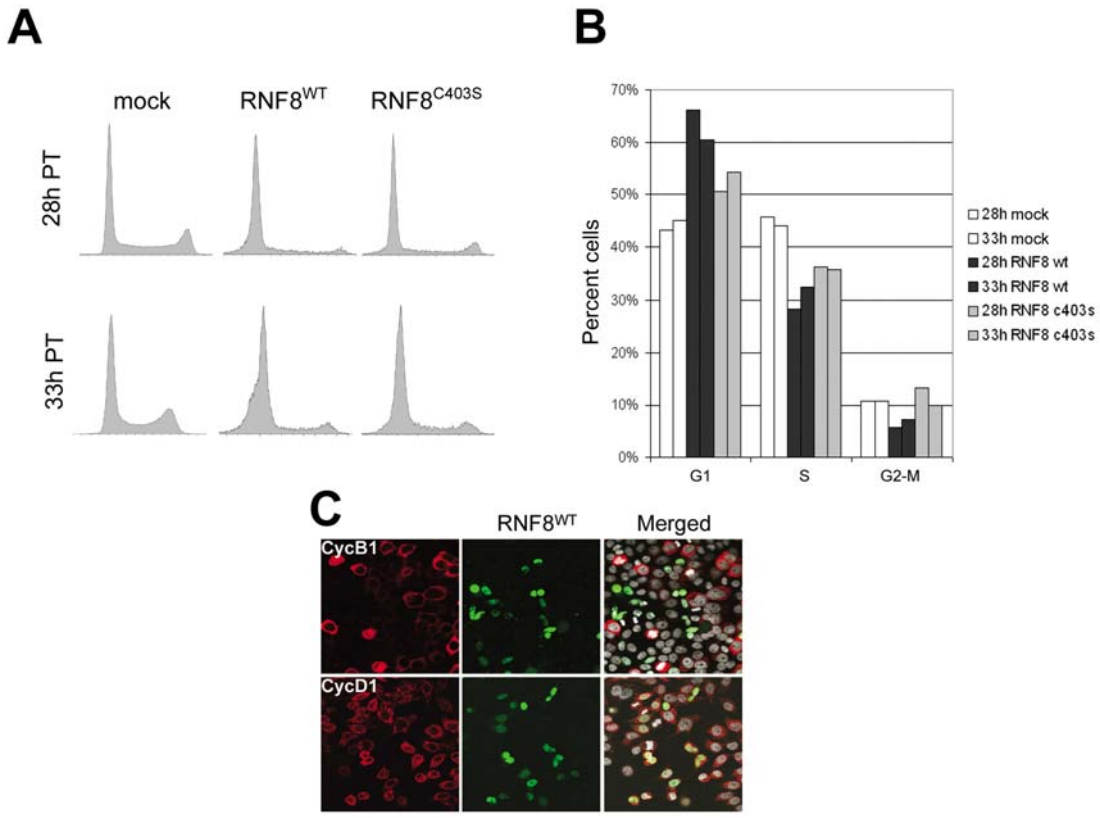

Fig. 23. RNF8 induces a block in G1. **A**, Flow cytometry analysis of HeLa cells transfected with GFP-RNF8^{WT} or GFP-RNF8^{C403S} 28 ND 33 hours post-transfection (PT), and control sham-transfected cells. **B**, The same experiment as in (**A**), analyzed by the Multicycler software, and expressed as the proportion of cells in the G1, S and G2-M fractions. **C**, Immunocytochemical detection of cyclin B1 or cyclin D1 in HeLa cells transfected with GFP-RNF8^{WT} showing predominance of undetectable cyclin B1, and of cytoplasmic cyclin D1 in GFP-RNF8^{WT}-positive cells. For best transfection efficiency cells were protected from apoptosis with 10 μM Z-DEVD.

Furthermore, when cells transfected with GFP-RNF8^{WT} were stained for cyclin D1, most GFP-positive cells showed cytoplasmic, but not nuclear, localization of cyclin D1 (Fig. 23C). Cyclin D1 is expressed in the cytoplasm in early G1, translocates into the nucleus at late G1 coincident with commitment to enter the S phase, and exits the nucleus at beginning of the S phase (Diehl et al., 1998). Consequently, the association of GFP-RNF8 transfected cells with a

cytoplasmic localization of cyclin D1 supported the conclusion that ectopic expression of RNF8 causes accumulation in early G1. Conversely, the majority of RNF8-transfected cells did not stain for cyclin B1, in contrast to the abundant cells in the same fields in which nuclear cyclin B1 was associated with mitotic figures (Fig. 23C). Nuclear entry of cyclin B1 signals the initiation of mitosis (Jin et al., 1998; Pines and Hunter, 1991), and its APC-targeted destruction permits the transition from metaphase into anaphase followed by completion of, and exit from, mitosis (Harper et al., 2002). Therefore, the absence of detectable cyclin B1 in GFP-RNF8 transfected cells suggested that they are either in a postmitotic phase or in early G1, before cyclin B1 accumulates in the cytoplasm. The same associations, cytoplasmic cyclin D1 and absence of cyclin B1, were seen in cells transfected with the RING-dead mutant GFP-RNF8^{C403S}, indicating that these associations are independent of the ubiquitin ligase activity of RNF8. Therfore, these observations indicate that the accumulation in early G_1 of cells transfected with GFP-RNF8 does not require its ubiquitin ligase function.

3. 2. Knock-down of RNF8 by siRNF8 does not affect the cell cycle

Because the localization and levels of RNF8 follow a cell-cycle dependent behavior and overexpression by transfection of GFP forms of RNF8 induce accumulation in G1, we decided to test the cell cycle distribution of cells in which RNF8 is depleted by siRNA. HeLa cells were double transfected at 48 h intervals with specific small interfering RNAs and collected for flow cytometry analysis (Fig24 A and B). Under such conditions, interfered cells show little

differences with untransfected cells and only slight decrease in the S population when comparing them with the cells interfered with a control siRNA. Such decrease is indeed too weak to postulate an effect of the lack of RNF8.

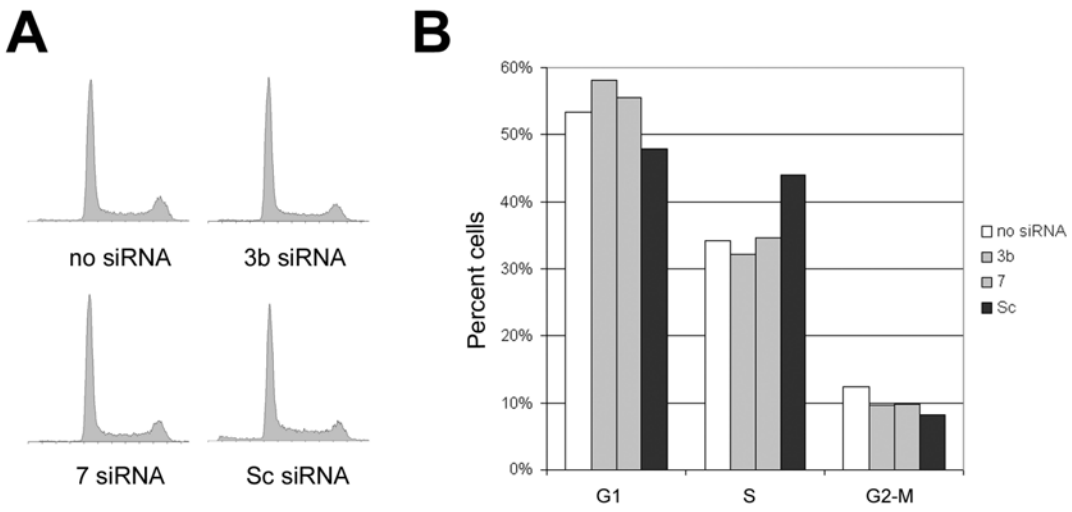

Fig 24. Depletion of RNF8 has no consequences on the basal cycle of HeLa cells. **A**, Flow cytometry analysis of untreated, interfered for RNF8 or scrambled siRNA transfected HeLa cells. **B**, The same experiment as in (**A**), analyzed by the Multicycler software, and expressed as the proportion of cells in the G1, S and G2-M fractions.

3. 3. Overexpression of RNF8 induces mitotic arrest evasion

The expression profile of RNF8 during the cell cycle, with levels slowly increasing during the S phase up to a maximum in mitosis, followed by a rapid decline from prophase to metaphase-anaphase suggested a role of the protein in the control of the G2-M transition. However, overexpression of RNF8 caused accumulation in G1 with little or no effect on G2-M and depletion by siRNF8

caused no significant effects on the basal cell cycle. We therefore tested whether manipulation of RNF8 levels had any consequences in the cellular response to mitotic stress. Consequently, we decided to create a mitotic arrest by preventing microtubule polymerization with nocodazole, followed by release from the block, in order to analyze the rate of mitotic exit. Mock transfected cells showed a proper synchronization in mitosis in response to nocodazole, with 70.8% of cells with a 4n DNA content. These cells promptly reenter the cell cycle, with a rapid decrease of the G2-M population to 26.5% 4 h after removal of nocodazole from the medium (Fig. 25A and B). The decline in the G2-M population was correlated with enrichment in the G1 population from 2.2% to 57.9% 4 h after release from the nocodazole block, and no significant sub-G1 population was observed. In contrast, cells transfected with GFP-RNF8^{WT} showed a negligible increase in the G2-M population with nocodazole treatment, which was only 8.3% of the cells. Nocodazole treatment produced a marked increase in the sub-G1 population of 52.3% 26 h post-transfection in comparison with the 24.1% 33 h post-transfection in the absence of nocodazole treatment (Fig 23A, 29A). Thus, GFP-RNF8^{WT} transfected cells fail to undergo mitotic arrest by nocodazole and show in contrast a very strong G_1 block. This lack of mitotic arrest remained even with nocodazole concentrations of to 0.5 μg/ml and/or exposure for to 20 h. In addition, stress from microtubule depolymerization seems to increase the sub-G1 population in GFP-RNF8^{WT}–transfected cells, and thus to enhance RNF8 mediated apoptosis (see below). It also suggests that GFP-RNF8^{WT} transfected cells are especially sensitive to microtubule stress which could be caused by an improper microtubule function due to the overexpression of RNF8^{WT}.

Cells transfected with GFP-RNF8^{C403S} also showed a poor block in mitosis after nocodazole treatment, although this failure was less pronounced than that caused by wild-type RNF8. Like with RNF8^{WT}, the sub-G1 population induced by transfection with RNF8^{C403S} was higher than without nocodazole treatment, 11.1% versus 3.8% (Fig. 25A).

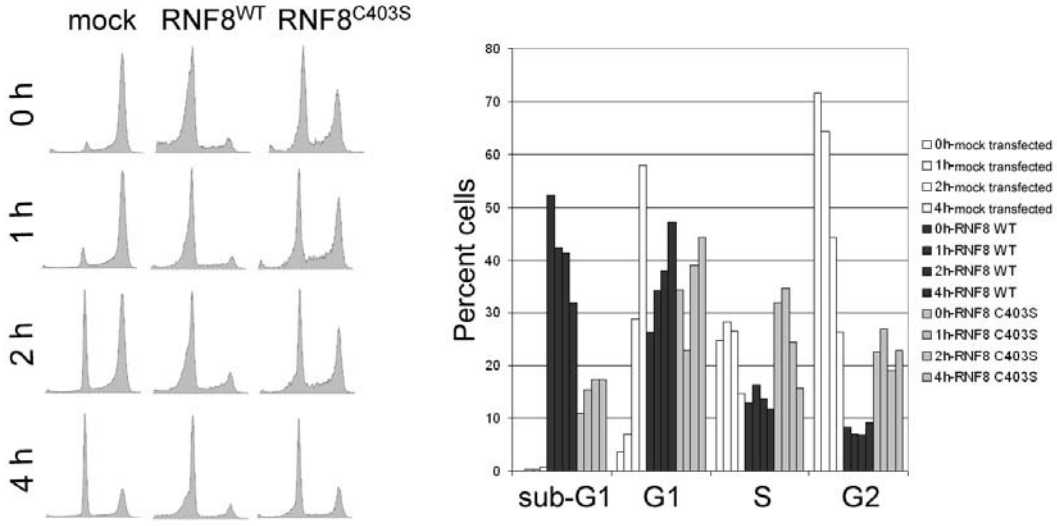

Fig 25. Bypass of nocodazole-induced mitotic arrest in cells with ectopic expression of RNF8. **A,** HeLa cells were transfected for 5 h with GFP-RNF8 WT and RING-dead, recovered for 9 h with complete medium, and incubated for 12 h with 0.1 μg/ml nocodazole. Cells were released from the block by removing nocodazole and providing fresh complete medium. Samples were collected from 0 h to 4 h after nocodazole wash out, and analyzed by flow cytometry. **B**, The same experiment as in (A), analyzed by the Multicycler analysis, and expressed as the proportion of cells in the sub-G1, G1, S and G2-M fractions.

3. 4. Depletion of RNF8 delays mitotic exit after nocodazole treatment

Since overexpression of RNF8 relieved cells from nocodazole-induced mitotic arrest and depletion of RNF8 induced no changes in the basal cell cycle, we decided to investigate the consequences of nocodazole treatment in RNF8-depleted cells. 0 h after nocodazole treatment, cell cycle distribution analyzed by flow cytometry of cells transfected with a scrambled siRNA, or siRNA's specific for RNF8 revealed a marked increase in the G2-M population regardless of treatment (Fig. 26A). Scrambled (control) siRNA-transfected cells recovered progressively from nocodazole exposure and showed 6 h after release a cell cycle distribution similar to basal conditions (Fig. 26A and B). In contrast, and although they also recover progressively from nocodazole treatment, RNF8-depleted cells showed a clear difficulty to exit mitosis. Thus, 6 h after nocodazole release, almost 50% of depleted cells had still 4n DNA content (Fig. 26 A and B). In an independent experiment, we analyzed mitotic exit of RNF8-depleted cells after nocodazole release by checking the levels of cyclin B1. APC-target destruction of cyclin B1 permits the transition from metaphase into anaphase followed by completition and thus exit from mitosis (Harper et al., 2002). The same samples were analyzed for actin levels for normalization. The levels of cyclin B1 in control cells were very high 0 h after nocodazole treatment and clearly declined 4 hours after release (Fig. 26C). In contrast, although they also experienced a significant decline in its level, cyclin B1 was still visible in RNF8-depleted up to 4 h after nocodazole release (Fig. 26C).

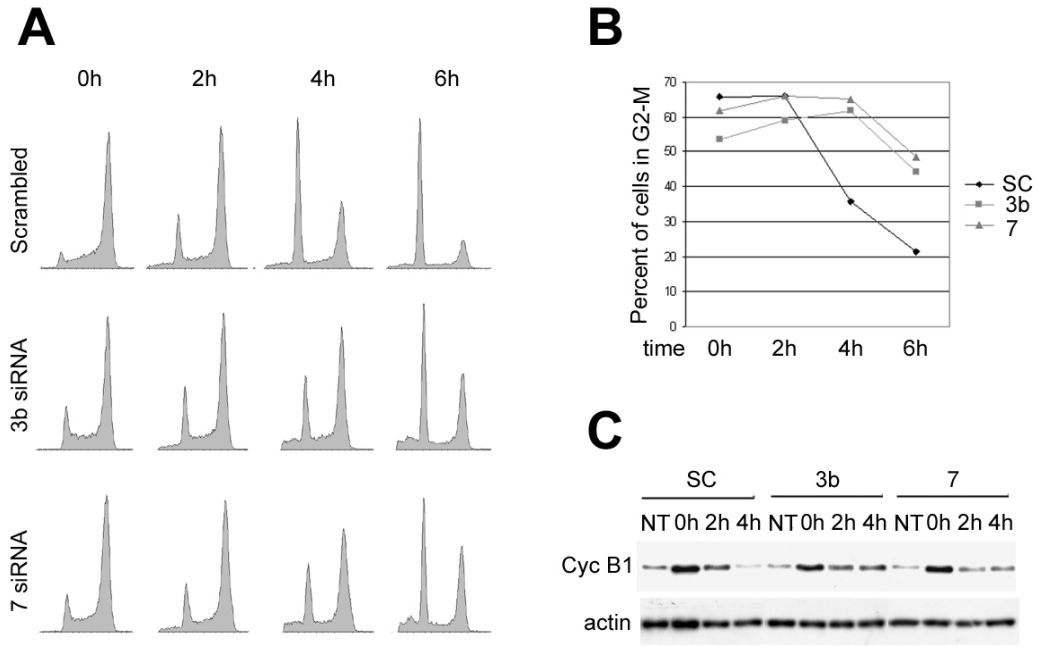

Fig. 26. Delay in mitotic exit in RNF8-depleted cells after nocodazole-induced mitotic arrest. HeLa cells were double transfected at 48 h intervals with a control siRNA or siRNA's specific for RNF8 depletion; 48 h after the last siRNA transfection, cells were incubated for 16 h with 0.1 μg/ml nocodazole. Subsequently, cells were washed and released from the block by providing fresh complete medium. Samples were collected at the indicated times and processed for flow cytometry or Western blotting analyses. **A**, Flow cytometry analisis of nocodazole arrested and released cells. **B**, Same experiment as in A analyzed by the Multicycler software. The graph shows only the proportion of cells in G2-M at each of the indicated time points after nocodazole release. **C**, Western blotting analysis of nocodazole-treated cells for cyclin B1. Actin levels were determined on the same membranes to normalize for protein loadings. *NT* stands for not treated and the indicated time points reflect hours after nocodazole release.

3. 5. Transfected GFP-RNF8 localizes in mitotic spindles and associates with aberrant cytokinesis figures

To reconcile the observations of block and death in G1 caused by ectopic expression of RNF8, and its cell-cycle pattern of expression, we hypothesized that excess levels, or untimely expression, of RNF8 can have a priming effect in late mitosis that becomes evident once the cells have completed cytokinesis, and thus with a G1 DNA content, resulting in either inability to progress beyond G1 or in apoptosis.

In order to study in better detail the localization and effects of transfected GFP-RNF8 at or beyond metaphase under conditions of cell viability, cells transfected with GFP-RNF8 were protected from apoptosis by treatment with the caspase inhibitor Z-VAD, and the localization of transfected and endogenous proteins were analyzed by confocal microscopy. Under these conditions, GFP-RNF8 was seen at localizations that were not generally observed in cells in which caspase-dependent apoptosis was not inhibited. In metaphase and anaphase, both wild-type and RING-dead mutant RNF8 associated with mitotic spindles, and also with the midzone spindle (Fig. 27A). In late telophase, GFP-RNF8 localized like the endogenous protein in the midbody of mitotic bridges, at the confluence of microtubule bundles converging from each of the two daughters cells (Fig. 27A). The localization of RNF8 to these mitotic structures was independent of its function as a ubiquitin ligase, since the mutant RNF8^{C403S} also showed similar localizations (Fig. 27B).

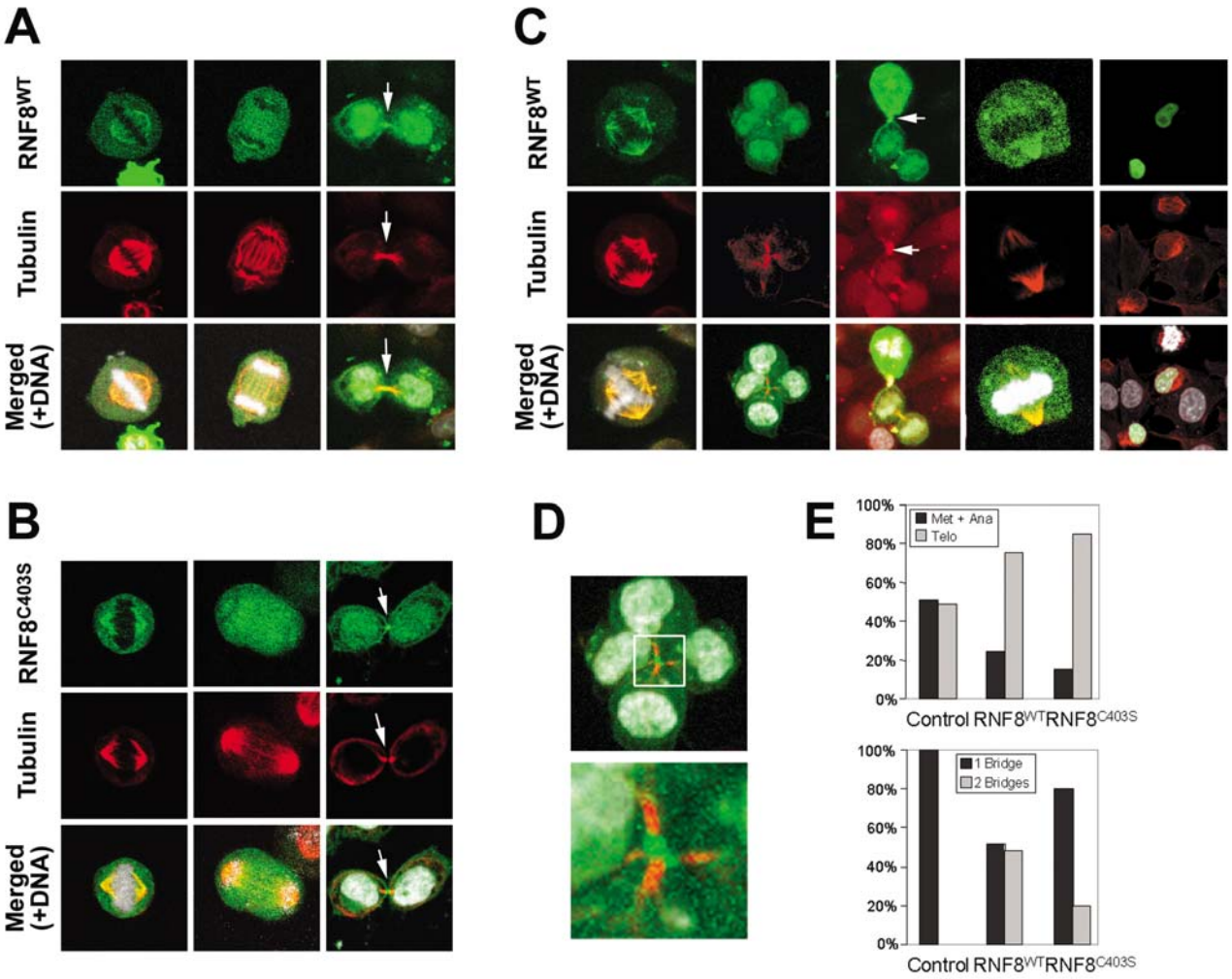

Fig 27. Localization of GFP-RNF8 to mitotic structures in HeLa cells protected from caspase-dependent apoptosis, and induction of aberrant mitosis and cytokinesis. **A**, HeLa cells transfected with GFP-RNF8WT and protected from apoptosis with Z-VAD were processed for immunocytochemistry for the detection of β-tubulin (red channel) and DNA (Hoechst 33258 staining). GFP-RNF8^{WT} co-localizes with tubulin in mitotic spindles with normal appearance (first column) and in central spindles (second column). In mitotic bridges at cytokinesis (third column), RNF8 localizes in the midbody (arrows), between two bundles of microtubules that converge from the dividing cells. **B**, Localization of the mutant GFP-RNF8^{C403S} in mitotic structures is similar to that of wild-type GFP-RNF8, in spindles and in the midbody of mitotic bridges (arrows). **C**, Overexpression of wild-type GFP-RNF8 into Z-VAD treated HeLa cells causes the appearance of aberrant mitotic figures, including multiple mitotic spindles (first column), unresolved mitotic bridges (second and third columns) and unbalanced mitotic spindles (fourth column). GFP-RNF8 transfected non mitotic cells show abnormally polymerized microtubules in comparison to mock transfected cells in

the same image (fifth column). **D**, Higher magnification of a double unresolved mitotic bridge shown in (C), with RNF8 localized to the double midbody into which four microtubule bundles converge from two attached cells. **E**, Overexpression of RNF8 in Z-VAD-treated HeLa cells causes an accumulation of mitotic cells in telophase (top panel), and of three cells attached to each other through two unresolved mitotic bridges (bottom panel). Cells transfected with GFP-RNF8^{WT} or GFP-RNF8^{C403S} were stained for β-tubulin and DNA, and GFP-positive cells analyzed for the appearance of mitotic structures that define each of the phases shown, metaphase, anaphase or telophase, or the presence of mitotic bridges indicated by the convergence of tubulin-positive bundles in two or more cells clearly seen as attached under transmission mode. The frequencies shown refer to more than 50 cells for each condition for the upper panel and to 25 independent mitotic events for each condition for the bottom panel.

In addition to mitotic structures with normal appearance, aberrant mitotic figures were seen in Z-VAD-treated cells transfected with wild-type RNF8, but not with the RING-dead mutant RNF8^{C403S}. Some aberrant figures consisted of three or more polar spindles, apparently originating from independent centrosomes, and associated with an aberrant distribution of condensed chromosomes (Fig. 27C). Several remarkable aberrant figures were observed, with two apparently adjacent midbodies containing GFP-RNF8, into which four separate bundles of microtubules converged from each of four cells (Fig. 27C, D).In addition, some GFP-RNF8-transfected metaphases showed clearly unbalanced microtubule spindles and non mitotic cells showed abnormally polymerized microtubules (Fig 27C). A proportion of RNF8-transfected and Z-VAD treated cells consisted of strings of 3 to 4 cells attached to each other by tubulin-containing mitotic bridges, with RNF8 localized at the midbodies (Fig.27C). In some instances, cells attached through mitotic bridges were

clearly in different phases of the cell cycle, for example with two attached cells in which nuclear division had been completed, suggestive of their being in G1 or S, and a third attached cell in mitosis (Fig. 27C, third column). This suggests that, in RNF8 transfected cells, mitotic bridges can form abnormally even with an ongoing metaphase or anaphase. Alternatively, it is possible that these multiple cell strings originated as a consequence of sequential cytokinesis before complete resolution of the first cytokinesis by abscission of the mitotic bridge. Determining DNA content of these aberrant figures would be as interesting as difficult due to the fact that they fall into the aggregate fraction when analyzing samples by flow cytometry or Laser Scan Cytometry.

Thirty hours after transfection of HeLa cells with GFP-RNF8^{WT} or with mutant GFP-RNF8^{C403S} and with caspase inhibitors, the proportion of mitotic cells in metaphase or anaphase was close to 20%, thus significantly lower than the more than 50% in control cells; supporting a faster chromosome segregation and entry into cytokinesis mediated by the overexpression of RNF8 (Fig 27E upper pannel). In addition, approximately half of the cells in late telophase and attached by tubulin bridges corresponded to strings of three or four cells attached to each other through double mitotic bridges (Fig. 27E downer pannel). The frequency of double mitotic bridges in cells transfected with the RING-dead mutant GFP-RNF8^{C403S} was reduced to approximately 20% of cells in late telophase, whereas no double bridges were found in control untransfected cells or cells transfected with GFP only (Fig. 27D).The fact that these aberrant cells attached through multiple unresolved mitotic bridges were not seen under conditions in which cell death is not prevented suggests that such aberrant mitoses are not viable.

Therefore, overexpression of RNF8 at metaphase and anaphase results in a subcellular localization at mitotic spindles. Overexpression of RNF8 causes a clear excess in the proportion of telophases among mitotic cells. In addition, a proportion of $RNF8^{WT}$ transfected cells fail to undergo normal cytokinesis associated with the formation of multiple microtubule bridges.

3. 6. Relationship between PLK1 and RNF8

Three major considerations argued in favor of Plk1 as a candidate protein for regulation by RNF8: First, Polo-like kinases regulate multiple events at different phases of the cell cycle. Plk1 activates the Cdk1 kinase for the initiation of mitosis (Patra and Dunphy, 1998) likely by phosphorylation and activation of Cdc25C (Ouyang et al., 1999) and also cyclin B (Jackman et al., 2003; Toyoshima et al., 1998), permits centrosome maturation (Lane and Nigg, 1996; Sunkel and Glover, 1988) and bipolar spindle formation (Ohkura et al., 1995), assists the APC by phosphodependent degradation of specific substrates (Kotani et al., 1999; Schmidt et al., 2005; Shirayama et al., 1998), and regulates cytokinesis (Guertin et al., 2002a; Lindon and Pines, 2004; Seong et al., 2002). Second, depletion of Plk1 causes apoptosis (Liu and Erikson, 2002). Third, all proteins containing FHA and RING finger domains are regulators of distinct G2-M transitions, and both CHFR and SpDma1p seem to act at least partly through targeted degradation or inhibition of Polo-like kinases. The metazoan protein CHFR acts at the onset of mitosis (Scolnick and

Halazonetis, 2000) and the fission yeast protein Dma1p at cytokinesis (Guertin et al., 2002).

We therefore studied whether RNF8 colocalized with PLK1 during mitosis and cytokinesis in cells protected with caspase inhibitors. Both wild-type RNF8 and its RING-dead mutant co-localized with PLK1 at the mitotic spindle in metaphase and anaphase and also in the mitotic furrow during anaphase (Fig 28A). In late telophase, they also co-localized in the midbody of mitotic bridges, with RNF8 tightly associated with the midbody but not the tubulin-containing bundles, whereas PLK1 extended its localization from the midbody onto the tubulin bundles attached to the midbody on both sides of the mitotic bridge (Fig. 28A). Under these conditions, and in late telophase, RNF8 showed additional localizations, including the nucleus and cell membranes (Fig. 28A). These observations suggest that RNF8 associates with PLK1 at specific mitotic structures.

If RNF8 has any regulatory function on PLK1, maybe by polyubiquitylating the protein either by K48 or K63, it may be reasonable to assume that the levels of the PLK protein should be modulated by overexpression of RNF8. HeLa cells were transfected with either GFP-RNF8^{WT} or GFP-RNF^{C403S} under inhibition of caspase-dependent apoptosis by adding caspase inhibitors to the medium. Thirty hours after transfection, cells were sorted and proteins analyzed by Western blotting. No significant changes in the levels of PLK1 were observed (Fig. 28B), suggesting that in spite of their co-localization at several mitotic structures, PLK1 may not be a direct target for ubiquitylation by RNF8.

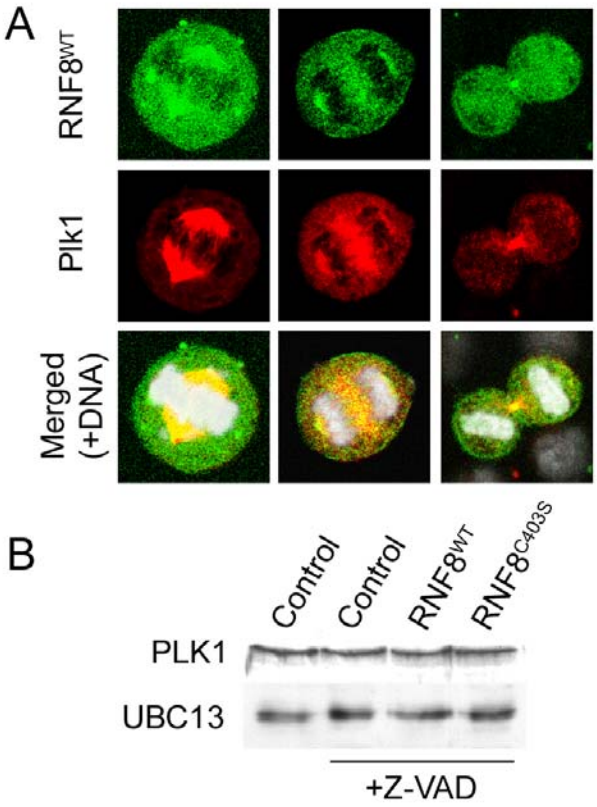

Fig 28. Co-localization of RNF8 and PLK1. HeLa cells were transfected with GFP-RNF8^{WT} and stained for PLK1 and DNA. **A**, In Z-VAD-treated HeLa cells, RNF8 and PLK1 partially co-localized in mitotic structures, such as the spindles (first column), the central spindle (second column) and the mitotic bridge (third column). RNF8 shows additional localizations in this stage of the cell cycle. **B**, Overexpression of RNF8 does not modulate PLK1 levels. HeLa cells were transfected with GFP-RNF8^{WT} or GFP-RNF8^{C403S}, sorted for GFP-positive cells (see Materials and Methods), and analyzed for levels of PLK1 protein by Western blotting. Each lane was loaded with extracts from 1.75 x 10^5 sorted cells, and the blots were further normalized for its levels of UBC13.

3. 7. Overexpression of RNF8 induces apoptosis

Flow cytometry analysis of the DNA content profile indicated that transfection with GFP-RNF8^{WT} caused the appearance of a significant population of cells with sub-G_1 DNA content, which, 28 hours after transfection, amounted to 4.5% of the cells expressing GFP-RNF8 (Fig. 29A) and increased up to 24.1% 33 hours post-transfection. This effect was significantly reduced when cells were transfected with mutant GFP-RNF8^{C403S} (Fig. 29A). Since sub-G1 DNA content is characteristic of apoptotic cells, we decided to analyze the cell cycle distribution of transfected cells treated with the caspase inhibitor Z-DEVD or vehicle (Fig. 29 B and C). Z-DEVD prevented the appearance of a sub-G1 cell population in cells transfected with GFP-RNF8 variants, indicating that this population corresponds to apoptotic cells, and that apoptosis depends on the activation of caspases. Prevention of apoptosis caused by GFP-RNF8^{WT} did not result in a significant increase in the G2-M population in these cells, but caused an increase in the population of cells in G1 (Fig. 29C and D). In contrast, cells transfected with the RING-dead form of RNF8 increased their G2-M population by two-fold. Therefore, the apoptotic population of cells overexpressing GFP-RNF8^{WT} appears to correspond to cells that would be otherwise in G_1, while there may be a G_2-M-associated mortality for the RING-dead mutant RNF8^{C403S}. Further experiments may need to be undertaken in order to confirm the DNA content of the dying cells over-expressing RNF8 RING-dead; maybe a third staining by tunnel assay or with anti-caspase-3 antibody could clarify it.

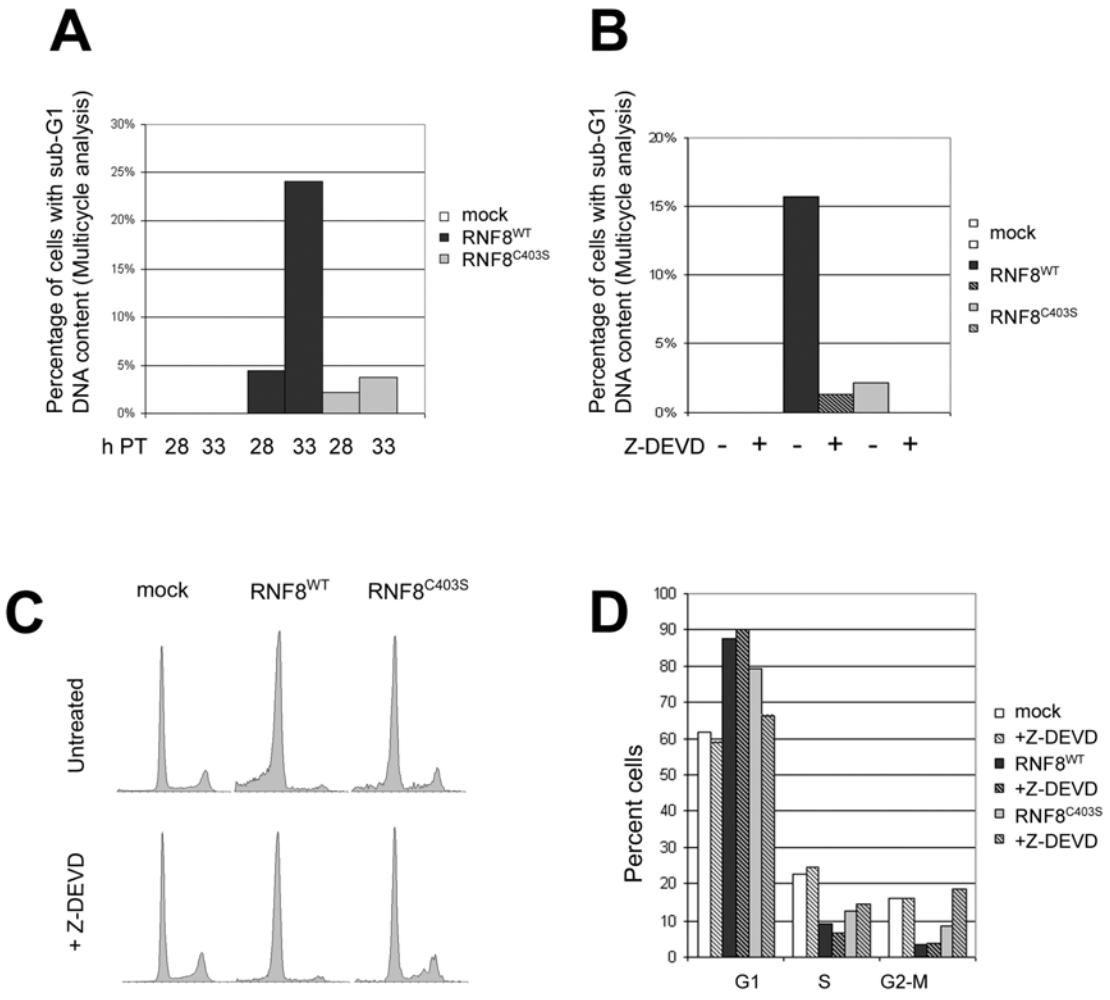

Fig 29. RNF8 causes apoptosis. **A**, Graphic representation of percentages of sub-G1 populations of HeLa cells transfected with GFP-RNF8^{WT} or GFP-RNF8^{C403S} 28 and 33 hours post-transfection (h PT), and control mock-transfected analyzed with the Multicycler software. See Fig 23A for histogram. **B**, Representation of sub-G1 populations of HeLa cells transfected with GFP-RNF8^{WT} or GFP-RNF8^{C403S} 30 hours post-transfection and treated with 10 μM Z-DEVD or vehicle, and control mock-transfected analyzed with the Multicycler software. **C**, Flow cytometry analysis from **B**. **D**, The same experiment as in (**C**), analyzed by the Multicycler software, and expressed as the proportion of cells in the G1, S and G2-M fractions.

Morphological evaluation after DNA staining of monolayers of HeLa cells untransfected or transfected with either empty vector (pEGFP), wild-type or RING-dead variants of RNF8 yielded, respectively, 0.2%, 8.9%, 24.6% and 7.2% of transfected cells with apoptotic nuclear appearance 24 hours after transfection and up to 49.3% ($RNF8^{WT}$) and 16.2% ($RNF8^{C403S}$) 48 hours after transfection (Fig. 30A), which is consistent with the flow-cytometry analysis. As described above, incubation with caspase inhibitors prevented the appearance of sub-G1 populations in transfected cells pointing to caspases mediated apoptosis. In agreement with this conclusion, transfection with $RNF8^{WT}$, but much less the RING-dead mutant $RNF8^{C403S}$, caused the appearance of proteolytic fragments of caspases -3 and -8 (Fig. 30C), indicating that the observed apoptosis is associated with the activation of these caspases. Also in transfected monolayers, treatment with the caspase inhibitor Z-VAD reduced the fraction of RNF8-induced apoptotic cells to less than 2% analyzed by morphologic criteria, showing that the sub-G_1 population in cells expressing GFP-RNF8 correspond to apoptotic cells, and confirming that death of these cells is executed by caspases (Fig. 30D).

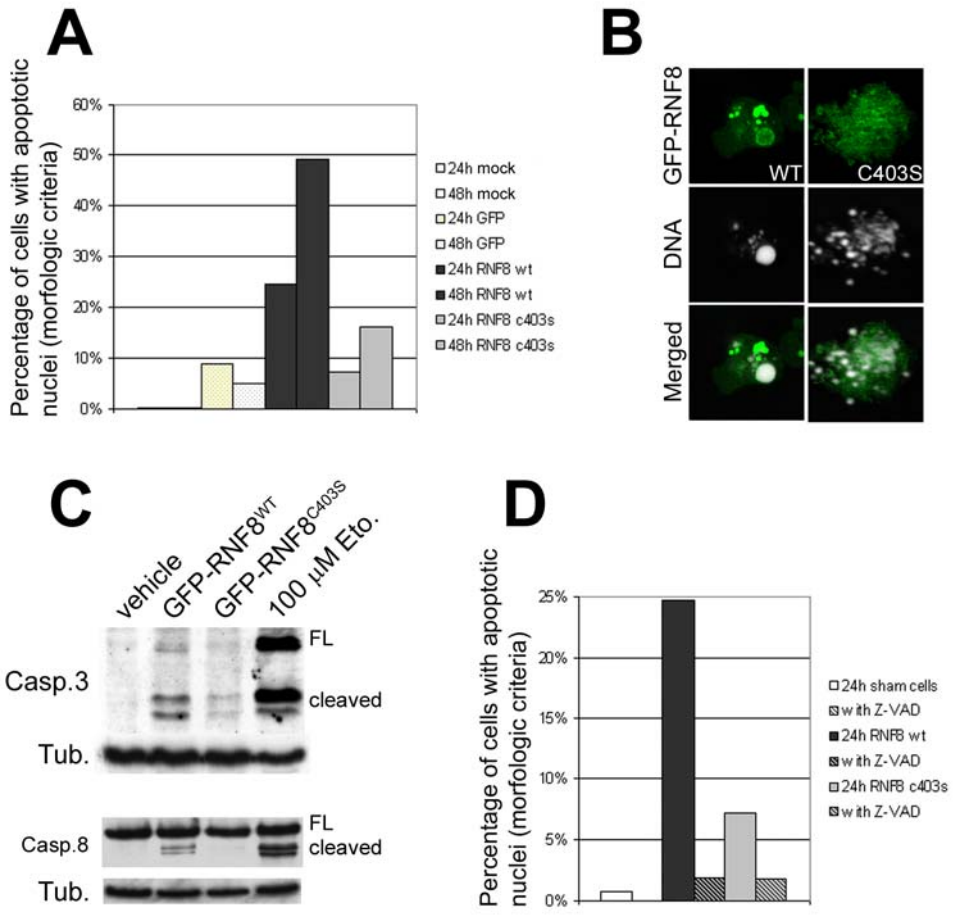

Fig 30. RNF8 over-expression induces apoptosis. **A**, Time-dependent accumulation of apoptotic cells in HeLa cells transfected with GFP, GFP-RNF8^{WT}, GFP-RNF8^{C403S} or mock-transfected. Transfected cells were processed at 24 or 48 h after transfection, stained for DNA with Hoechst 33258, and GFP-positive cells assessed for apoptotic appearance. Histogram shows the mean of at least three independent experiments in which between 150 and 200 cells were counted. **B**, Confocal image of HeLa cells transfected with GFP-RNF8 or RING-dead mutant and stained for DNA with Hoechst 33258 with the characteristics of an apoptotic cell. **C**, Induction of proteolytic cleavage of caspase-8 and caspase-3 in HeLa cells transfected with GFP-RNF8^{WT} but not GFP-RNF8^{C403S}. Thirty-six hours after transfection, cell extracts were analyzed by Western blotting with antibodies specific for caspase-8 and caspase-3. As a positive control for apoptosis, HeLa cells were treated in parallel with etoposide (100 μM) over-night. The proteolytic fragments of activated caspase-8 and caspase-3 are indicated on the right by "Cleaved". **D**, Z-VAD-dependent accumulation of apoptotic RNF8-transfected cells. Cells were treated with 30μM Z-VAD containing DMEM immediately after transfection, fixed for DNA staining 24h later and counted for apoptotic appearance as in A.

3. 8. Endogenous RNF8 protein levels increase under pro-apoptotic stimuli

Since RNF8 over-expression caused apoptosis, we decided to test whether RNF8 endogenous levels increased in cells undergoing DNA damage. Cells were seeded and treated with increasing concentrations of cis-Platinium, etoposide and UV light. Cis-Platinum can form DNA-protein crosslinks, DNA monoadducts and both interstrand and intrastrand crosslinks (Meyers et al., 2004). Etoposide acts by stabilizing the complex formed by DNA and topoisomerase II, which results in the increase of double-strand DNA breaks (Meresse et al., 2004). Ultraviolet light induces cyclobutane pyrimidine dimers that cause lesions on DNA (Sonneveld et al., 2001). Cell lysates were quantified and analyzed by Western blotting for RNF8 expression, the appearance of proteolytic forms of caspase-3 were used as an apoptosis marker, and β-tubulin levels were used for normalization (Fig. 31A). Levels of endogenous RNF8 were induced by all these stimuli in a dose-dependent manner, independently of their ability to activate caspase-3. Notably, treatment of cells with UV light caused both an increased of RNF8 protein levels and a high mortality, apparently without caspase-3 activation. Immunostaining of etoposide-treated cells showed that RNF8 localized intensely in cells with micro or collapsed nuclei (Fig. 31B).

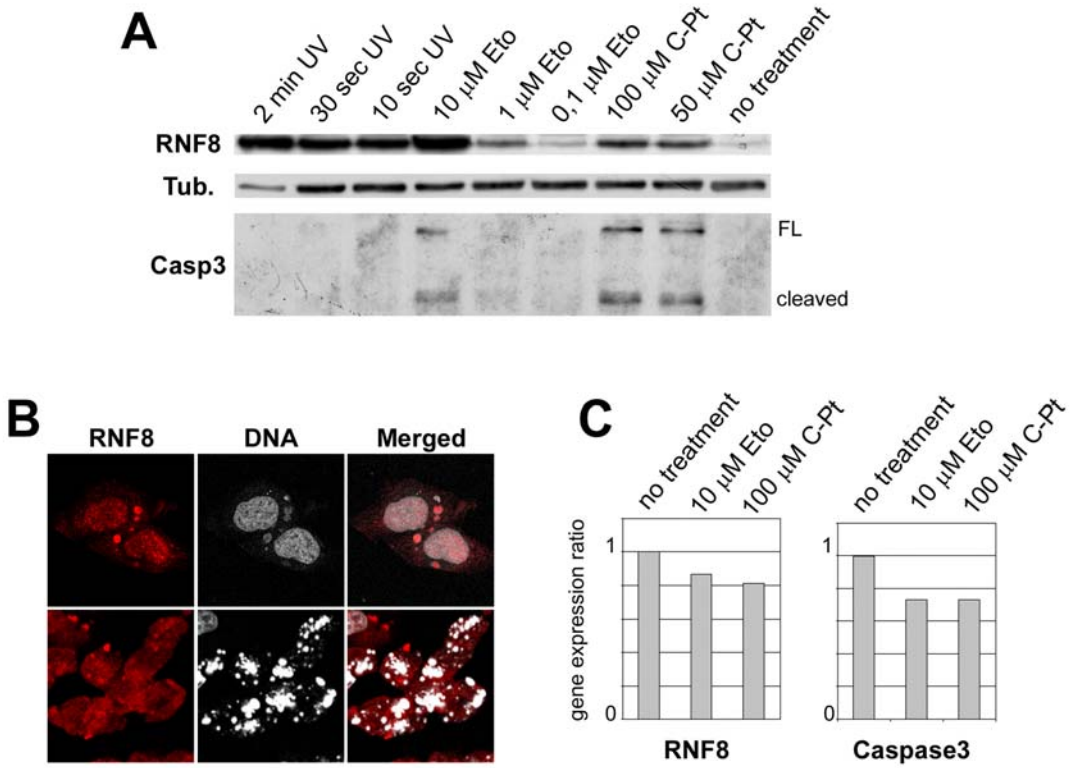

Fig. 31. Endogenous RNF8 protein and transcript levels under drug treatments. **A**, HeLa cells were treated with several proapoptotic stimuli for 24 h as indicated in the figure and protein levels were analyzed after quantification by Western blotting. FL stands for full length, which is the non active form of caspase-3, cleaved stands for the active form of caspase-3. **B**, Immunocytochemistry staining of RNF8 of cells treated with 10 or 25 μM Etoposide. DNA was stained with either Toto iodide 3 or Hoechst. The first panel shows cells with micronuclei and bottom panel cells with collapsed nuclei. **C**, Transcript levels, shown as ratios determined by real-time RT-PCR. Cells were treated with the corresponding drugs for 24 h and RNA was isolated reverse transcribed and cDNAs were used as templates in Sybr-Green PCR reactions with specific primers for the genes RNF8, caspase-3 and S14r. Real-time C_T levels were determined on a ABI 7700 instrument (see Materials and Methods). C_T values were normalized in each case for values obtained for the reference gene S14r, and then further normalized relative to the non treated cells.

The induction of RNF8 protein levels by pro-apoptotic stimuli could be caused by either an increase in gene transcription or/and a stabilization of the

protein. To determine RNF8 transcript levels, total RNA was extracted from HeLa cells, untreated or treated with etoposide 10μM or cis-Platinum 100μM. RT-Real-time PCR was performed as shown in Fig. 31C. RNF8 transcript levels did not increase with these treatments but instead they experienced a small decrease, determined after normalization for ribosomal S14 rRNA. This suggested that the increase in RNF8 protein levels induced by apoptotic stimuli is not caused by increased transcription but possibly by stabilization of the protein.

3. 9. Depletion of RNF8 by siRNA makes cells more resistant to the apoptosis induced by etoposide.

The combined observations that overexpression of RNF8 by transfection causes apoptosis and that apoptotic stimuli such as etoposide treatment induce higher levels of endogenous RNF8 led us to propose that RNF8 could mediate at least part of the pro-apoptotic response to such treatments, and that its depletion could protect cells from pro-apoptotic stimuli. To test this hypothesis, HeLa cells were depleted of RNF8 by siRNA and treated for 12 h with 25 μM etoposide. Morphological evaluation after both RNF8 and DNA staining revealed a significant decrease in the apoptotic population in RNF8-depleted cells in comparison to control cells transfected with non specific siRNA duplexes (Fig 32A). Cells transfected with the non-specific scrambled siRNA showed an apoptosis rate of 36.91%, while cells depleted of RNF8 with either 3b or 7 siRNA showed an apoptosis rate of 4.27% and 4.10%, respectively. In parallel experiments, cells were treated as above and collected for Western blotting

analysis with anti-caspase-3 antibody and anti-tubulin for normalization. Caspase-3 remained undetectable in the absence of a pro-apoptotic stimulus, but etoposide treatment induced the appearance of both the full-length and the cleaved form of the protein in control cells (Fig 32B). In cells depleted of RNF8, etoposide treatment induced markedly less pro-caspase-3 levels than in control cells, with much less significant changes in the appearance of the cleaved forms, suggesting that the induction of caspase-3 is dependent on the presence of RNF8. These data support the conclusion that overexpression of RNF8 regulates the activity of caspase-3. The molecular mechanisms by which RNF8 accomplishes this regulation still remain to be identified.

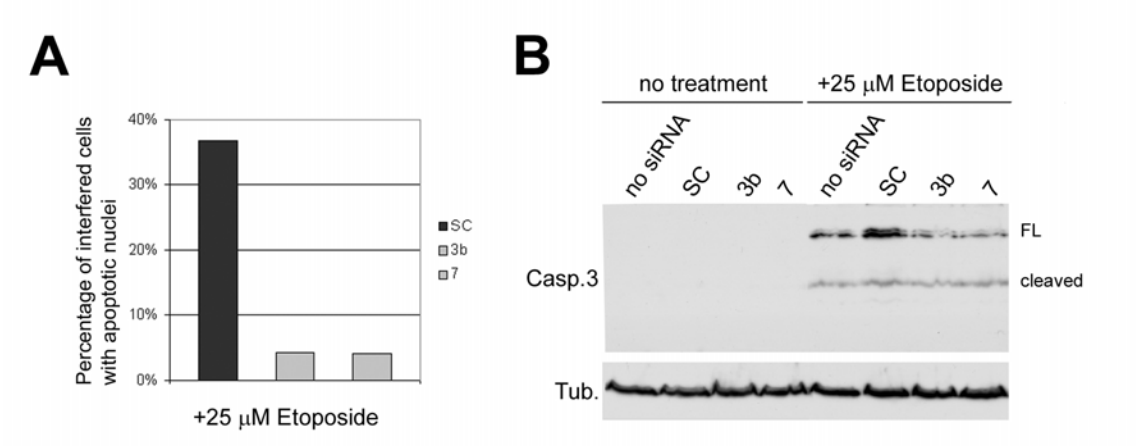

Fig. 32. Depletion of RNF8 makes cells more resistant to etoposide-induced apoptosis. **A**, RNF8-dependent apoptosis in HeLa cells treated with 25 μM etoposide. Double transfected cells at 48 h intervals were treated with 25 μM etoposide in DMEM 10% FBS for 12 h, fixed and immunoassayed for RNF8 and stained for DNA with Hoechst 33258, RNF8 positive or negative cells were assessed for apoptotic appearance. Each column represents the average of triplicate experiments where around 200 cells where counted. **D**, Immunodetection of caspase-3 in interfered HeLa cells treated or not with 25 μM Etoposide for 12h. The same membrane was blotted with anti-tubulin for loading calibration.

3. 10. Overexpression of RNF8 does not enhance caspase-3 gene transcription

Since RNF8 over-expression increased pro-caspase-3 protein levels, we tested if the protein induction was due to an increase of the corresponding transcript levels. RT-PCR of *caspase-3* on cDNA's from non transfected cells or cells transfected with GFP alone or fused to both wild type or RING-dead RNF8 showed that there was no significant increase of the mRNA levels (Fig 33). Thus, the increase of caspase-3 protein levels caused by RNF8 overexpression is possibly caused by stabilization of the protein.

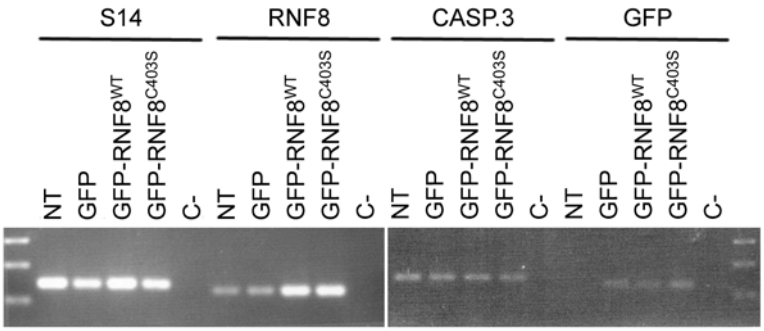

Fig 33. Ectopic expression of RNF8 does not induce changes in the levels of caspase-3 transcripts. HeLa cells were transfected with vehicle alone, with GFP or with GFP-RNF8^{WT} and GFP-RNF8^{C403S} and lysed for total RNA isolation. Reverse transcription was performed from 2 μg of RNA followed by PCR amplification with specific primers of the ribosomal S14 (as a normalizer) and for the genes of study: RNF8, caspase-3 and GFP.

4. Forth objective

To identify molecular partners of RNF8 that might help to understand the phenotype caused by RNF8 overexpression or knock-down.

4.1. Yeast two-hybrid screening to search for RNF8 interactors

Full length RNF8 was cloned in frame with the Gal4 DNA binding domain and used as bait for a yeast two hybrid screening of the same human fetal brain cDNA library used to search for UBC13 binding partners. Out of 3.0 x 10^6 independent clones screened, we confirmed interactions with RNF8 for 17 clones, corresponding to three distinct proteins (Figure 34A). The ribosomal subunit S40 was the first interaction partner (10 clones). The second interacting partner of RNF8 was HERC2, with two classes of clones of different insert size (5 clones). Finally, Huntingtin Interacting Protein 1, or HIP1, was the third interacting partner, with two positive clones. In contrast to the screening of UBC13 interactors, no sequence or domain motif was found to be in common to the three RNF8 interacting partners. Deletion mutants of RNF8 containing only the FHA domain or both the coil and the RING finger domain were generated to further characterize the regions of interaction of these positive clones. All three RNF8-associated proteins interacted both with the FHA domain and with the full length RNF8 protein, but not with deletion variants lacking the FHA domain (Fig 34B).

S40 is a protein of 295 amino acids that shows a homology to laminin receptor-1 and with the ribosomal protein SA (LOC92215) (Fig 35). There is little available data about the protein, whose function has not been studied. The clone that interacted with RNF8 included the carboxy-terminal 200 amino acids from a total of 326.

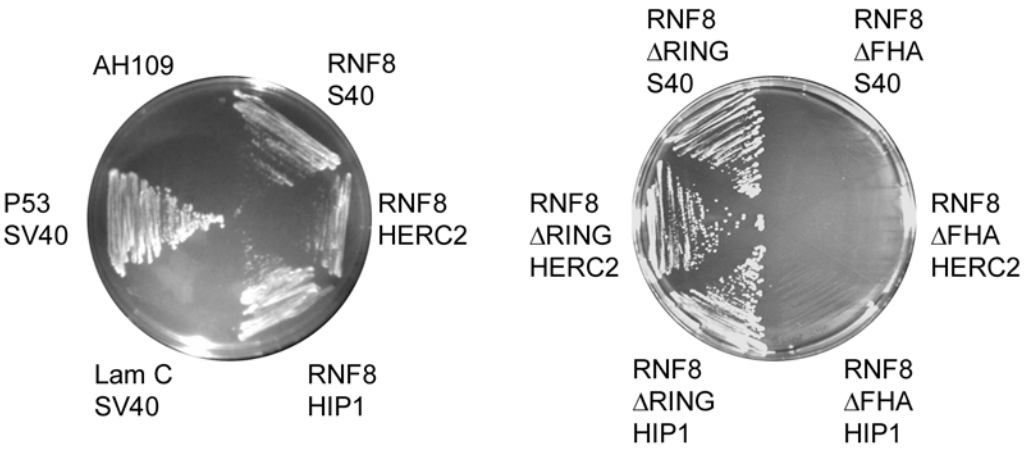

Fig 34. RNF8 interactors found by yeast two-hybrid analysis. **A**, Results of yeast two-hybrid screening of human fetal brain cDNA library using RNF8 as a bait. Negative controls included the untransfected strain AH109 and cells co-transfected with laminin C and SV40 large T. As a positive control for interaction, cells were co-transfected with p53 and SV40 large T. The symbols for the interacting proteins are shown adjacent to each of the sectors of the plate. **B**, Interaction of S40, HERC2 and HIP1 with the FHA domain of RNF8. RNF8ΔRING construct includes only the FHA domain of the protein, while RNF8ΔFHA contains both the coiled-coil domain plus the RING domain.

The second RNF8 binding partner, HERC2, is a large protein of 4834 amino acids whose gene is located on chromosome 15q. The biggest clone isolated from the library included only the last 219 amino acids of the protein and the smallest the carboxy-terminal 47 residues. HERC2 contains a HECT domain (Homologous to E6-AP Carboxyl Terminus) located between positions 4463 and 4790 (Fig. 35), which is typical of a class of E3 ubiquitin ligases (see introduction, E3 or ubiquitin ligases). This domain was partially contained within the longest clone interacting with RNF8, but not in the shortest. This suggests that the interaction of HERC2 with the FHA domain of RNF8 is mediated by the last 47 amino acids in the carboxy terminus of HERC2. In addition to its HECT

domain, HERC2 presents three RCC-like domains (positions 437 to 786, 2952 to 3323 and 3945 to 4328), which are domains involved in chromosome condensation and guanidine nucleotide exchange (GEF activity) of small GTP binding proteins (Dasso, 2001; Hetzer et al., 2000; Zhang et al., 2000). Notably, HERC1, a related protein, also contains RCC1-like domains which stimulate guanine nucleotide exchange on ARF1 and on members of the Rab related proteins, but not on Ran or R-Ras2/TC21 (Rosa et al., 1996). HERC2 has not been studied for such an activity. Besides, HERC2 is predicted to contain a steroid binding domain at position 1209 to 1282, a zinc finger domain similar to the ones found in CREB-binding protein/p300 and dystrophin-like proteins from position 2702 to 2745 and an anaphase-promoting complex sub-unit 10 domain at position 2803 to 2922, a domain that has been shown to bind to the Smad3 MH2 domain (Nourry et al., 2004) (Fig 35). HERC2 has orthologs in rodents and *Drosophila*. Loss of the HERC2 gene in the *rdf2* mouse causes abnormal juvenile development, juvenile lethally and infertility phenotype (Lehman et al., 1998). Interestingly, it has been described that the HERC2 gene is duplicated at the breaking points of chromosome 15q11-q13, providing END-repeats for potential chromosome homologue recombination, and that there exists rearranged transcripts in Prader-Willi syndrome (PWS) and Angelman syndrome (AS) patients (Amos-Landgraf et al., 1999).

In collaboration with Dr. José Luis Rosa, we tested also by yeast two hybrid assays if the full length or a C-terminal form of RNF8 containing the coil and the RING domains interacted either with a partial clone of HERC1 (from the HECT domain to the end of the protein) and/or the full length of HERC3 or the same proteins carrying a point mutation of the catalytic cysteine of their HECT

domain. None of these proteins interacted with RNF8. Therefore, we conclude that RNF8 interacts with HERC2 but not with HERC1 or HERC3. The interaction of HERC2 with RNF8 is carried out by its carboxy end, the segment where the HERC proteins share the lowest similarity.

The third RNF8 interacting partner identified in our screening corresponded to HIP1, a protein involved in cell survival, protein trafficking and tumorigenesis. Initially, HIP1 was reported to function as a pro-apoptotic protein that activated both the caspase-8-independent or intrinsic and the caspase-8-dependent or extrinsic death-receptor execution pathways (Gervais et al., 2002; Hackam et al., 2000). It was reported that HIP1 binds huntingtin (HTT) or the protein Hippi (HIP1 protein interactor) depending on the length of the polyglutamine expansion in the HTT protein (Gervais et al., 2002), an expansion that causes Huntington's disease (HDCRG, 1993). It was also reported that HIP1 mediates apoptosis through components of the extrinsic cell death pathway by binding HIPPI and then recruiting procaspase-8 (Gervais et al., 2002; Hackam et al., 2000).

In seeming contradiction, more recent reports indicated that over-expression of HIP1 does not induce apoptosis, whereas transfection of HIP1 mutants lacking the N-terminal domain cause apoptosis in multiple cell types (Rao et al., 2003; Rao et al., 2002). The apoptosis mediated by the HIP1 deletion mutant could be inhibited by a dominant-negative version of caspase-9, suggesting that the intrinsic mitochondrial pathway was responsible for the observed cell death (Rao et al., 2002). In an activity that is probably closer to its actual physiologic function, HIP1 mediates receptor uptake at the plasma membrane via endocytosis (Kaksonen et al., 2003; Metzler et al., 2003) of

several receptors such as the epidermal growth factor receptor (EGFR) or transferrin receptor, an activity that confers the protein the ability to transform fibroblasts when stably overexpressed (Rao et al., 2003).

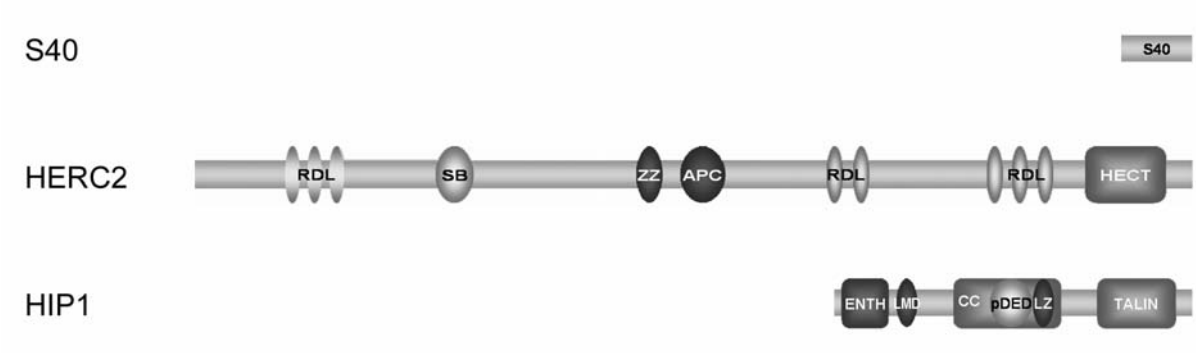

Fig 35. Schematic depiction of the domain architecture of the RNF8 interacting proteins. HERC2 contains RCC1-like domains (RLD), a domain homologous to E6-AP carboxyl terminus (HECT), a steroid binding domain (SB), a zinc finger domain (ZZ) and an anaphase-promoting complex sub-unit 10-like domain (APC10). HERC2 predictions were performed on two domain prediction servers, SMART (http://smart.emblheidelberg. de/) and NCBI Conserved Domain Search (http://www.ncbi.nlm.nih.gov/Structure/cdd/wrpsb.cgi). HIP1 contains an epsin N-terminal homology domain (ENTH), a clathrin binding site (LMD) a central coiled-coil region (CC), overlapping with this domain a pseudo death-effector motif (pDED). a leucine zipper (LZ) and, at the carboxy terminus, a talin-like domain (TALIN) (Gervais et al., 2002; Rao et al., 2001; Rao et al., 2002). S40 has no defined motives or domains.

HIP1 contains an ENTH (Epsin N-terminal Homology) domain at positions 38 to 160, a clathrin binding site at positions 332 to 361, a pseudo-DEAD domain at positions 422 to 503 (involved in procaspase-8 recognition together with Hippi pseudo-DEAD), and a leucine zipper at position 534 to 556. Overlapping with the pseudo-DEAD domain and the leucine zipper, other authors predict a coiled-coil region with multiple interaction motives with the

cytoskeleton. Finally, HIP1 carries a talin-like domain at positions 814 to 1012 (Gervais et al., 2002; Rao et al., 2001; Rao et al., 2002). The HIP1 clone that interacts with RNF8 contained the last 654 amino acids of the protein and thus all the domains described for HIP1 except the ENTH and LMD domains. HIP1 is a highly conserved protein and has homologues from yeast to humans. In humans, there is a HIP1 related protein (HIP1r) with which it shares the central leucine zipper and the actin binding talin homology domain and is more related to endocytic regulation (Engqvist-Goldstein et al., 1999).

4. 2. Proposal of a candidate consensus sequence for recognition by the FHA domain of RNF8

Although the three RNF8 interactors found in our screening do not share any obvious common domain, they all interacted with the FHA domain of RNF8. The FHA domain recognizes phosphoprotein motifs within characteristic sequence strings. Consequently, we tried to identify a consensus sequence present in all RNF8 interactors that could fit known consensus phosphorylation sites, and also the established consensus sequence for recognition by FHA domains. Data obtained from a peptide library screening on several FHA domains revealed a preferential binding for phosphopeptides with the consensus pT-x-x-I/L (Fig. 36, left). Also in this study, Y127_MYCTU FHA and FHA1 of Rad53 showed affinity towards peptides containing a glutamine in position +1 (Durocher et al., 2000). Therefore, we reasoned that a good RNF8-

interacting sequence should contain at least a potentially phosphorylable threonine.

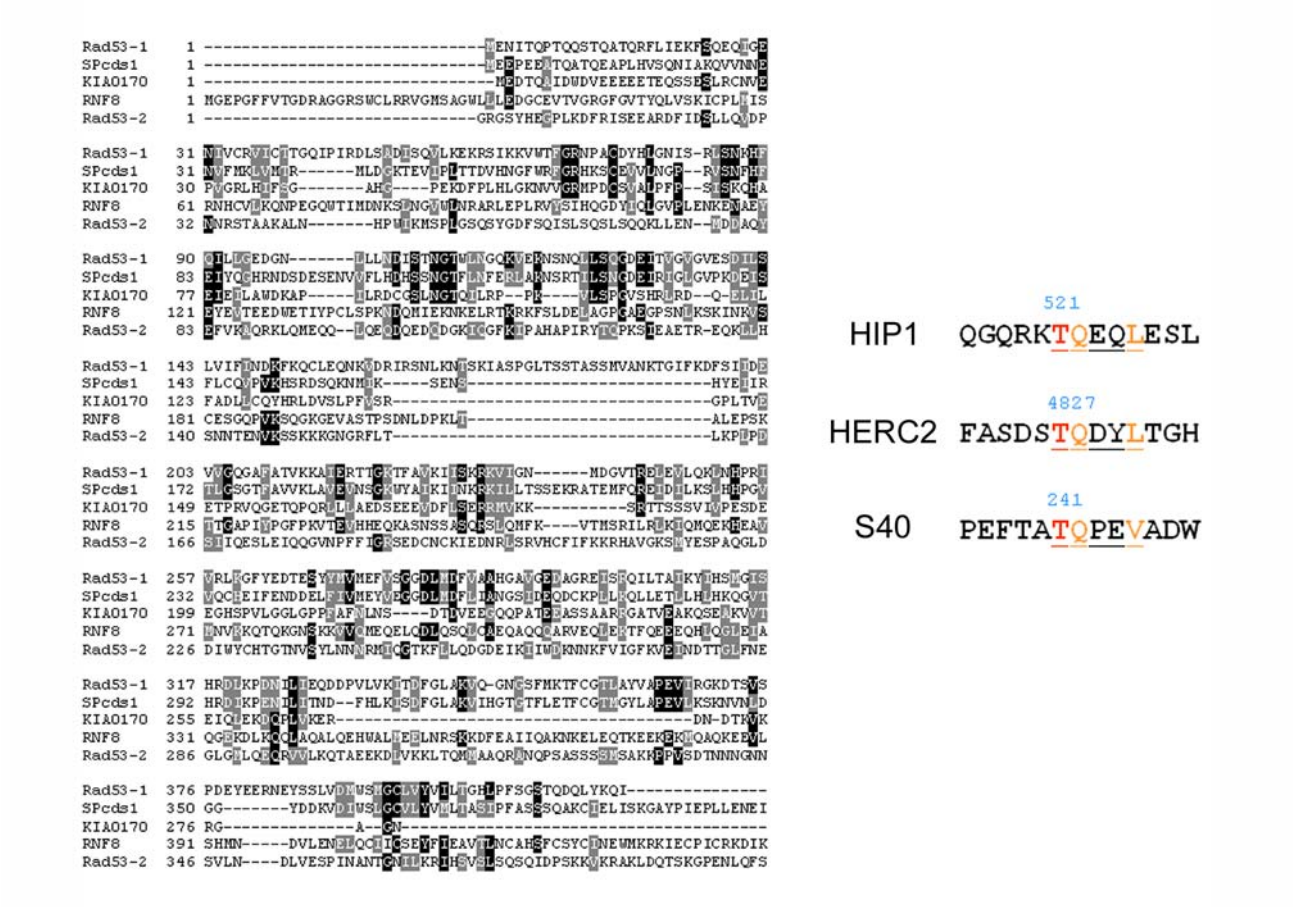

Fig 36. Alignment of FHA domains from several proteins, for comparison with the FHA domain of RNF8. The FHA domains of Rad53 (Rad53-1 and -2), *S.pombe* cds1, KIAA0170, (Durocher et al., 2000) were aligned with the FHA domain of RNF8 using ClustalW. On the right are shown potential phospho-threonine residues on the three RNF8 interactors HIP1, HERC2 and S40. The sequences are consistent with the consensus sequences recognized by FHA domains (Durocher et al., 2000), and they are also putative sites of recognition and phosphorylation by ATM or DNA-dependent kinases (http://scansite.mit.edu).

We compared the sequences of the RNF8 interactors, which revealed a threonine residue within sequences potentially recognized by FHA domains, located at position 521 in HIP1, 4827 in HERC2 and 241 in S40 (Fig. 36, right). Therefore, this threonine seemed to be a good candidate for phosphorylation and subsequent recognition by the FHA domain of RNF8. The consensus sequence containing this threonine is pTQXXL/V. When looking for kinases potentially able to phosphorylate such a site using the scansite tool, only ATM (Ataxia Telangiectasia Mutated) and DNA dependent kinase appear to be good candidates to phosphorylate the above identified threonine residue. It is important to remark that both kinases are activated by DNA breaks and promote a p53 response (Vogelstein et al., 2000b).

4. 3. Confirmation of interaction of RNF8 with HIP1

Of the RNF8 interactors, HIP1 is the only protein for which functional information is available. Consequently, we decided to confirm this interaction in mammalian cells. The plasmid pFlag-HIP1 was kindly provided to us by Michael Hayden (Hackam et al., 2000). RNF8 associated with HIP1 in mammalian cells *in vivo*, as shown by co-immunoprecipitation experiments in Cos-7 cells co-transfected with pHA-RNF8 and pFlag-HIP1 (Fig. 37A). This co-immunoprecipitation required the presence of phosphatase inhibitors in the lysis buffer, suggesting the requirement of phosphorylation for an appropriate interaction. As shown before, HA-tagged wild-type RNF8, when transfected alone, was detected exclusively in the cell nucleus (Fig. 13B). In contrast, HIP1

(also when transfected alone) was observed only in cytoplasmic localizations, in agreement with its original description (Fig. 37C) (Gervais et al., 2002; Hackam et al., 2000). Upon co-transfection of both plasmids in Cos-7 cells, the expression of RNF8 is unexpectedly absent or very weakly expressed 24 h after transfection, at which time HIP1 was seen exclusively in the cytoplasm. Very few co-transfected cells showed a minimal colocalization of both proteins (Fig. 37B). Forty eight hours after co-transfection, both proteins showed a more widespread co-localization, which included an unexpected localization of HIP1 in the nucleus and cytoplasmatic localizations for RNF8. In some cases, RNF8 was again detected in the plasma membrane like the endogenous or GFP-fused protein in telophase (Fig. 20C and 27A). In HeLa cells co-transfected with the two plasmids, both HA-RNF8 and GFP-RNF8 colocalized with Flag-HIP1 already at 24 h post-transfection. These observations indicate that a striking shift in the default subcellular localization of both proteins occurs as a consequence of their overexpression, possibly mediated by their interaction. Interestingly, a potential nuclear localization signal (NSL) could be predicted on HIP1 with the PROSITE motif search starting at lysine 996 to lysine 1007 with the sequence KERQKLGELRKK. Although the nuclear localization for HIP1 observed in our experiments has not been described before, RNF8 can be considered as the third interacting partner for HIP1 that can localize in the nucleus, since Hippi also localizes in the nucleus (Gervais et al., 2002) and sumoylated Htt can localize in the cell nucleus where it promotes its repression of transcription (Steffan et al., 2004b).

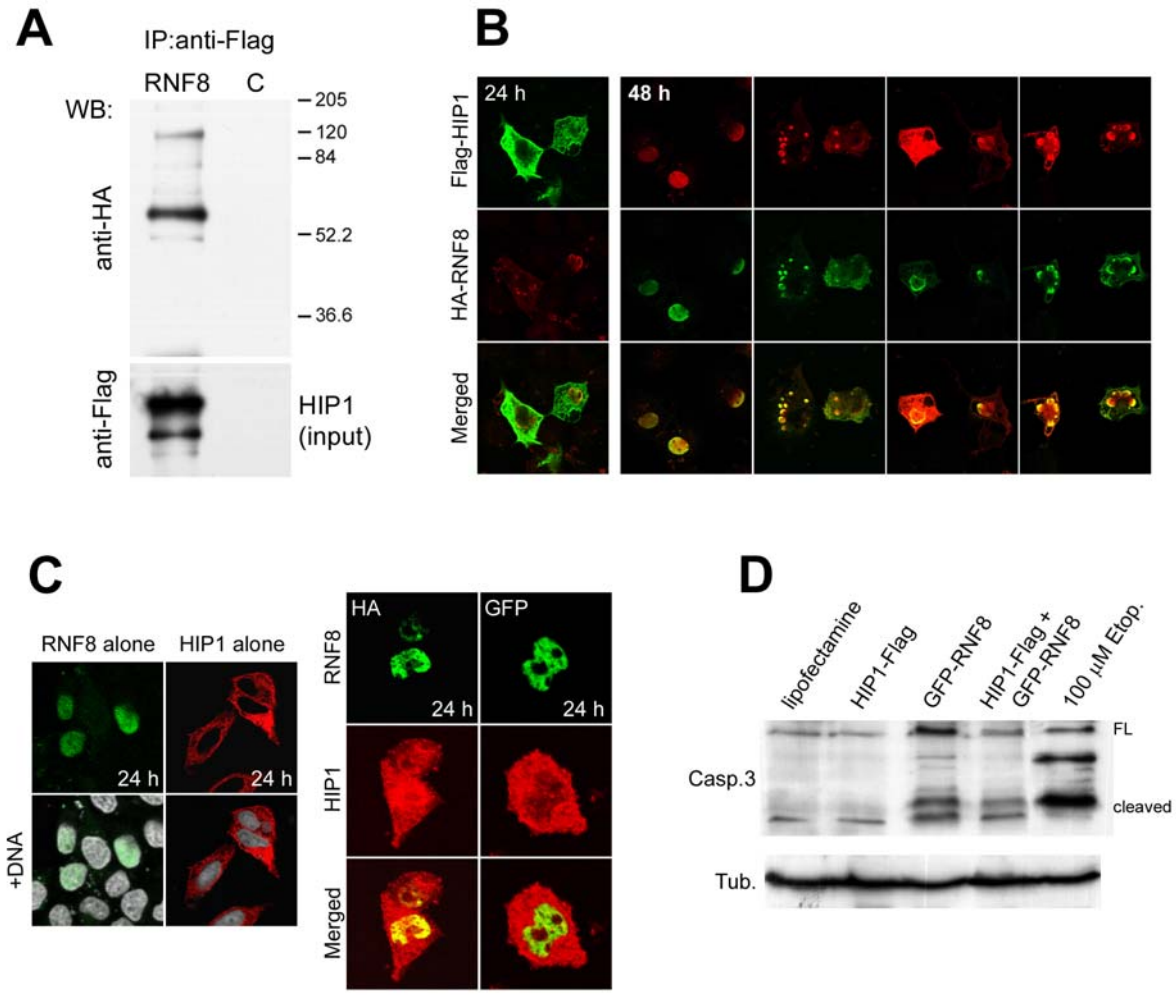

Fig 37. Interaction between RNF8 and HIP1 in mammalian cells. **A**, HIP1 pulls down wild-type RNF8. Extracts of Cos-7 cells co-transfected with Flag-HIP1 and HA-tagged RNF8 were immunoprecipitated with anti-Flag and blotted with either anti-HA for the detection of HA-RNF8, or anti-Flag for the detection of HIP1 (bottom). **B**, Subcellular localizations of HA-RNF8 and of FLAG-HIP1 in transfected Cos-7 cells stained with anti-HA or anti-Flag 24 or 48 h post-transfection analyzed by confocal microscopy. **C**, Immunolocalization of transfected HA-RNF8 and Flag-HIP1 in HeLa cells 24h post-transfection, left panel, or co-transfected Flag-HIP1 with either HA-RNF8 or GFP-RNF8 24h post-transfection. **D**, Caspase-3 protein determination in GFP-RNF8 and Flag-HIP1 transfected HeLa cells. As negative and positive controls lysates from cells treated with Lipofectamine only or 100 μM etoposide were used. “FL” stands for Full-length and “cleaved” for the cleaved form of caspase-3. Normalization was performed by determining tubulin levels on the same membranes.

Real-time RT-PCR analysis shows that HIP1 is expressed mostly in adult testis, brain and kidney. In fetal tissues, HIP1 is also widely expressed, with the highest levels in brain. Therefore, RNF8 and HIP1 are co-expressed in a wide range of tissues and they show a similar expression pattern. (Fig 38)

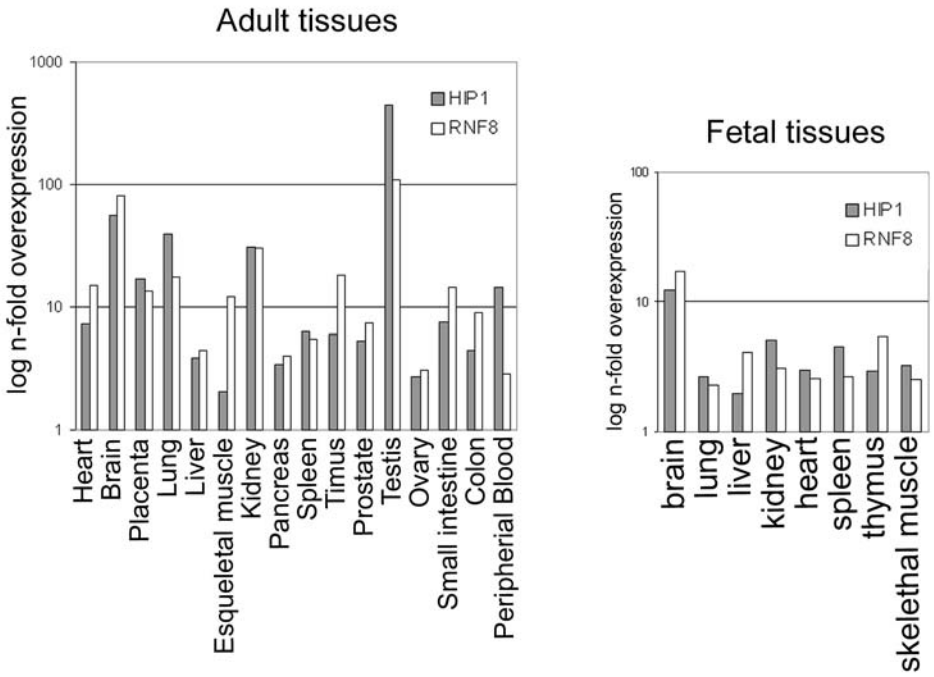

Fig 38. Relative expression levels of the genes HIP1 and RNF8 in normal human adult and fetal tissues, determined by semiquantitative real-time RT-PCR. cDNA collections from adult or fetal tissues were used as templates in Sybr-Green PCR reactions with specific primers, and real-time C_T levels were determined in on a ABI 7700 instrument (see Materials and Methods). C_T values were normalized in each case against values obtained for the reference gene S14r, and then further normalized against the tissue with the lowest expression levels in each set, adult or fetal.

Since both RNF8 and HIP1 are involved in the regulation of apoptosis, we decided to test the effects of their transfection on HeLa cells, using caspase-3 levels and proteolytic activation as an apoptosis marker. The levels of pro-

caspase-3 and active caspase-3 proteolytic forms were not enhanced upon HIP1 over-expression in comparison to the control (Fig. 37D), which is more in agreement with the proposed non-apoptotic nature of the protein (Rao et al., 2003; Rao et al., 2002). Also in agreement with an anti-apoptotic activity, overexpression of HIP1 prevented the increase in pro-caspase-3 and active caspase-3 that were stimulated by over-expression of RNF8 (Fig. 37D). Further experiments need to be undertaken in order to determine if the RNF8 pro-apoptotic activity is enhanced in HIP1 deficient cells and if RNF8 overexpression can revert the transforming phenotype of HIP1.

DISCUSSION

1. K63-polyubiquitylation

Polyubiquitylation that uses the lysine on position 63 of ubiquitin is mediated by the heterodimeric E2 formed by UBC13 and UEV, in which UBC13 is the catalytic subunit and UEV is the regulatory subunit (Hofmann and Pickart, 1999). This heterodimeric arrangement is unique for an E2 enzyme in that it serves the purpose to force the positioning of lysine 63, rather than 48, 29 or other lysines on the ubiquitin polypeptide, as the residue available for isopeptide bond formation with the carboxyterminal glycine of the following ubiquitin in the elongation of polyubiquitin chains (VanDemark et al., 2001). Tagging of substrate proteins with this modification does not appear to target them for destruction by the proteasome (Spence et al., 2000b; Wang et al., 2001b), and this modification is essential for the regulation of relevant biochemical pathways and cellular processes, including postreplicative DNA repair (Broomfield et al., 1998; Ulrich and Jentsch, 2000; Xiao et al., 2000) in yeasts, or signal transduction (Deng et al., 2000a; Shi and Kehrl, 2003; Wang et al., 2001b) and cell motility (Didier et al., 2003) in mammalian cells. It is therefore of great interest to identify which substrates and biochemical pathways are potentially susceptible of regulation by K63 polyubiquitylation. Our yeast two-hybrid screening of a human fetal brain library using UBC13 as a bait yielded as interaction partners UEV1 and two additional proteins, RNF8 and KIAA0675. Both proteins contain RING finger proteins, through which they interact with

UBC13. Additional screenings of other cDNA libraries have also yielded, in addition to UEV1 or UEV2, other RING finger proteins as the only interaction partners for UBC13 (data from our lab, not shown). This suggests that only two surfaces on UBC13 are used for high affinity protein-protein interactions, one with UEV proteins, and the second with RING finger domains. Both RNF8 and KIAA0675, which interacted with UBC13, also interacted with a second E2, UBE2E2, the human homologue of yeast Ubc4/5p. The occurrence of these cross interactions between different E2's with a variety of RING finger domains is well documented (Ito et al., 2001; Ulrich, 2003; Winkler et al., 2004), and reflects the fact that a given RING finger domain can recruit more than one type of E2's to an E3. In most cases the different E2's thus recruited may have interchangeable functions in the ubiquitylation of substrates simultaneously recruited to the E3, and the choice of E2 to be tethered to the complex may depend solely on its availability in a particular cell type or process, or coincident subcellular localizations. The recruitment of UBC13 and other E2's to the RING finger domain of RNF8 or KIAA0675 implies that the same E3 can function as a ligase in more than one class of polyubiquitylation, and therefore the specific E2 recruited determines the function of the E3 in the final fates of the modified substrate proteins. This is likely to be the case for CHFR in K48 and K63 polyubiquitylations (Bothos et al., 2003; Chaturvedi et al., 2002; Kang et al., 2002; Scolnick and Halazonetis, 2000), and in this sense would be similar to the recruitment of Ubc9 or UbcH7 for the alternative functions of Mdm2 and other E3's in either sumoylation or K48 polyubiquitylation of substrates (Buschmann et al., 2000).

Both RNF8 and KIAA0675 have features characteristic of ubiquitin ligases. They both contain a RING finger domain which functions by recruiting ubiquitin-conjugating enzymes (Ciechanover et al., 2000; Joazeiro and Weissman, 2000), namely RNF8 is able to recruit UBE2E2 (Ito et al., 2001) and UBC13 (Plans et al, in press) and KIAA0675 UBC13, UBCH6 and UBE2E2 (Plans et al, in press). In addition, both proteins contain other domains involved in protein recognition, namely FHA in the case of RNF8 and Tetratricopeptide repeats in the case of KIAA0675 apart from their coiled-coil domains. Both proteins can function as self-ubiquitin ligases *in vivo* (Kreft and Nassal, 2003; Moore et al., 2003)(Plans et al., in press). $RNF8^{WT}$ can be modified by polyubiquitin chains that use predominantly the lysines at positions 29, 48 and 63. In contrast, the RING-dead mutant $RNF8^{C403S}$ fails to be modified by UbK29,63R and UbK29,48R but is still modified by UbK48,63R. Therefore, RNF8 functions as a self ubiquitin ligase for polyubiquitylation through lysines 48 and 63 of ubiquitin, probably mediated by UBE2E2 and UBC13, respectively. However, polyubiquitylation of RNF8 with K29-type polyubiquitin chains does not require its own functional RING finger domain, suggesting that this modification of RNF8 is mediated by a different E3, rather than by itself. The lack of detectable polyubiquitylation of the RING-dead mutant of RNF8 by the ubiquitin variants with lysines mutated at residues 48 and 63 would argue that lysines on the ubiquitin molecule other than those at positions 29, 48 or 63 are not likely to be used to a significant degree for the polyubiquitylation of RNF8.

2. Possible functions of RNF8 in the metaphase-anaphase transition

Beyond its activity as a ubiquitin ligase, we have studied several biological properties of RNF8. We have found that the localization and the levels of this protein are modulated in a cell-cycle specific manner. The localization of RNF8 in well-defined mitotic structures such as the polar and central microtubule spindles and the midbody of mitotic bridges during cytokinesis strongly suggests that this protein plays a role in several mitotic transitions. Furthermore, our observation that RNF8 protein levels increase steadily until reaching a peak before metaphase, followed by an abrupt disappearance in anaphase, suggests that either it is necessary for a critical function in metaphase, or its destruction is required for progression beyond metaphase, or both. However, depletion of RNF8 by means of specific siRNAs does not produce any obvious consequences in the cycle of HeLa cells. And, somewhat contrary to what we had expected, overexpression of RNF8 by transient transfection caused an accumulation of cells in G1, but not G2-M. Yet, the existence of a functional connection of RNF8 with mitosis is hinted from the facts that the cells in which this protein is overexpressed fail to undergo mitotic arrest by the microtubule depolymerizing drug nocodazole and simultaneously become sensitized to nocodazole-induced apoptosis. Moreover, RNF8 depleted cells show difficulties in recovering from nocodazole treatment which results in a delay in mitotic exit.

Taken together, these observations may point to a link of RNF8 to the control of mitotic checkpoints, but not to the regulation of mitotic transitions in a

“basal” cell cycle. A mitotic checkpoint can be defined as the activation of processes that prevent progression through mitosis in response to defects in structures or proteins whose functions are necessary for the transitions between the different mitotic phases. For example, depolymerization of microtubules by nocodazole during mitosis prevents the attachment of spindle microtubules to kinetochores, which results in condensed chromosomes that are not subjected to mechanical tension and biorientation. This sets in action a number of mechanisms that prevent the activation of the anaphase promoting complex (APC), which would otherwise result in untimely and fatal separation of sister chromatids through degradation of securins. Removal of nocodazole permits the polymerization and growth of microtubules, and kinetochores can become attached to the plus end of spindle microtubules and they are then subjected to sufficient bipolar tension, which eventually relieves APC-C inhibition (Gorbsky, 2001; Hongtao, 2002; Hoyt, 2001; Millband et al., 2002; Shah and Cleveland, 2000). Several molecules are involved in blocking APC-C activity in response to mitotic stress, including the checkpoint proteins Mad2, BubR1, Bub1 or Bub3, that sequester the APC-C regulatory protein Cdc20, thus preventing the function of this complex in the ubiquitin and proteasome-dependent degradation of substrates such as cyclin B, Pds1 or securin (Gorbsky, 2001; Hongtao, 2002; Hoyt, 2001; Millband et al., 2002; Shah and Cleveland, 2000). The molecules that sense a failed microtubule attachment to kinetochores or loss of bipolar tension have not been identified unambiguously, but the ternary complex formed by the serine-threonine kinase Aurora B, the IAP-related protein survivin, and the histone-like protein INCENP appears to play a fundamental role in this process (Stern, 2002; Stern and Murray, 2001; Tanaka, 2002;

Tanaka et al., 2002). The details of how this sensing directs mitotic checkpoint proteins to Cdc20 and APC-C for its inhibition are only partially known.

The relief of nocodazole-induced checkpoint activation and subsequent arrest in mitosis by overexpression of RNF8 as well as the delayed exit from mitosis observed in the absence of RNF8 might suggest that RNF8 regulates either checkpoint proteins, or proteins that regulate the sensing of kinetochore-microtubule attachment. The sensitization of cells to nocodazole-induced apoptosis when RNF8 is overexpressed also indicates a functional association of this protein with the mitotic checkpoint. For example, downregulation or depletion of the Mad2 mitotic checkpoint protein permits the escape from the checkpoint arrest induced by nocodazole, and at the same time causes a p53-dependent apoptosis that is associated with aberrant chromosome segregation and micronucleation (Wang et al., 2004), which are phenotypes strikingly reminiscent of those induced by overexpression of RNF8. Other laboratories have also shown that functional disruption of the mitotic checkpoint components mediates either apoptosis or arrest in G1 following evasion of mitotic arrest by inhibitors of microtubule assembly (Bharadwaj and Hongtao, 2004; Hongtao, 2002; Margolis et al., 2003). In this context, it should be mentioned that, once the mitotic structures are in order, this must be sensed, and the checkpoint must be inactivated to allow mitotic progression. How this occurs is not known at present.

In addition, the domain architecture of RNF8, consisting of one RING finger domain, and one FHA domain, can be found in only 4 other proteins, CHFR in metazoans, Dma1p in *S. pombe* and Dma1/2p in *S. cerevisisae*, all which are known to participate in G2-M checkpoints (Chaturvedi et al., 2002;

Fraschini et al., 2004; Guertin et al., 2002b; Murone and Simanis, 1996; Scolnick and Halazonetis, 2000).

Interestingly, survivin plays a dual role in the regulation of apoptosis and mitotic spindle checkpoint control, and disruption of survivin-microtubule interactions results in the caspase 3-dependent death of HeLa cells (Beltrami et al., 2004; Li et al., 1998). These functional similarities make the Aurora B-survivin- INCENP complex an attractive candidate for regulation by RNF8. However, in our experiments RNF8 does not appear to localize to kinetochores in metaphase chromosomes (which Aurora B, survivin and INCENP do), and therefore how this potential functional link can be explained by such divergent localizations remains to be seen. In this regard, it should be mentioned that we have not determined the localization of RNF8 under mitotic stress. A reasonable approach to answer these questions is to undertake unbiased searches for RNF8 interaction partners. As discussed below, our yeast two-hybrid survey using RNF8 as bait has not provided clear-cut and direct answers that help to define the function of RNF8 in the mitotic checkpoint. A second approach would be to pull down RNF8-interacting proteins from a lysate of synchronized cells followed by mass spectroscopy analysis, a technologically demanding project but potentially very rewarding.

3. Possible function of RNF8 in cytokinesis

Our observations show that the expression of RNF8 attains peak levels before metaphase, after which the protein all but disappears and becomes

barely detectable by immunocytochemistry until cells exit mitosis. At cytokinesis RNF8 is associated both with the nucleus and the midbody of the mitotic bridge. When RNF8 is overexpressed, and the cell death that usually results from this overexpression is prevented by treatment with caspase inhibitors, the association of the transfected protein with the mitotic bridge midbody remains. Hence, this localization is physiological and could reflect a function in cytokinesis for RNF8. In addition to its localization in the mitotic bridge midbody, ectopically expressed RNF8 localized at the mitotic spindles. Although we have not seen such localizations for the endogenous protein, this has not been studied under conditions of mitotic stress, which, as mentioned in Results first objective, increase the levels of endogenous RNF8. Indeed, our overexpression experiments suggest that the function of RNF8 in this localization is to accelerate chromosome segregation. In addition, our RNF8 depletion experiments by siRNA show that a delay in mitotic exit occurs only under conditions of mitotic stress. This suggests once more that the putative function of RNF8 in mitotic exit or cytokinesis is not engaged under basal cell cycle conditions, but only under stress or signals that disrupt the cell cycle.

Faithful chromosome segregation requires the mitotic spindle to be correctly positioned with respect to the cell division axis, and cytokinesis takes place only after this task is achieved and the two sets of chromosomes are sufficiently far apart. Unscheduled cytokinesis before proper chromosome segregation leads to formation of anucleate and polyploidy cells. Eukaryotic cells prevent these harmful events by a surveillance mechanism, called spindle position checkpoint, that delays cytokinesis in the presence of mispositioned or misoriented spindles until errors are corrected. This control is particularly critical

for organisms, such yeasts and higher plants, which specify the site of cytokinesis before spindle assembly, but may also be functional in mammalian cells.

The spindle position checkpoint is well characterized in *S. cerevisiae* and requires the Bub2 and Bfa1 proteins (Bardin et al., 2000; Bloecher et al., 2000; Pereira et al., 2000), which form a two-component GTPase-activating protein inhibiting the G protein Tem1 (Geymonat et al., 2002), which is in turn required to activate the mitotic exit network (MEN) in telophase (Simanis, 2003). Tem1-dependent activation of the MEN leads to the release from the nucleolus of the Cdc14 protein phosphatase, which is crucial to promote inactivation of cyclinB-dependent CDKs at the end of mitosis (Visintin et al., 1998). Inhibition of such CDKs is an essential prerequisite for spindle disassembly and cytokinesis at the end of the cells cycle and is obtained in budding yeast by both anaphase promoting complex (APC)- mediated proteolysis of their cyclin subunits and accumulation of the CDK inhibitor Sci1 (Zachariae and Nasmyth, 1999). The MEN has a similar structural organization to fission yeast septation initiation network (SIN), which is required for cytokinesis but not for mitotic exit (Simanis, 2003). *Schizosaccharomyces pombe* Dma1 is required for SIN inhibition in the presence of spindle damage (Guertin et al., 2002; Murone and Simanis, 1996). Fraschini et al. (2004) have shown that *S. cerevisiae* Dma1 and Dma2 are involved in proper septin ring positioning and cytokinesis, such that the simultaneous lack of Dma1 and Dma2 leads to spindle mispositionting and defects in the spindle position checkpoint. Conversely, they have shown that overexpression of Dma2 caused cytokinetic defects that were partially suppressed by hyperactivation of the MEN by either Bub2 deletion or Tem1

overexpression. As described above, these proteins are homologous to human CHFR (Scolnick and Halazonetis, 2000), sharing a forkhead-associated domain and a RING finger motif.

Although only partially characterized, the regulation of mitotic exit and cytokinesis in mammalian cells shares many structural and regulatory features with yeasts. And, again, the similar domain composition of RNF8 to the FHA- and RING finger bearing mitotic checkpoint proteins, and its specific localization and effects on cytokinesis observed in our study, lead us to consider its possible involvement also in the regulation of cytokinesis and the mammalian equivalent of the yeast spindle position checkpoint. Depletion of RNF8 followed by mitotic stress produced by nocodazole delayed cyclin B1 degradation and mitotic exit. In addition, in the presence of caspase inhibitors, ectopic expression of RNF8 caused accelerated mitosis, as deduced from the presence of an excess of mitotic cells with uncleaved mitotic bridges, and of cells attached through multiple mitotic bridges. Also, cells that are still in metaphase appear attached through mitotic bridges to cells that are in other phases, which indicates that ectopic expression of RNF8 can trigger initiation of cytokinesis without completion of mitosis. This unscheduled triggering of cytokinesis could be due to the inactivation of a spindle position checkpoint in the presence of ectopic RNF8. This checkpoint should normally be activated by the aberrant chromosome segregation or incorrectly positioned spindles that would result from bypassing the spindle assembly checkpoint by overexpression of RNF8, as discussed above. Instead, ectopic expression of RNF8 appears to also inactivate the cytokinesis checkpoint, leading to either untimely entry into the G1 phase of the following cycle, or to apoptosis.

Dysfunction of cytokinesis can cause arrest in G1, for example by activation of the p53-dependent tetraploidy checkpoint (Margolis et al., 2003). However, the accumulation in G1 of HeLa cells expressing ectopic RNF8 is not accompanied by increased protein levels of p53 or $p21^{CIP/WAF}$, or by changes in the levels of transcripts for p53, $p21^{CIP/WAF}$, $p15^{INK4B}$, $p27^{KIP1}$ or $p57^{KIP2}$ (V.P., J.D.M., and T.M.T., unpublished observations). Although a more detailed study of the status of these proteins in RNF8-overexpressing cells is needed, our preliminary observations suggest that other proteins or mechanisms are involved in the RNF8-induced arrest of HeLa cells in G1.

4. RNF8 and apoptosis

Concomitant with the effects related to the two mitotic checkpoints discussed above, spindle assembly and cytokinesis, ectopic expression of RNF8 invariably triggers caspase-dependent apoptosis. This could be a direct consequence of aberrant chromosome segregation that occurs in the absence of appropriate activation of the spindle assembly checkpoint, accompanied by untimely DNA replication (Castedo et al., 2004; Margolis et al., 2003). Additional observations described in this study, however, also suggest that RNF8 may play more general roles in apoptosis that are not necessarily linked to the regulation of mitotic checkpoints. We have shown that the apoptosis caused by wild-type RNF8 induces, and depends on, the activation of caspases, in particular caspases 3 and 8. This is accompanied by increased levels of pro-caspase-3, probably by stabilization or diminished degradation of the protein,

since transcript levels remain unchanged. Furthermore, proapoptotic stimuli, such as incubation with the topoisomerase inhibitor etoposide, the alkylating agent cis-platinium, or exposure to ultraviolet light, all induce a marked dose-dependent accumulation of RNF8, again not due to increased gene transcription but likely to enhanced protein stability. Finally, depletion of RNF8 by specific siRNA duplexes protects the cells from the caspase-dependent apoptosis induced by etoposide.

Together, these observations suggest that RNF8 is a pro-apoptotic protein and that its ubiquitin ligase activity is critical to achieve this function. The observed activation of caspase-8 but not caspase-9 might imply that RNF8 targets the extrinsic death-receptor apoptotic pathway. However, the fact that depletion of RNF8 is accompanied by a significant decrease in the etoposide-induced levels of full-length pro-caspase-3 might suggest that RNF8 directly or indirectly regulates caspase-3 protein stability. One might speculate that RNF8 could bind directly to caspase-3 or other caspases, and target them for modification by K63-dependent polyubiquitylation or even sumoylation for protection from K48-dependent polyubiquitylation and proteasome-dependent degradation. Although this is an interesting possibility, it should be mentioned that RNF8 lacks known caspase recognition domains.

The inhibitors of Apoptosis Proteins are a family of proteins characterized by one or more BIR domains (baculoviral IAP repeat) by which they bind caspases and function as endogenous caspase inhibitors (Liston et al., 2003). RING finger domains are also characteristic from this family and can be found in XIAP, c-IAP1 c-IAP2 and Livin carboxy terminal (Duckett et al., 1996; Lin et al., 2000; Liston et al., 1996; Rothe et al., 1995; Uren et al., 1996). However the

best studied IAP, survivin, does not have a RING finger domain (Li et al., 1998). All these proteins can inhibit effector caspases (3 and 7) and notably XIAP and c-IAP2 function as ubiquitin ligases to modify caspase-3 and -7 by polyubiquitylation and proteasomal degradation (Huang et al., 2000; Suzuki et al., 2001b). In turn, IAPs are regulated by mainly three proteins, XAF1, Smac/Diablo and Omi which can either delocalize IAPs from the cytoplasm to the nucleus and inhibit their binding or their E3 activity towards caspases (Creagh et al., 2004; Liston et al., 2001; Suzuki et al., 2001a). Although RNF8 does not have a BIR domain, its RING finger domain and ubiquitin ligase activity could be involved in the regulation of caspases, as hypothesized above, or IAPs. IAPs are rapidly degraded by the proteasome under proapoptotic stimuli such as etoposide (Liston et al., 2003; Yang et al., 2000). It would be very interesting to investigate if RNF8 exerts its apoptotic activity by binding, and promoting the degradation (or misslocalization) of one or more of the IAP that regulate caspase-3. From their known subcellular localizations and functions both in cell survival/apoptosis and cell cycle, the most likely IAPs that would be candidates for functional interaction with RNF8 are cIAP and survivin. A recent report reveals that cIAP1 localizes to the nuclear compartment and modulates the cell cycle (Samuel et al., 2005).

5. Possible stabilization of RNF8 by posttranslational modifications

We have shown that RNF8 can be the subject of several posttranslational modifications such as K48- and K63 based polyubiquitylations and sumoylation. However, the biological significance of these modifications remains to be analyzed. It is possible that K63-polyubiquitylation and sumoylation of RNF8 target the same lysine residue on RNF8 that is modified by K48-polyubiquitylation and hence protects the protein from degradation, in a situation akin to PCNA (Hoege et al., 2002). Such RNF8 stabilization could be useful in certain situations such as when the cell undergoes programmed cell death, to signal DNA damage response or for recovery after spindle checkpoint activation. This regulation could acutely alter the normal cell cycle turnover of RNF8 by rapidly increasing the protein levels without new protein synthesis.

We have tried to investigate RNF8 sumoylation with respect to PML-bodies and their ability to function as transcriptional platforms (Hofmann and Will, 2003), notably for p53 or for other FHA-containing transcriptional factors to trigger several responses including cell death (Rokudai et al., 2002; Sax et al., 2002). Several proteins localize in PML nuclear bodies after sumoylation, including PML itself, Sp100, Daxx, p53 and CBP (Girdwood et al., 2003; Gostissa et al., 1999; Ishov et al., 1999; Jang et al., 2002; Sternsdorf et al., 1997). In addition, RNF8 had been reported to interact with Retinoid X Receptor α and to enhance its transcriptional activity (Takano et al., 2004). Although RNF8 localizes mainly in the cell nucleus forming a dense dotted pattern, it colocalized only partially with PML-bodies. Our data suggests that the

regulation of caspase-3 by RNF8 does not imply an increase on caspase-3 mRNA levels and that overexpression of RNF8 has no influence in the levels of transcripts for p53, $p21^{CIP/WAF}$, $p15^{INK4B}$, $p27^{KIP1}$ or $p57^{KIP2}$ (V.P., J.D.M., and T.M.T., unpublished observations). Hence, none of the conditions to postulate that sumoylation of RNF8 target the protein to PML nuclear bodies where it would enhance gene transcription of target genes that would explain the phenotype observed under overexpression conditions were satisfied.

6. RNF8-interacting proteins

Our yeast two-hybrid screening using RNF8 as bait has found three RNF8 interactors: the actin-associated protein HIP1 (huntingtin-interacting protein 1), the large HECT domain protein HERC2, and the ribosomal protein S40. All three proteins interact with the FHA domain of RNF8, which suggests that RNF8 recognizes specific phosphoaminoacid sequences on these three proteins.

Human HIP1 was found as a protein that interacts with the large protein huntingtin (htt), the mutation of which is causally associated with Huntington's disease, a severely disabling neurodegenerative disorder (HDCRG, 1993). The best known function of HIP1 is as a regulator of endocytosis and vesicular traffic, functions similar to those of the HIP1 orthologue in the yeast *S. cerevisiae*, Sla2p (Hyun and Ross, 2004). A great deal of interest was generated when the laboratory of Michael Hayden reported that HIP1 mediated the recruitment and activation of caspases 3 and 8, resulting in apoptosis,

especially in the presence of htt forms bearing a polyglutamine expansion (Gervais et al., 2002). Subsequent reports have qualified this putative proapoptotic function of HIP1, in that only partial fragments of the protein may be proapoptotic, while full-length HIP1 may actually protect cells from caspase-dependent apoptosis (Rao et al., 2003; Rao et al., 2002). In fact, HIP1 has been found to be expressed at high levels in a number of neoplasias (Rao et al., 2002), and its overexpression induces a transformed phenotype in fibroblasts (Rao et al., 2003). Therefore, our finding that HIP1 protects cells from RNF8-induced death is consistent with an antiapoptotic function, rather than the proapoptotic function proposed by the Hayden lab for HIP1.

How HIP1, a protein that is predominantly cytoplasmic and associated with the Golgi network and vesicles, encounters RNF8, which localizes predominantly in the nucleus, is an interesting question. Our co-transfection experiments suggest that both HIP1 and RNF8 shift their predominant subcellular localizations when they are both expressed ectopically. Also, our analysis of the localization of RNF8 throughout the cell cycle has shown that it can localize in the cytoplasm and in a subcortical compartment at the end of mitosis. Therefore, it is possible that high levels of HIP1 favor the maintenance of extranuclear localizations of RNF8. In other words, HIP1 might sequester RNF8 from the nucleus, thus preventing its possible functions as an apoptosis. This interaction does not help to answer the question of the mechanisms by which RNF8 triggers apoptosis or its role in checkpoint monitoring and activation. In any case, and in view of the interaction between HIP1 and Huntingtin, it would be interesting to explore whether RNF8 plays any role in the

apoptosis and neuronal degeneration that results from disease-generating variants of Huntingtin.

The second RNF8 interactor, HERC2, contains a HECT domain at its carboxy terminus, and several RCC1 repeats. The study of the functional consequences of this interaction is greatly hampered because the function of HERC2 has not been characterized in any detail (although there is a spontaneous mouse mutant in which Herc2 has been found to be defective; (Lehman et al., 1998)). From its domain composition one can deduce that HERC2 is a ubiquitin ligase through its HECT domain, and one can speculate that it might have a function in chromatin architecture or in nucleo-cytoplasmic transport associated with its RCC1 domains. RCC1 stimulates the rate of exchange of GTP for GDP on Ran in the vicinity of chromosomes. As a result of this activity, Ran-GTP releases NuMa and TPX2 which stimulate microtubule stabilization and spindle assembly (Carazo-Salas et al., 1999; Kahana and Cleveland, 2001). Should HERC2 display a GEF activity on Ran, there would be a direct connection between RNF8 and spindle assembly.

7. A function for RNF8: hypotheses and proposals

RNF8 is one of only four proteins in all organisms that contain both a FHA domain and a RING finger domain. The other three proteins are, in metazoans, CHFR, and in yeasts, Dma1p (and its paralogue Dma2p) and Dun1p. Of these four proteins, three, CHFR, Dma1p (and Dma2p), and Dun1p have been shown to regulate distinct mitotic checkpoints. The studies described

here also suggest a participation of the fourth FHA-RING finger protein, RNF8, in at least two mitotic checkpoints, spindle assembly and cytokinesis. However, the mode of participation of RNF8 in these checkpoints, as deduced from our observations, appears to be quite unique: its overexpression apparently disables both checkpoints, ushering the cells out of mitosis even in the presence of aberrant mitotic structures or incorrect chromosome segregation. This is a fatal combination of events that sooner or later leads to apoptosis.

One lingering question could be: what might be the use of a protein that appears to counter the beneficial effects of checkpoint activation in the face of problems in mitosis? One possible answer might be that RNF8 is a mediator of programmed death of cells in which mitotic structures damaged beyond possible repair. The molecular couplings that link mitotic damage sensing, RNF8 activation, and then caspase recruitment and activation are areas of study that need to be resolved in the future. These links could be associated with either direct protein-protein interactions, or through transcriptional regulation, given the fact that RNF8 has been reported to function as a transcriptional co-factor for the nuclear receptor RXRα (Takano et al., 2004).

Yet, granting that directing mitosis defective cells to their death is one function of RNF8, what might be the need to disable two checkpoints, spindle assembly and cytokinesis, and bring the damaged cells all the way to the next G1 before triggering apoptosis? One possible answer might be that RNF8 has a second function, perhaps in sensing and signalling the correction of the damage, which has not been explored in our studies. Different stimuli that induce mitotic (nocodazole and taxol) or DNA (etoposide, cis-Pt, UV light) damage cause markedly increased levels of endogenous RNF8. These levels

are not as high as those attained with ectopic expression by transient transfection, and there might be a critical threshold of expression of RNF8 above which caspase-dependent death is the prevailing effect, while below the threshold the prevailing effect might be that of relief from checkpoint blocks once the damage has been corrected. A possible approach to study these possibilities would be to engineer cells in which RNF8 expression levels can be modulated experimentally by addition or removal of molecules that do not affect the cell cycle, such as a tet-off conditional expression system, A second approach would be to carefully quantitate the damage caused by mitotic or genotoxic stress in cells depleted of RNF8. Our experiments have shown that depletion of RNF8 protects cells from death by genotoxic agents, but we have not determined the level of damage sustained by these cells, and, more importantly, the extent or rate of damage correction. Direct assessment of mitotic or DNA damage repair is certainly not an easy task, and these are usually determined through indirect evidence, such as the rate of cell cycle progression. Nevertheless, one could design experiments to detect and quantitate the re-attachment of spindle microtubules to kinetochores, or to estimate the rate of repair of damaged DNA by genetic monitoring.

CONCLUSIONS

1. Our yeast two hybrid screening of a human fetal brain library revealed three interacting partners for the ubiquitin conjugating enzyme UBC13: UEV1, RNF8 and KIAA0675. The last two are RING finger proteins, a domain through which they interact with UBC13 and other E2 enzymes, such as UBE2E2 and UBCH6. RNF8 and KIAA0675 are co-expressed in multiple adult and fetal tissues.

2. RNF8 co-immunoprecipitates and colocalizes with UBC13 in Cos-7 cells. This interaction depends on the integrity of the RING finger domain of RNF8, suggesting that this domain is essential for the interaction.

3. RNF8 has ubiquitin ligase activity on itself for K48- and K63-polyubiquitylations. K63-autopolyubiquitylation of RNF8 requires the catalytic activity of UBC13. RNF8 may be ubiquitylated by another E3 which promotes K29-based polyubiquitylation. In addition, RNF8 can be sumoylated.

4. Endogenous RNF8 localizes mainly in the cell nucleus forming a dotted pattern which colocalize only partially with some nuclear structures, the nuclear or PML bodies. UBC13 localizes more widely, notably in the nucleus, cytoplasm and plasma membrane. RNF8 has a cell cycle-dependent turnover with levels of the protein increasing from S to G2-M phases, followed by an abrupt decline in metaphase-anaphase. RNF8 can localize in several mitotic structures such as

polar and central mitotic spindles and at the midbody between the two daughter cells in cytokinesis.

5. RNF8 over-expression arrests HeLa cells in early G1. This arrest is more efficient with wild type RNF8 than with the RING-dead variant of the protein. G1 arrest persists when protecting cells from death for the WT protein and the RING-dead mutant shows a significant increase in the G2-M population. Depletion of RNF8 has no effect on the basal cell cycle.

6. Over-expression of RNF8 causes escape from the mitotic arrest induced by nocodazole, a drug that prevents microtubule polymerization. Depletion of RNF8 delays mitotic exit after nocodazole treatment and release.

7. RNF8 over-expression promotes cell death executed by caspases in a RING-dependent manner. Depletion of RNF8 in HeLa cells results in a protection from the apoptosis induced by treatment with the drug etoposide. Several pro-apoptotic stimuli enhance protein levels of RNF8 without involving new gene expression. In apoptotic cells, RNF8 is associated with micronuclei and collapsed nuclei. Hence, RNF8 is a pro-apoptotic protein that triggers cell death and it participates in the apoptosis induced by several damaging stimuli.

8. In addition to its E2 interactions through its RING finger domain, RNF8 interacts with three other proteins through its FHA domain: Huntingtin interacting protein 1 (HIP1), HERC2 and S40. Simultaneous over-expression of HIP1 and RNF8

can shift their default subcellular localizations. Overexpression of HIP1 protects cells from the death induced by RNF8 over-expression.

RESUM EN CATALÀ

1. INTRODUCCIÓ

1.1. Característiques generals de la ubiquitinació

La ubiquitinació és una modificació post-traduccional de les proteïnes. Durant molt de temps es va creure que la ubiquitinació era una modificació post-traduccional limitada que permetia només senyalitzar la degradació de proteïnes no desitjades pel proteasoma. Estudis recents han evidenciat que la ubiquitinació pot implicar un gran ventall de possibilitats per a la proteïna així modificada, potser tant ampli com la fosforilació, i que es poden transmetre senyals únics mitjançant diferents tipus d' ubiquitinació (Fig 1). La ubiquitinació regula molts tipus diferents de senyalitzacions cel·lulars i processos biològics com l'endocitosi, el tràfic vesicular, la reparació del DNA, la transcripció, el control de qualitat de proteïnes, el cicle cel·lular, l'apoptosi, la resposta immune, la transducció del senyal o la degeneració neuronal (Hershko and Ciechanover, 1998; Hicke and Dunn, 2003; Jesenberger and Jentsch, 2002; Kloetzel, 2001; Muratani and Tansey, 2003; Reed, 2003).

1. 2. La molècula ubiquitina

La ubiquitina és una molècula molt conservada de 76 aminoàcids (~8 kDa) que trobem en tots els organismes eucariotes (Ozkaynak et al., 1984). La ubiquitina posseeix set lisines que poden potencialment promoure la seva conjugació a la proteïna substrat o a una altra ubiquitina (Fig2).

1. 3. Mecanismes de catàlisi de la ubiquitina i particularitats de cada enzim

La ubiquitinació es dóna en tres passos enzimàtics catalitzats per (1) una E1 o enzim activador de ubiquitines, (2) una E2 o enzim de conjugació de ubiquitines, i (3) una E3 o lligasa de ubiquitines (Hershko and Ciechanover, 1998; Pickart, 2001). Primer, una E1 activa la ubiquitina de forma ATP depenent gràcies a l'adenilació de la part C-terminal de la ubiquitina i seguidament es forma un enllaç tioèster entre la glicina terminal de la ubiquitina i la cisteïna catalítica de la E1 (Haas and Rose, 1982; Haas et al., 1982). Seguidament, la ubiquitina així activada es transfereix també mitjançant un enllaç tioéster a la cisteïna catalítica de la E2. Finalment, la ubiquitina es transfereix de la E2 al substrat formant un enllaç isopeptídic amb catàlisi i/o presència d' una E3 de tipus HECT o RING (Fig 3).

Els enzims activadors de ubiquitines son proteïnes abundants del citoplasma i el nucli però poc diverses ja que un sol E1 pot activar una gran quantitat de E2 diferents (Mahajan et al., 1997; McGrath et al., 1991; Zacksenhaus and Sheinin, 1990). Els enzims E2 comparteixen un domini estructural comú anomenat UBC (Fig 4) i poden interactuar amb igual afinitat amb diferents E3 tant si aquests són de tipus HECT o de tipus RING. Aquests enzims poden determinar en alguns casos, si no en tots, el tipus de ubiquitinació que rebrà el substrat. Els enzims E3 son molt més nombrosos i confereixen especificitat de substrat. Els E3 poden tenir dos tipus de domini: el domini HECT, que participa activament en la catàlisi de la reacció (Verdecia et al., 2003a) i el domini RING, que permet d'aproximar de forma adient l'E2 i el substrat (Passmore and Barford, 2004; Pickart, 2001).

Les cadenes de poliubiquitines es poden allargar cap a l'últim amb enzims allargadors de la cadena anomenats E4 (Koegl et al., 1999). A més, existeixen enzims deubiquitinadors anomenats DUB capaços d' hidrolitzar les ubiquitines un cop conjugades al substrat o que pertanyen a la ruta biosintètica de la ubiquitina processant les pro-ubiquitines (Wilkinson, 2000).

1. 4. Modificacions proteiques per la ubiquitina

La monoubiquitinació consisteix en afegir a la proteïna substrat només una ubiquitina. Aquest tipus de ubiquitinació regula transcripció, endocitosi, funció de les histones i tràfic de membrana (Hicke, 2001; Hicke and Dunn, 2003; Katzmann et al., 2002; Muratani and Tansey, 2003). Per exemple, la monubiquitinació, multimonoubiquitinació o poliubiquitinació mitjançant lisina 63 de proteïnes clau permet l'endocitosi de vesícules, tant per que modifica l'activitat proteica de la maquinària de transport com per que senyalitza el destí de la vesícula cap a diferents compartiments cel·lulars (Hicke and Dunn, 2003; Shih et al., 2000). Monoubiquitinar una proteïna no es suficient per a degradar-la via proteasoma (Thrower et al., 2000). A més, existeixen proteïnes que protegeixen la molècula única de ubiquitina de l'elongació amb altres ubiquitines (Shekhtman and Cowburn, 2002).

La poliubiquitinació canònica consisteix en la formació de cadenes de ubiquitina sobre un determinat substrat mitjançant la formació d'enllaços isopeptídics entre la glicina terminal de la ubiquitina donant i la lisina 48 de la ubiquitina acceptora (Chau et al., 1989; Shekhtman and Cowburn, 2002; Thrower et al., 2000). Una cadena de tetraubiquitines unides de forma canònica és suficient per que el proteasoma la reconegui i degradi la proteïna que la

porta (Thrower et al., 2000). Aquest tipus de modificació permet la degradació de forma ràpida i irreversible de proteïnes no desitjades. Existeixen dos multicomplexos proteics encarregats de reconèixer i poliubiquitinar proteïnes involucrades en el cicle cel·lular de forma que permeten a la cèl·lula avançar en aquest. Així, l' APC juga un paper clau en la transició G2-M i l' SCF en la transició G1-S (Hershko and Ciechanover, 1998; Reed, 2003). A més, existeixen mecanismes que coordinen la poliubiquitinació amb el proteasoma aconseguint així una degradació més eficient dels substrats (Kleijnen et al., 2000; Seeger et al., 2003).

La poliubiquitinació per lisina 63 consisteix en la formació de cadenes de poliubiquitines unides per enllaços isopeptídics entre la G76 de la ubiquitina donant i la K63 de la ubiquitina acceptora. Aquestes particulars cadenes només estan catalitzades per l'E2 format per l'heterodímer UBC13-UEV1/2 (Hofmann and Pickart, 1999; VanDemark et al., 2001). La poliubiquitinació de substrats via K63 és important per a la transducció del senyal a través del receptor de interleuquines, la reparació del DNA, la resposta a l'estrés i l'endocitosi (Deng et al., 2000a; Galan and Haguenauer-Tsapis, 1997a; Hoege et al., 2002; Spence et al., 2000b). Aquest tipus d'enllaç entre ubiquitines es caracteritza per una conformació més extensa, fet que els impedeix d'ésser reconegudes pel proteasoma (Cook et al., 1994; Varadan et al., 2003; Varadan et al., 2002a).

S'han descrit cadenes de poliubiquitines via K11 i K29 que serien reconegudes pel proteasoma i implicarien la degradació dels substrats així modificats (Baboshina and Haas, 1996; Johnson et al., 1995; Liu et al., 1996). També s'han descrit cadenes unides via K6 que serien disgregades pel proteasoma (Baboshina and Haas, 1996; Lam et al., 1997; Nishikawa et al.,

2004). En cap cas, però, s'han descrit cadenes híbrides de poliubiquitines, fet que implicaria que aquestes cadenes no es poden ramificar.

1. 5. Proteïnes semblants a la ubiquitina: UBL

Les UBL son una família de petites proteïnes que inclou Rub1p, NEDD8, URCP, Apg12 i SUMO i es caracteritza per tenir similituds estructurals amb la ubiquitina així com per que també es poden conjugar a determinats substrats. SUMO, la proteïna més estudiada de la família, es conjuga mitjançant la E2 UBC9 i permet la repressió transcripcional, està involucrada en el transport nucli-citoplasma i permet l'establiment dels cossos PML (Mahajan et al., 1997; Matunis et al., 1996; Muller et al., 1998; Shiio and Eisenman, 2003). El més interessant de SUMO és que es pot conjugar al substrat pel mateix residu en que es conjugaria la ubiquitina, de forma recíprocament excloent (Hoege et al., 2002). Aquestes dues modificacions competitives permeten una regulació molt fina del destí final de la proteïna substrat.

1. 6. Ubiquitinació i cicle cel·lular

La poliubiquitinació i degradació proteica pel proteasoma de substrats juga un paper essencial en la regulació de gairebé tots els estadis del cicle cel·lular i de la proliferació (Fig. 8); així les proteïnes APC, SCF, MDM2, Smurf1/2, CHFR i les IAPs claus en la regulació d'aquests processos són lligases de ubiquitines de múltiples substrats mitjançant totes les formes de ubiquitinació a dalt esmentades. Ubiquitinar una proteïna pot modular l'activitat

bioquímica d'aquesta o alterar la seva localització subcel·lular (Liston et al., 2003; Margolis et al., 2003; Pray et al., 2002; Vogelstein et al., 2000a).

1. 7. Ubiquitinació i malalties neurodegeneratives

El mal funcionament del sistema ubiquitina-proteasoma és responsable de múltiples desordres neurològics com ara les síndromes d'Angelman, de Parkinson, de Alzheimer, la demència frontotemporal, la corea de Huntington i les malalties priòniques (Fig. 9, (Baek, 2003; Hardy, 1997; Layfield et al., 2001; Leroy et al., 1998; Steffan et al., 2004b)). Tota una sèrie de proteïnes que inclouen lligases de ubiquitines com Parkin o E6-AP, enzims deubiquitinadors com PGP9.5, substrats com les Presinilines o la Huntingtina i la ubiquitina ella mateixa han estat identificades com a responsables directes de la patogènesi.

2. OBJECTIUS

- Identificar molècules que interactuen amb l'enzim de conjugació de ubiquitines via K63 UBC13 mitjançant l'assaig de dos híbrids en llevat i confirmar-ne la interacció en cultius cel·lulars.
- Estudiar el sentit funcional de les interaccions tipus UBC de RNF8 i determinar si aquesta és una lligasa de ubiquitines.
- Estudiar el funcionament de RNF8 en processos cel·lulars mitjançant la sobreexpressió i la tècnica de l'RNA d'interferència.
- Identificar proteïnes que interactuen amb RNF8 per tal d'entendre millor el fenotip obtingut per la sobreexpressió o la interferència d' RNF8.

3. RESULTATS

3. 1. Identificació de proteïnes que interactuen amb UBC13

Després de descobrir en el nostre laboratori les proteïnes UEV (Sancho et al., 1998a) i posterior descobriment per part del laboratori de Cecile Pickart en que relacionava aquestes proteïnes amb una nova forma de poliubiquitinació que utilitzava la lisina en posició 63 en lloc de la 48; vàrem decidir de buscar proteïnes que interactuen amb UBC13 mitjançant la tècnica dels dos híbrids en llevat. Es van identificar tres proteïnes diferents: UEV, RNF8 i KIAA0675 (Fig 12A). Tant RNF8 com KIAA0675 contenen un domini RING finger que és típic de les lligases de ubiquitines o E3. A més del domini RING (aa 402 al aa 440), RNF8 presenta un domini coiled-coil (aa 45 al aa 390) i un domini FHA (aa 45 al aa 109). Només quatre proteïnes, CHFR, ScDma1/2p i SpDma1p, presenten aquesta composició de dominis (FHA+RING) i totes participen en *check-points* en la transició G2/M o en la sortida de mitosi (Fig 13). Pel que fa a KIAA0675 conté a més del domini RING (aa 1148 al aa 1187) un domini coiled-coil (aa 784 al aa 905) i quatre repeticions tetratricopèptid (aa 21 al aa 68 i del aa 126 al aa 349) (Fig. 15). A més de interactuar amb UBC13, RNF8 interactua amb UBE2E2 i KIAA0675 ho fa amb UBE2E2 i UBCH6 (Fig 12B).

Seguidament vàrem demostrar que RNF8 interactua amb UBC13 *in vivo*, ja que ambdues proteïnes co-immunoprecipiten quan es sobreexpressen amb un epítop en cèl·lules cos7. Per aquesta interacció, és necessari el domini RING finger de RNF8 ja que la mutació puntual C403S implica una pèrdua total d' interacció. RNF8 salvatge ($RNF8^{WT}$) es localitza en el nucli de la cèl·lula, on

també colocalitza amb UBC13, mentre que RNF8^{C403S} es pot localitzar tant a nucli com al citoplasma (Fig. 17).

L'anàlisi del patró d'expressió de UBC13, RNF8 i KIAA0675 per RT-PCR sobre una llibreria de cDNAs humans de diferents teixits, va demostrar que E2 i proteïnes RING finger es coexpressaven en un gran nombre de teixits tant adults com fetals amb especial èmfasi en el cervell, el tímus i els testicles (Fig. 18).

Un cop confirmada la interacció entre RNF8 i UBC13 vàrem decidir generar anticossos policlonals de conill contra dos pèptids que corresponien a part de les seqüències d'RNF8 i UBC13. Després d'assegurar-nos del bon funcionament dels anticossos (Fig. 10 i 11), vàrem estudiar la localització sub-cel·lular d'RNF8 i UBC13. RNF8 es localitza en el nucli de la cèl·lula formant un patró de punts discrets que recorda el patró observat en les proteïnes associades als cossos PML (Ishov et al., 1999; Salomoni and Pandolfi, 2002; Zhong et al., 2000). Tanmateix, la colocalització d'RNF8 amb PML és tan sols parcial, tot i que augmenta una mica quan es tracten les cèl·lules amb estímuls pro-apoptòtics com la llum ultravioleta, l'etopòsid o el cis-platí. La proteïna UBC13 es localitza tant en la membrana plasmàtica com en el citoplasma i el nucli (Fig 19).

Degut a les semblances entre CHFR i RNF8, vàrem investigar el comportament d'RNF8 al llarg del cicle cel·lular. Després d'un doble bloqueig amb timidina, vàrem recollir mostres per a citometria de flux, western blot i immunocitoquímica. Així vàrem poder determinar que els nivells d'RNF8 oscil·len al llarg del cicle cel·lular de forma que pugen progressivament durant S i G2 i desapareixen de forma abrupta entre metafase i anafase. A més, si les

cèl·lules es tracten amb nocodazole o taxol que arresten les cèl·lules en mitosi, es produeix una acumulació d'RNF8. Sempre que el nucli era present, RNF8 es localitzava en aquest. A més en telofase, RNF8 es localitza a la membrana plasmàtica i més especialment en la juntura dels dos fusos de tubulina que separen les dues cèl·lules filles. Contràriament a RNF8, els nivells de UBC13 no varien al llarg del cicle i tan sols s'observa un enriquiment nuclear de la proteïna en avançar en la fase S (Fig 20).

3. 2. RNF8 té una activitat lligasa d'ubiquitines

RNF8 és una proteïna amb un RING finger que interactua com a mínim amb dues E2 diferents: UBC13 i UBE2E2. A més moltes lligases d'ubiquitines tenen activitat lligasa sobre sí mateixes. Per aquest motiu, vàrem generar un seguit de construccions per tal d'expressar HA-ubiquitina salvatge i HA-Ubiquitina amb les mutacions següents: K48,63R, K29,63R i K29,48R així com His_6-$RNF8^{WT}$ o His_6-$RNF8^{C403S}$. L'anàlisi per *western blot* dels lisats de cèl·lules cotransfectades amb una combinatòria de construccions abans esmentades i purificades per afinitat amb una columna de níquel varen demostrar que RNF8 es pot poliubiquitinar via K29, K48 i K63. A més, RNF8 té una activitat autocatalítica per a les poliubiquitinacions que utilitzen les lisines K48 i K63, ja que aquestes es perden quan el domini RING no és funcional (Fig. 21). En un altre experiment, vàrem demostrar que la poliubiquitinació d'RNF8 via K63 necessita d'UBC13 ja que aquesta es perd quan es sobreexpressa un dominant negatiu d'UBC13 que porta la mutació C87A.

En un altre experiment de western blot a partir d'extractes cel·lulars de cèl·lules transfectades amb His_6-$RNF8^{WT}$ o vector buit, purificats per cromatografia d'afinitat en columnes de níquel i blotades amb anti-sumo, vàrem poder determinar que RNF8 es pot sumoïlar. Analitzant la seqüència aminoacídica d'RNF8 es varen poder determinar dos possibles dianes de sumoïlació en les posicions 190 i 264 d'RNF8 (Fig. 22). Per tant, RNF8 es pot modificar com a mínim per quatre tipus de modificacions post-traducionals diferents.

3. 3. RNF8: cicle cel·lular i apoptosi

Degut a l'associació de l'expressió d'RNF8 amb diferents estadis del cicle cel·lular vàrem decidir d'estudiar l'efecte de la sobreexpressió d'RNF8 sobre aquest. Per aquest motiu vàrem generar les construccions que permetien expressar les proteïnes quimeres GFP-$RNF8^{WT}$ i GFP-$RNF8^{C403S}$ i les vàrem transfectar en cèl·lules HeLa per tal d'analitzar-ne la distribució segons el seu contingut de DNA. Com a controls vàrem utilitzar les cèl·lules no transfectades de la mateixa placa que les transfectades. Sobreexpressar RNF8 comporta un important augment de la fase G1 amb una corresponent baixada de les fases S i G2-M respecte les cèl·lules control (Fig 23). Aquest fenotip no era tant fort quan el que es sobreexpressava era la quimera amb el domini RING mutat. La tinció per immunocitoquímica de les ciclines D1 i B1 en cèl·lules transfectades amb les construccions quimeres corroboraven les dades de citometria de flux. Per altra banda, vàrem suprimir l'expressió d'RNF8 en cèl·lules HeLa amb la tècnica de l'RNA de interferència per tal d'observar-ne la distribució al llarg del

cicle cel·lular. En aquestes condicions, no es varen detectar grans canvis entre la presencia o absència d'RNF8 (Fig. 24).

L'expressió d'RNF8 al llarg del cicle cel·lular i la relació amb altres proteïnes de dominis similars suggeria per a RNF8 un paper en la transició G2-M. Per això vàrem decidir crear un arrest mitòtic amb nocodazole que impedeix la polimerització de microtúbuls. Així vàrem poder observar que malgrat les cèl·lules control es sincronitzaven correctament el mitosi a les 0h, les cèl·lules que sobreexpressen $RNF8^{WT}$ eren incapaces de fer-ho i presentaven una major apoptosi que la observada en condicions basals (Fig. 25). Per tant la sobreexpressió d'RNF8 permet a les cèl·lules escapar d'un arrest mitòtic per nocodazole i les fa més sensibles a la mort cel·lular.

Seguidament vàrem analitzar la sortida de mitosi de cèl·lules deplecionades d'RNF8 sota estrès mitòtic. La manca d'RNF8 després del tractament amb nocodazole produeix una baixada més tardana del percentatge de cèl·lules amb un contingut 4n de DNA respecte el control, analitzat per citometria de flux. A més, els nivells de ciclina B1 desapareixen també de forma més tardana en absència d'RNF8 (Fig. 26). Per tant, la manca d'RNF8 provoca un retard en la sortida de mitosi després d'un estrès mitòtic com el produït pel tractament amb nocodazole.

Per tal de mirar d'entendre les discrepàncies entre l'expressió temporal d'RNF8 i l'arrest observat en G1, vàrem hipotetitzar que un excés d'RNF8 o una expressió inadequada d'aquesta podia implicar la realització d'una mitosi defectuosa, i que aquest defecte seria evident un cop la cèl·lula hagués completat la citoquinesi i per tant amb un contingut de DNA equivalent a G1. Vàrem transfectar cèl·lules amb GFP-$RNF8^{WT}$ i ^{C403S} i vàrem analitzar les

mitosis per microscopia confocal en condicions de protecció de mort cel·lular. En aquestes mitosi, GFP-RNF8^{WT} i ^{C403S} es localitzen sobre els fusos mitòtics i sobre els fusos de la zona mitja en anafase el que representa una nova localització respecte la proteïna endògena. Un cop en telofase, RNF8 es localitza de forma molt similar a la proteïna endògena (Fig. 27A, B). El percentatge de metafases-anafases respecte el total de mitosis en les cèl·lules que sobreexpressen RNF8 és d'aproximadament el 20% i per tant marcadament inferior al 50% observat en els controls. Aquestes dades recolzen la hipòtesi que la sobreexpressió d'RNF8 accelera la separació de cromosomes i l'entrada en citoquinesi. A més, a part d'observar estructures mitòtiques d'aparença normal, es varen veure figures aberrants per a GFP-RNF8^{WT}, que consistien en la formació de fusos mitòtics multipolars associats amb una distribució aberrant dels cromosomes condensats així com fusos mitòtics clarament descompensats. La freqüència d'aquestes estructures era d'aproximadament la meitat per a GFP-RNF8^{WT} i d' un 20% per a GFP-RNF8^{C403S} (Fig. 27C, D, E). El fet que aquestes estructures aberrants no es veiessin sense inhibidors de caspases suggereix que aquest tipus de mitosis no són viables.

PLK1 era un bon candidat a ser subjecte de regulació per part d'RNF8. Per tant, vàrem estudiar si les dues proteïnes colocalitzaven en les diferents fases de la mitosi. Ambdues proteïnes colocalitzen en els fusos mitòtics polars i de la zona mitja i amb el cos mitjà en telofase (Fig 28). Llavors, vàrem hipotetitzar que si RNF8 tenia algun paper regulador sobre la proteïna PLK1, ja sigui per poliubiquitinació via K48 o K63, llavors els nivells de PLK1 haurien de variar sota condicions de sobreexpressió d'RNF8. L'anàlisi per *western blot*

dels nivells de PLK1 en cèl·lules que sobre-expressen RNF8, va revelar que no existien diferències en l'expressió de PLK1, i que per tant era poc provable que RNF8 tingués un paper regulador sobre PLK1.

L'anàlisi per citometria de flux va permetre observar l'aparició d'una població sub-G1 quan es sobreexpressa RNF8 de 4.5% a les 28 hores post-transfecció i de 24.1% a les 33 hores post-transfecció (Fig 29). Per això vàrem analitzar de nou els cicles en presència inhibidors de caspases, fet que causà un augment de la fase G1 per a les cèl·lules transfectades amb $RNF8^{WT}$ i un augment en G2-M per a les transfectades amb $RNF8^{C403S}$, a més de la desaparició de la fracció sub-G1. Per tant, la sobreexpressió d'$RNF8^{WT}$ causa una mortalitat en G1 i es provable que la de $RNF8^{C403S}$ la causi en G2-M.

Seguidament, vàrem caracteritzar millor l'apoptosi per contatges sobre monocapes transfectades i tenyides amb Hoechst 33258. Els contatges respectius de cèl·lules no transfectades, transfectades amb GFP, GFP-$RNF8^{WT}$ i GFP-$RNF8^{C403S}$ eren a les 24h post-transfecció de 0.2%, 8.9%, 24.6% i 7.2% mentre que 48h post-transfecció eren de 0.4%, 5.0%, 49.3% i 16.2% (Fig. 30). Per tant, els resultats no contradiuen les dades de citometria. L'anàlisi per western blot de lisats de cèl·lules transfectades va revelar la presència dels fragments proteolítics tant de la caspasa-3 com de la -8, suggerint que la mort cel·lular observada està associada amb activació d'aquestes caspases. A més, en tractar les cèl·lules amb inhibidors de caspases es reduïa substancialment la mort cel·lular observada.

Un cop caracteritzada l'apoptosi sota la sobreexpressió d'RNF8, vàrem estudiar la resposta de la proteïna endògena front a estímuls pro-apoptòtics

que causen dany al DNA. Existeix un augment d'RNF8 dosi-resposta depenent sota estímuls com cis-platí, etopòsid o la llum ultravioleta, tant si es dóna o no una activació de caspasa-3 (Fig 31). Aquest augment, no és degut a un augment en la transcripció sinó que possiblement es deu a una estabilització de la proteïna (Fig 31).

El següent pas va consistir en analitzar la resposta de cèl·lules deplecionades d'RNF8 front a un estímul proapoptòtic com el tractament amb etopòsid. Vàrem analitzar monocapes de HeLa interferides per a RNF8 amb dos siRNAs diferents i amb un siRNA control que no baixa l'expressió de la proteïna després de tractar-les durant 12h amb etopòsid. Les cèl·lules interferides per a RNF8 presentaven apoptosis al voltant del 4% mentre que les cèl·lules no interferides el presentaven gairebé del 40%. En analitzar l'estat de la caspasa-3 en cèl·lules tractades de la mateixa manera es va poder observar una baixada significativa de la pro-caspasa malgrat que no hi havia baixada de les formes proteolitzades. Aquests resultats confirmen les dades observades sota condicions de sobreexpressió d'RNF8.

Finalment, vàrem comprovar que l'augment de caspasa-3 degut a la sobreexpressió d'RNF8 no implicava un augment en la transcripció del mRNA d'aquesta, sinó que provablement es dóna per estabilització de la proteïna (Fig. 32).

3. 4. Identificació de proteïnes que interactuen amb RNF8

Per tal d'entendre millor la funció d'RNF8 vàrem realitzar un segon crivatge de la llibreria de cervell fetal humà per la tècnica dels dos híbrids en llevat utilitzant RNF8 com a esquer. Vàrem identificar tres proteïnes diferents d'

un total de 3.0 milions de clons crivats, que corresponien a les proteïnes S40, HERC2 i HIP1 (Fig. 33 esquerra). Malgrat totes interactuaven amb una construcció parcial d'RNF8 a la qual li faltava el domini coiled-coil i el domini RING, no vàrem identificar un domini comú entre elles responsable de la interacció (Fig. 33 dreta). En HERC2 vàrem poder predir un domini HECT, típic de les lligases d'ubiquitines, tres dominis semblants a RCC1, un domini d'unió d'esteroids i un domini semblant al de la subunitat número 10 de l'APC (Fig 34). HIP1, *Huntington Interacting Protein 1*, és una proteïna molt més coneguda i està involucrada en supervivència cel·lular, tràfic vesicular i tumorigènesi. Existeix gran controvèrsia en el paper pro- o anti-apoptòtic d'aquesta proteïna, que és capaç d'unir-se a la Huntingtina només quan aquesta no esta mutada (Gervais et al., 2002; HDCRG, 1993; Rao et al., 2003; Rao et al., 2002). HIP1 conté, segons aquests mateixos autors, un domini ENTH, un domini pseudo-DEAD, una cremallera de leucina, un domini *coiled-coil* i una regió d'homologia a Talina (Fig 34).

Tenint en compte que els dominis FHA tenen una unió preferencial per a les seqüències tipus pT-X-X-I/L (Das et al., 1998; Durocher et al., 2000) i que aquesta hauria d'estar continguda en els tres positius de dos híbrids, vàrem poder determinar una potencial seqüència de fosforilació reconeguda pel FHA d'RNF8; aquesta seria pT-Q-X-X-L/V i podria ésser fosforilada per ATM o la kinasa depenent de DNA, ja que acompleix el consensus de fosforilació d'aquestes kinases (Fig 35).

Seguidament, vàrem co-immunoprecipitar RNF8 i Hip1 en cèl·lules de mamífer. A més, vàrem observar un canvi en la localització subcel·lular tant de Hip1 com d'RNF8 (Fig. 36). RNF8 i HIP1 es coexpressen en gran varietat de

teixits adults i fetals, especialment en cervell i testicle (Fig. 37). En cotransfectar HIP1 amb RNF8 i analitzar per *western blot* l'expressió de la caspasa-3, vàrem poder demostrar que en les nostres cèl·lules HIP1 no és pro-apoptòtic, sinó que al contrari, aquesta proteïna contraresta l'efecte apoptòtic d'RNF8 (Fig. 36D).

4. DISCUSSIÓ

4. 1. K63-poliubiquitinació

La poliubiquitinació que utilitza la lisina en la posició 63 de la ubiquitina està mediada únicament per l'heterodímer format per UBC13-UEV1 (Hofmann and Pickart, 1999). Aquesta modificació no promou la degradació de la proteïna substrat (Spence et al., 2000b; Wang et al., 2001b) i sembla essencial per a la regulació de certs processos com la reparació del DNA en llevats (Broomfield et al., 1998; Ulrich and Jentsch, 2000; Xiao et al., 2000) o la transducció del senyal (Deng et al., 2000a; Shi and Kehrl, 2003; Wang et al., 2001b) i la motilitat cel·lular (Didier et al., 2003) en cèl·lules de mamífer. És per tant de gran interès biològic l'estudi dels mecanismes que promouen aquesta modificació. Hem identificat tres proteïnes que interactuen amb UBC13 per la tècnica dels dos híbrids en llevat: UEV1, i dues proteïnes amb dominis RING finger RNF8 i KIAA0675. En resultat d'aquest i altres cribatges (dades del nostre laboratori) recolzen que la proteïna UBC13 ofereix tant sols dues superfícies per a la interacció amb altres proteïnes, una per a proteïnes amb dominis UEV i una altra per a proteïnes amb dominis RING finger. A més el domini RING finger permet la interacció de la proteïna que el porta amb

diferents enzims tipus E2 com UBC13. Això implica que la proteïna RING finger pot desenvolupar diferents classes d'activitat lligasa de ubiquitines depenent de amb quina E2 està interactuant i determinar destins oposats per a la proteïna substrat.

Tant RNF8 com KIAA0675 compleixen les característiques típiques de les E3, ja que contenen un domini RING finger que recluta E2 a més d'altres dominis que promouen interaccions proteïna-proteïna com l'FHA d'RNF8 o els dominis tetratricopèptid de KIAA0675 (Ciechanover et al., 2000; Joazeiro and Weissman, 2000) i son autolligases d'ubiquitines *in vivo* (Kreft and Nassal, 2003; Moore et al., 2003)(Plans et al., pendent de publicació). RNF8 autocatalitza la formació de cadenes tipus K48 i K63 sobre sí mateixa provablement gràcies a la interacció amb UBE2E2 i UBC13, mentre que segurament requereix d'una altra E3 per a la poliubiquitinació via K29. A més, és poc provable que RNF8 es poliubiquitini mitjançant alguna altra lisina en la molècula de la ubiquitina.

4. 2. Possibles funcions d'RNF8 en la transició metafase-anafase

A més de la seva activitat E3, hem estudiat diferents propietats biològiques d'RNF8. La localització subcel·lular i els nivells d'RNF8 estan regulats al llarg del cicle cel·lular. RNF8 pot localitzar-se en els fusos mitòtics en metafase i anafase i a la zona mitja del pont de tubulina en citoquinesi, fets que suggereixen un paper d'aquesta en les transicions mitòtiques. Tanmateix, la manca d'RNF8 no produeix canvis substancials en el cicle cel·lular, i la sobreexpressió transitòria d'aquesta produeix una acumulació en G1 més que en G2-M. La connexió funcional entre RNF8 i mitosi es fa però evident en el fet

que la sobreexpressió d'RNF8 incapacita les cèl·lules a bloquejar-se en mitosi, les sensibilitza a la mort cel·lular sota estrès mitòtic i que la manca d'RNF8 retarda la sortida de mitosi en les mateixes condicions d'estrès.

RNF8 podria estar participant en el control de *checkpoints* mitòtics però no regulant el cicle de base. Un *checkpoint* es un procés que es desencadena sota un estrés com a resposta a un dany. El *checkpoint* del fus mitòtic desencadenat pel tractament amb nocodazole conté mecanismes que impedeixen l'activació de l'APC i per tant l'entrada en anafase (Gorbsky, 2001; Hongtao, 2002; Hoyt, 2001; Millband et al., 2002; Shah and Cleveland, 2000). Les molècules que participen en aquesta inhibició son Mad2, BubR1, Bub1 i Bub3, captant la molècula reguladora de l'APC Cdc20. A més, hi han molècules parcialment conegudes que censen el dany. Entre elles, el complex ternari format per l'Aurora B kinasa, la IAP survivina i la proteïna semblant a les histones INCENP (Stern, 2002; Stern and Murray, 2001; Tanaka, 2002; Tanaka et al., 2002).

És possible que RNF8 reguli alguna proteïna del *checkpoint* del fus mitòtic o alguna proteïna encarregada de censar l'ocupació dels quinetocors per microtubuls del fus mitòtic. El fenotip observat per a RNF8 s'assembla al de la manca de Mad2 o altres proteïnes del *checkpoint,* en que les cèl·lules escapen al bloqueig en G2-M causat pel tractament amb nocodazole i moren per apoptosi p53 depenent (Bharadwaj and Hongtao, 2004; Hongtao, 2002; Margolis et al., 2003).

A més l'estructura en dominis d'RNF8 (RING finger i FHA) tant sols es troba en 4 altres proteïnes conegudes: CHFR en metazous, Dma1 en *S. pombe* i Dma1/2 en *S. Cerevisisae.* Totes elles participen en *checkpoints* en la

transició G2-M (Chaturvedi et al., 2002; Fraschini et al., 2004; Guertin et al., 2002b; Murone and Simanis, 1996; Scolnick and Halazonetis, 2000).

4. 3. Possible funció d'RNF8 en citoquinesi

En citoquinesi, RNF8 s'associa amb el nucli però també en la zona mitja del pont de tubulina que separa les dues cèl·lules. Quan es sobreexpressa, la proteïna transfectada també es localiza en la zona mitja del pont de tubulina i per tant aquesta localització es fisiològica i reflecteix una possible funció d'RNF8 en citoquinesi. A més, RNF8 sobreexpressada es localitza sobre els fusos mitòtics, localització que podria reflexar la localització de la proteïna endògena sota estrés mitòtic. Els nostres experiments de sobreexpressió suggereixen que la funció d'RNF8 sobre el fus mitòtic és la d'accelerar la segregació cromosòmica, fet que es corrobora pel retard en la sortida de mitosi en cèl·lules deplecionades d'RNF8 sota estrés mitòtic.

La segregació fidedigna dels cromosomes requereix la bona disposició dels fusos mitòtics respecte l'eix de divisió cel·lular. L'entrada en citoquinesi abans de la segregació cromosòmica provoca la formació de cèl·lules filles anucleades o poliploids. Les cèl·lules eucariotes tenen un mecanisme per a evitar els possibles danys causats per una acceleració de la citoquinesi anomenat *checkpoint* del posicionament del fus mitòtic que retarda la citoquinesi en presència de fusos mal posicionats o mal orientats fins que es corregeixen els errors.

En *s. cerevisiae*, el *checkpoint* del posicionament del fus mitòtic requereix la participació de les proteïnes Bub2 i Bfa1 a més de Tem1 per tal d'inhibir la maquinaria de sortida de mitosis (MEN) (Bardin et al., 2000; Bloecher et al.,

2000; Geymonat et al., 2002; Pereira et al., 2000; Simanis, 2003). La MEN té una composició estructural semblant a la SIN (maquinaria d'iniciació de la septació) en *s. pombe*, que es pot inhibir per Dma1 en presència de dany en el fus mitòtic (Guertin et al., 2002; Murone and Simanis, 1996). La manca de Dma1 i 2 provoca un mal funcionament del *checkpoint* del posicionament del fus mitòtic en el llevat. A més, la sobreexpressió de Dma2 causa defectes en la citoquinesi del llevat (Fraschini et al., 2004). Les proteïnes Dma1 són homologues a CHFR, com també podrien ser-ho d' RNF8 tenint en compte la composició en dominis de les proteïnes.

La manca d'RNF8 afegida a un estrés mitòtic provoca un retard en la sortida de mitosi; a més, la sobreexpressió d'RNF8 accelera aquest mateix procés si tenim en compte els percentatges de metafases-anafases en el total de cèl·lules mitòtiques i la presència amb inhibidors de caspases de més de dues cèl·lules unides per més d'un pont de tubulina, éssent fins i tot alguna d'elles clarament en metafase. La sobreexpressió d'RNF8 provoca l'entrada en citoquinesi abans de completar la mitosi, fet que podria explicar-se per una inactivació del *checkpoint* del posicionament del fus mitòtic.

4. 4. RNF8 i apoptosi

A part de defectes en dos *checkpoints*, la sobre-expressió d'RNF8 provoca apoptosi depenent de l'activació de les caspases 3 i 8, a més d'un augment en els nivells proteics de pro-caspasa-3. Estímuls pro-apoptòtics com la llum ultravioleta, l'etopòsid i el cis-platí provoquen un augment d'RNF8 endògena dosi-depenent sense augmentar la transcripció del gen. A més, la depleció en cèl·lules per a RNF8 protegeix de la mort per etopòsid.

Pertant, RNF8 és una proteïna pro-apoptòtica que podria estar activant la via extrínseca de l'apoptosi al mateix temps que podria estar regulant directament l'estabilitat proteica de la caspasa-3. RNF8 podria estabilitzar la caspasa-3 gràcies a la seva activitat lligasa però cal destacar que RNF8 no té dominis de reconeixement de caspases.

Existeix una família de proteïnes anomenades IAPs que contenen dominis BIR i RING finger que funcionen com a inhibidors endògens de caspases (Liston et al., 2003). XIAP, c-IAP1, c-IAP2, Livin i survivin en son membres i estan regulades per XAF1, Smac/Diablo i Omi, les quals poden canviar la localització citoplasmàtica de les IAPs, inhibir la seva activitat lligasa de ubiquitines o directament la seva unió a caspases (Creagh et al., 2004; Liston et al., 2001; Suzuki et al., 2001a). Seria interessant investigar si RNF8 regula l'estabilitat de la caspasa-3 mitjançant la regulació d'alguna IAP. Els candidats més interessants de regulació serien survivina i cIAP per la seva localització subcel·lular i el seu paper dual en cicle i apoptosi (Beltrami et al., 2004; Li et al., 1998; Samuel et al., 2005).

4. 5. Possible estabilització d'RNF8 per modificacions postraduccionals

Hem demostrat que RNF8 pot patir diferents modificacions postraducionals que impliquen la conjugació de cadenes de poliubiquitines K29, K48, K63 i sumo. Malgrat els nostres esforços, no hem pogut determinar el lligam entre aquestes modificacions i el paper que RNF8 desenvolupa en la cèl·lula. Tanmateix, és possible que tant la sumoilació com la poliubiquitinació via K63 d'RNF8 permetin una estabilització de la proteïna de forma similar al funcionament de PCNA (Hoege et al., 2002). Aquesta hipotètica i ràpida

estabilització permetria modular els nivells cíclics d'RNF8 en condicions d'estímuls pro-apoptòtics o d'estrés mitòtic.

4. 6. Proteïnes que interactuen amb RNF8

Mitjançant la tècnica dels dos híbrids en llevat, hem trobat tres proteïnes que interactuen amb l'FHA d'RNF8: S40, HERC2 i HIP1. A més d' interactuar amb la proteïna Htt responsable de la Corea de Huntington (Gervais et al., 2002; HDCRG, 1993), HIP1 regula l'endocitosi i el tràfic vesicular (Hyun and Ross, 2004). Malgrat estudis inicials, HIP1 sembla ser una proteïna antiapoptòtica sobreexpressada en nombroses neoplàsies capaç de transformar fibroblasts (Gervais et al., 2002; Hyun and Ross, 2004; Rao et al., 2003; Rao et al., 2002). Per tant, el fet que HIP1 protegeixi de la mort induïda per la sobreexpressió d'RNF8 està en acord amb la funció d'HIP1. Ara, el mecanisme pel qual una proteïna citoplasmàtica es troba amb una proteïna nuclear es una pregunta interessant. Quan es troben doblement sobreexpressades, HIP1 i RNF8 poden canviar la seva localització subcel·lular. És possible, per tant, que alts nivells d'HIP1 deslocalitzin RNF8 del nucli prevenint-ne l'apoptosi. Seria per tant de gran interès investigar si RNF8 juga algun paper en la mort i degeneració neuronal que acompanyen a la malaltia de Huntington.

La segona proteïna que interactua amb RNF8, HERC2, conté un domini lligasa d'ubiquitines tipus HECT a part de dominis tipus RCC1. Degut a la manca de dades funcionals més consistents, es podria especular que HERC2 té una funció semblant a RCC1, permetent entre altres el transport nucli-citoplasma i la formació i estabilització de microtúbuls del fus mitòtic en la

proximitat de cromosomes condensats (Carazo-Salas et al., 1999; Kahana and Cleveland, 2001). Si HERC2 tingués activitat GEF sobre Ran, llavors s'establiria una connexió directa entre RNF8 i la formació del fus mitòtic.

4. 7. Una funció per a RNF8 hipòtesis i propostes

La composició particular en dominis d'RNF8 s'assembla només a la de 3 altres proteïnes, totes elles involucrades en la regulació de *checkpoints* mitòtics. Els nostres estudis suggereixen la regulació per part d'RNF8 de dos checkpoints, però de forma única ja que és una regulació negativa d'aquests.

Per què seria important desactivar dos checkpoints beneficiosos per a la cèl·lula en condicions d'estrés? Una possible resposta seria que RNF8 està involucrada en la mediació d'una resposta apoptòtica quan la reparació del dany no és possible. Tantmateix, per què caldria portar la cèl·lula danyada fins a G1 per tal de fer-la entrar en apoptosi? Potser RNF8 té una segona funció, que consistiria en evaluar i senyalitzar la correcció del dany, funció que no hem explorat en aquest treball. Estímuls tant diferents com inducció d'estrés mitòtic o de dany al DNA incrementen notablement els nivells d'RNF8 endògena però no pas tant com els nivells assolits per sobreexpressió, i per tant podria existir un llindar crític d'expressió d'RNF8 que decidiria entre mort cel·lular per caspases o alliberament del checkpoint un cop superat el dany. Per tant, potser caldrà establir un sistema on els nivells d'RNF8 son modulables, tipus tet-off, i quantificar el dany causat per estrés mitòtic o genotòxic en cèl·lules deplecionades per a RNF8 així com el nivell de correcció d'aquest.

5. CONCLUSIONS

1. Mitjançant un cribatge per la tècnica dels dos híbrids en llevat hem identificat tres proteïnes que interactuen amb l'enzim de conjugació d'ubiquitines UBC13: UEV1, RNF8 i KIAA0675. Les dues últimes són proteïnes que contenen dominis RING finger, a través del quals interactúen amb UBC13, així com altres enzims tipus E2 com UBE2E2 i UBCH6. UBC13, RNF8 i KIAA0675 es co-expressen en diversos teixits adults i fetals.

2. RNF8 interactúa i co-localitza amb UBC13 en cèl·lules Cos-7 i HeLa. Aquesta interacció depèn de la integritat del domini RING finger, fet que demostra que aquest domini és essencial per a la interacció.

3. RNF8 té activitat lligasa de ubiquitines sobre sí mateixa per a les cadenes que utilitzen la K48 i la K63. La K63-autopoliubiquitinació d'RNF8 requereix l'activitat catalítica de UBC13. RNF8 es pot poliubiquitinar per al menys una altra E3. Aquesta promou una poliubiquitinació sobre RNF8 basada en unions que utilitzen la K29. A més, RNF8 es pot modificar també mitjançant sumoïlació.

4. La proteïna RNF8 endògena es localitza principalment en el nucli de la cèl·lula amb un patró puntejat que colocalitza tant sols parcialment amb unes estructures nuclears anomenades cossos nuclears. UBC13 es localitza de forma més extensa, en particular en el nucli, el citoplasma i la membrana plasmàtica de la cèl·lula. Els nivells de RNF8 estan regulats al llarg del cicle

cel·lular, augmentant progressivament al llarg de S fins a G2-M amb una baixada brusca en metafase-anafase. RNF8 es pot localitzar a diverses estructures mitòtiques, incloent-hi els fusos polars, fusos centrals, i el cos central dels ponts mitòtics durant la citoquinesi.

5. La sobreexpressió d'RNF8 promou l'arrest de cèl·lules HeLa a l' inici de la fase G1. Aquest arrest és més eficient per part de $RNF8^{WT}$ que no per part de un mutant on el domini RING no és funcional. L'arrest en G1 persisteix quan es protegeixen les cèl·lules de la mort per apoptosi amb inhibidors de caspases per a la forma salvatge d'RNF8.

6. La sobreexpressió d'RNF8 permet a les cèl·lules d'escapar de l' arrest mitòtic provocat pel nocodazole, droga que despolimeritza els microtúbuls; mentre que la depleció d'RNF8 provoca un retard en la sortida de mitosi amb el mateix tractament.

7. La sobreexpressió d'RNF8 promou la mort cel·lular depenent de caspases, efecte que requereix de la integritat del domini RING finger. La depleció d'RNF8 mitjançant la transfecció de dúplexes de siRNA específics protegeix les cèl.lules de l'apoptosi causada per diversos estímuls genotòxics. Finalment, diversos estímuls pro-apoptòtics augmenten els nivells d'RNF8 endògen, sense augmentar-ne els nivells d'mRNA. En cèl·lules apoptòtiques, RNF8 es localitza en micronuclis i en nuclis col·lapsats. Per tant, RNF8 és una proteïna proapoptòtica que participa causalment en la mort cel·lular induïda per diferents estímuls apoptòtics.

8. A més d' interactuar amb enzims E2 a través del seu domini RING finger, RNF8 interactúa amb tres proteïnes mitjançant el seu domini FHA: les proteïnes huntingtin-interacting protein 1 (HIP1), HERC2 i S40. La simultània sobreexpressió d'RNF8 i HIP1 pot causar un canvi en la localització d'ambdues proteïnes, i protegeix les cèl·lules de l'apoptosi induïda per sobreexpressió d'RNF8.

BIBLIOGRAPHY

Amos-Landgraf, J. M., Ji, Y., Gottlieb, W., Depinet, T., Wandstrat, A. E., Cassidy, S. B., Driscoll, D. J., Rogan, P. K., Schwartz, S., and Nicholls, R. D. (1999). Chromosome breakage in the Prader-Willi and Angelman syndromes involves recombination between large, transcribed repeats at proximal and distal breakpoints. Am J Hum Genet *65*, 370-386.

Baboshina, O. V., and Haas, A. L. (1996). Novel Multiubiquitin Chain Linkages Catalyzed by the Conjugating Enzyme E2-EPF and RAD6 Are Recognized by 26 S Proteasome Subunit 5. J Biol Chem *271*, 2823-2831.

Baek, K. H. (2003). Conjugation and deconjugation of ubiquitin regulating the destiny of proteins. EXPERIMENTAL and MOLECULAR MEDICINE *35*, 1-7.

Bardin, A. J., Visintin, R., and Amon, A. (2000). A mechanism for coupling exit from mitosis to partitioning of the nucleus. Cell *102*, 21-31.

Beltrami, E., Plescia, J., Wilkinson, J. C., Duckett, C. S., and Altieri, D. C. (2004). Acute Ablation of Survivin Uncovers p53-dependent Mitotic Checkpoint Functions and Control of Mitochondrial Apoptosis. J Biochem *279*, 2077-2084.

Bernier-Villamor, V., Sampson, D. A., Matunis, M. J., and Lima, C. D. (2002). Structural basis for E2-mediated SUMO conjugation revealed by a complex between ubiquitin-conjugating enzyme Ubc9 and RanGAP1. Cell *108*, 345-356.

Bharadwaj, R., and Hongtao, Y. (2004). The spindle checkpoint, aneuploidy, and cancer. Oncogene *23*, 2016-2027.

Bloecher, A., Venturi, G. M., and Tatchell, K. (2000). Anaphase spindle position is monitored by the BUB2 checkpoint. Nat Cell Biol *2*, 556-558.

Bloom, J., Amador, V., Bartolini, F., DeMartino, G., and Pagano, M. (2003). Proteasome-mediated degradation of p21 via N-terminal ubiquitinylation. Cell *115*, 71-82.

Borden, K. L. (2000). RING domains: master builders of molecular scaffolds? J Mol Biol *295*, 1103-1112.

Borden, K. L., and Freemont, P. S. (1996). The RING finger domain: a recent example of a sequence-structure family. Curr Opin Struct Biol *6*, 395-401.

Bothos, J., Summers, M. K., Venere, M., Scolnick, D. M., and Halazonetis, T. D. (2003). The Chfr mitotic checkpoint protein functions with Ubc13-Mms2 to form Lys63-linked polyubiquitin chains. Oncogene *22*, 7101-7107.

Broomfield, S., Chow, B. L., and Xiao, W. (1998). MMS2, encoding a ubiquitin-conjugating-enzyme-like protein, is a member of the yeast error-free postreplication repair pathway. Proc Natl Acad Sci U S A *95*, 5678-5683.

Burbea, M., Dreier, L., Dittman, J. S., Grunwald, M. E., and Kaplan, J. M. (2002). Ubiquitin and AP180 regulate the abundance of GLR-1 glutamate receptors at postsynaptic elements in C. elegans. Neuron *35*, 107-120.

Buschmann, T., Fuchs, S. Y., Lee, C. G., Pan, Z. Q., and Ronai, Z. (2000). SUMO-1 modification of Mdm2 prevents its self-ubiquitination and increases Mdm2 ability to ubiquitinate p53. Cell *101*, 753-762.

Büttner, C., Stadtler, S., Leyendecker, A., Laube, B., and Griffon, N. (2001). Ubiquitination precedes internalization and proteolytic cleavage of plasma membrane-bound glycine receptors. J Biol Chem *276*, 42978-42985.

Carazo-Salas, R. E., Guarguaglini, G., Gruss, O. J., Segref, A., Karsenti, E., and Mattaj, I. W. (1999). Generation of GTP-bound Ran by RCC1 is required for chromatin-induced mitotic spindle formation. Nature *400*, 178-181.
Carbone, R., Pearson, M., Minucci, S., and Pelicci, P. G. (2002). PML NBs associate with the hMre11 complex and p53 at sites of irradiation induced DNA damage. Oncogene *21*, 1633-1640.
Carrano, A. C., Eytan, E., Hershko, A., and Pagano, M. (1999). SKP2 is required for ubiquitin-mediated degradation of the CDK inhibitor p27. Nat Cell Biol *1*, 193-199.
Castedo, M., Perfettini, J. L., Roumier, T., Andreau, K., Medema, R., and Kroemer, G. (2004). Cell death by mitotic catastrophe: a molecular definition. Oncogene *23*, 2825-2837.
Chaturvedi, P., Sudakin, V., Bobiak, M. L., Fisher, P. W., Mattern, M. R., Jablonski, S. A., Hurle, M. R., Zhu, Y., Yen, T. J., and Zhou, B. B. (2002). Chfr regulates a mitotic stress pathway through its RING-finger domain with ubiquitin ligase activity. Cancer Res *62*, 1797-1801.
Chau, V., J.W., T., A., B., D, M., D.J., E., D.K., G., and Varshavsky, A. (1989). A multiubiquitin chain is confined to specific lysine in a targeted short-lived protein. Science *243*, 1576-1583.
Chen, Z., and Pickart, C. M. (1990). A 25-kilodalton ubiquitin carrier protein (E2) catalyzes multi-ubiquitin chain synthesis via lysine 48 of ubiquitin. J Biol Chem *265*, 21835-21842.
Ciechanover, A., Elias, S., Heller, H., Ferber, S., and Hershko, A. (1980). Characterization of the heat-stable polypeptide of the ATP-dependent proteolytic system from reticulocytes. J Biol Chem *255*, 7525-7528.
Ciechanover, A., Orian, A., and Schwartz, A. L. (2000). Ubiquitin-mediated proteolysis: biological regulation via destruction. Bioessays *22*, 442-451.
Cook, W. J., Jeffrey, L. C., Carson, M., Chen, Z., and Pickart, C. M. (1992). Structure of a diubiquitin conjugate and a model for interaction with ubiquitin conjugating enzyme (E2). J Biol Chem *267*, 16467-16471.
Cook, W. J., Jeffrey, L. C., Kasperek, E., and Pickart, C. M. (1994). Structure of tetraubiquitin shows how multiubiquitin chains can be formed. J Mol Biol *236*, 601-609.
Cook, W. J., Jeffrey, L. C., Xu, Y., and Chau, V. (1993). Tertiary structures of class I ubiquitin-conjugating enzymes are highly conserved: crystal structure of yeast Ubc4. Biochemistry *32*, 13809-13817.
Creagh, E. M., Murphy, B. M., Duriez, P. J., Duckett, C. S., and Martin, S. J. (2004). Smac/Diablo antagonizes ubiquitin ligase activity of inhibitor of apoptosis proteins. J Biol Chem *279*, 26906-26914.
Das, A. K., Cohen, P. W., and Barford, D. (1998). The structure of the tetratricopeptide repeats of protein phosphatase 5: implications for TPRmediated
protein-protein interactions. EMBO J *17*, 1192-1199.
Dasso, M. (2001). Running on Ran: nuclear transport and the mitotic spindle. Cell *104*, 321-324.
Deng, L., Wang, C., Spencer, E., Yang, L., Braun, A., You, J., Slaughter, C., Pickart, C., and Chen, Z. J. (2000a). Activation of the IkappaB kinase complex by TRAF6 requires a dimeric ubiquitin-conjugating enzyme complex and a unique polyubiquitin chain. Cell *103*, 351-361.

Deng, L., Wang, C., Spencer, E., Yang, L., Braun, A., You, J., Slaughter, C., Pickart, C. M., and Chen, Z. J. (2000b). Activation of the IkapaB kinase complex by TRAF6 requires a dimeric ubiquitin-conjugating enzyme complex and a unique polyubiquitin chain. Cell *103*, 351-361.
Desterro, J. M., Rodriguez, M. S., and Hay, R. T. (1998). SUMO-1 modification of IkappaBalpha inhibits NF-KappaB activation. MolCell *2*, 233-239.
Didier, C., Broday, L., Bhoumik, A., Israeli, S., Takahashi, S., Nakayama, K., Thomas, S. M., Turner, C. E., Henderson, S., Sabe, H., and Ronai, Z. (2003). RNF5, a RING finger protein that regulates cell motility by targeting paxillin ubiquitination and altered localization. Mol Cell Biol *23*, 5331-5345.
Diehl, J. A., Cheng, M., Roussel, M. F., and Sherr, C. J. (1998). Glycogen synthase kinase-3beta regulates cyclin D1 proteolysis and subcellular localization. Genes Dev *12*, 3499-3511.
Duckett, C. S., Nava, V. E., Gedrich, R. W., Clem, R. J., Van Dongen, J. L., Gilfillan, M. C., Shiels, H., Hardwick, J. M., and Thompson, C. B. (1996). A conserved family of cellular genes related to the baculovirus iap gene and encoding apoptosis inhibitors. Embo J *15*, 2685-2694.
Durocher, D., Taylor, I. A., Sarbassova, D., Haire, L. F., Westcott, S. L., Jackson, S. P., Smerdon, S. J., and Yaffe, M. B. (2000). The molecular basis of FHA
domain:phosphopeptide binding specificity and implications for phosphodependent
signaling mechanisms. Mol Cell *6*, 1169-1182.
Ebisawa, T., Fukuchi, M., Murakami, G., Chiba, T., Tanaka, K., Imamura, T., and Miyazono, K. (2001). Smurf1 interacts with transforming growth factor-beta type I receptor through Smad7 and induces receptor degradation. J Biol Chem *276*, 12477-12480.
Eki, T., Abe, M., Naitou, M., Sasanuma, S. I., Nohata, J., Kawashima, K., Ahmad, I., Hanaoka, F., Murakami, Y. C. a. c., of novel gene, D., expressed from Down's syndrome critical region of, and human chromosome 21q22.2. DNA Seq 7, -. (1997). Cloning and characterization
of novel gene, DCRR1, expressed from Down's syndrome critical region of human chromosome 21q22.2. DNA Seq *7*, 153-164.
Engqvist-Goldstein, A. E., Kessels, M. M., Chopra, V. S., Hayden, M. R., and Drubin, D. G. (1999). An actin-binding protein of the Sla2/Huntingtin interacting protein 1 family is a novel component of clathrin-coated pits and vesicles. J Cell Biol *147*, 1503-1518.
Etlinger, J. D., and Goldberg, A. L. (1977). A soluble ATP-dependent proteolytic system responsible for the degradation of abnormal proteins in reticulocytes. Proc Natl Acad Sci U S A *74*, 54-58.
Fields, S., and Song, O.-K. (1989). A novel genetic system to detect protein-protein interactions. Nature *340*, 245-246.
Fraschini, R., Bilotta, D., Lucchini, G., and Piatti, S. (2004). Functional Characterization of Dma1 and Dma2, the Budding Yeast Homologues of Schizosaccharomyces pombe Dma1 and Human Chfr. Mol Biol Cell *15*, 3796-3810.
Galan, J. M., and Haguenauer-Tsapis, R. (1997a). Ubiquitin lys63 is involved in ubiquitination of a yeast plasma membrane protein. Embo J *16*, 5847-5854.
Galan, J.-M., and Haguenauer-Tsapis, R. (1997b). Ubiquitin Lys63 is involved in ubiquitination of a yeast plasma membrane protein. Embo J *16*, 5847-5854.

Gervais, F. G., Singaraja, R., Xanthoudakis, S., Gutekunst, C.-A., Leavitt, B. R., Metzler, M., Hackam, A. S., Tam, J., Vaillancourt, J. P., Houtzager, V.*, et al.* (2002). Recruitment and activation of caspase-8 by the Huntingtin-interacting protein Hip-1 and a novel partner Hippi. *4*, 95-105.
Geymonat, M., Spanos, A., Smith, S. J., Wheatley, E., Rittinger, K., Johnston, L. H., and Sedgwick, S. G. (2002). Control of mitotic exit in budding yeast. In vitro regulation of Tem1 GTPase by Bub2 and Bfa1. J Biol Chem *277*, 28439-28445.
Girdwood, D., Bumpass, D., Vaughan, O. A., Thain, A., Anderson, L. A., Snowden, A. W., Garcia-Wilson, E., Perkins, N. D., and Hay, R. T. (2003). P300 transcriptional repression is mediated by SUMO modification. Mol Cell *11*, 1043-1054.
Glickman, M. H., and Ciechanover, A. (2002). The ubiquitin-proteasome proteolytic pathway: destruction for the sake of construction. Physiol Rev *82*, 373-428.
Goebl, M., and Yanagida, M. (1991). The TPR snap helix: a novel protein repeat motif from mitosis to transcription. Trends Biochem Sci *16*, 173-177.
Goldknopf, I. L., and Busch, H. (1977). Isopeptide linkage between nonhistone and histone 2A polypeptides of chromosomal conjugate-protein A24. Proc Natl Acad Sci U S A *74*, 864-868.
Goldstein, G., Scheid, M., Hammerling, U., Schlesinger, D. H., Niall, H. D., and Boyse, E. A. (1975). Isolation of a polypeptide that has lymphocyte-differentiating properties and is probably represented universally in living cells. Proc Natl Acad Sci U S A *72*, 11-15.
Gorbsky, G. J. (2001). The mitotic spindle checkpoint. Curr Biol *11*, R1001-1004.
Gostissa, M., Hengstermann, A., Fogal, V., Sandy, P., Schwarz, S. E., Scheffner, M., and Del Sal, G. (1999). Activation of p53 by conjugation to the ubiquitin-like protein SUMO-1. Embo J *18*, 6462-6471.
Guertin, D. A., Trautmann, S., and McCollum, D. (2002a). Cytokinesis in eukaryotes. Microbiol Mol Biol *Rev 66*, 155-178.
Guertin, D. A., Venkatram, S., Gould, K. L., and McCollum, D. (2002). Dma1 prevents mitotic exit and cytokinesis by inhibiting the septation initiation network (SIN). Dev Cell *3*, 779-790.
Guertin, D. A., Venkatram, S., Gould, K. L., and McCollum, D. (2002b). Dma1prevents mitotic exit and cytokinesis by inhibiting the septation initiation network
(SIN). Dev Cell *3*, 779-790.
Guo, A., Salomoni, P., Luo, J., Shih, A., Zhong, S., Gu, W., and Paolo Pandolfi, P. (2000). The function of PML in p53-dependent apoptosis. Nat Cell Biol *2*, 730-736.
Haas, A. L., and Rose, I. A. (1982). The mechanism of ubiquitin activating enzyme. A kinetic and equilibrium analysis. J Biol Chem *257*, 10329-10337.
Haas, A. L., Warms, J. V., Hershko, A., and Rose, I. A. (1982). Ubiquitin-activating enzyme. Mechanism and role in protein-ubiquitin conjugation. J Biol Chem *257*, 2543-2548.
Habelhah, H., Takahashi, S., Cho, S. G., Kadoya, T., Watanabe, T., and Ronai, Z. (2004). Ubiquitination and translocation of TRAF2 is required for activation of JNK but not of p38 or NF-kappaB. Embo J *23*, 322-332.
Hackam, A. S., Yassa, A. S., Singaraja, R., Metzler, M., Gutekunst, C. A., Gan, L., Warby, S., Wellington, C. L., Vaillancourt, J., Chen, N.*, et al.* (2000).

Huntingtin interacting protein 1 induces apoptosis via a novel caspase-dependent death effector domain. J Biol Chem *275*, 41299-41308.
Haglund, K., Di Fiore, P. P., and Dikic, I. (2003). Distinct monoubiquitin signals in receptor endocytosis. Trends Biochem Sci *28*, 598-603.
Hamilton, K. S., Ellison, M. J., Barber, K. R., Williams, R. S., Huzil, J. T., McKenna, S., Ptak, C., Glover, M., and Shaw, G. S. (2001). Structure of a conjugating enzyme-ubiquitin thiolester intermediate reveals a novel role for the ubiquitin tail. Structure (Camb) *9*, 897-904.
Hardy, J. (1997). Amyloid, the presenilins and Alzheimer's disease. Trends Neurosci *20*, 154-159.
Harper, J. W., Burton, J. L., and Solomon, M. J. (2002). The anaphase-promoting complex: it's not just for mitosis any more. Genes Dev *16*, 2179-2206.
Hartmann-Petersen, R., Hendil, K. B., and Gordon, C. (2003). Ubiquitin binding proteins protect ubiquitin conjugates from disassembly. FEBS Lett *535*, 77-81.
Hatakeyama, S., and Nakayama, K. (2003). U-box proteins as a new family of ubiquitin ligases. Biochem Biophys Res Commun *302*, 635-645.
HDCRG (1993). A novel gene containing a trinucleotide repeat that is expanded and unstable on Huntington's disease chromosomes. The Huntington's Disease Collaborative Research Group. Cell *72*, 971-983.
Henry, K. W., Wyce, A., Lo, W. S., Duggan, L. J., Emre, N. C., Kao, C. F., Pillus, L., Shilatifard, A., Osley, M. A., and Berger, S. L. (2003). Transcriptional activation via sequential histone H2B ubiquitylation and deubiquitylation, mediated by SAGA-associated Ubp8. Genes Dev *17*, 2648-2663.
Hershko, A., and Ciechanover, A. (1998). The ubiquitin system. Annu Rev Biochem *67*, 425-479.
Hetzer, M., Bilbao-Cortes, D., Walther, T. C., Gruss, O. J., and Mattaj, I. W. (2000). GTP hydrolysis by Ran is required for nuclear envelope assembly. Mol Cell *5*, 1013-1024.
Hicke, L. (2001). Protein regulation by monoubiquitin. Nat Rev Mol Cell Biol *2*, 195-201.
Hicke, L., and Dunn, R. (2003). Regulation of membrane protein transport by ubiquitin and ubiquitin-binding proteins. Annu Rev Cell Dev Biol *19*, 141-172.
Hochstrasser, M. (1996). Protein degradation or regulation: Ub the judge. Cell *84*, 813-815.
Hoege, C., Pfander, B., Moldovan, G. L., Pyrowolakis, G., and Jentsch, S. (2002). RAD6-dependent DNA repair is linked to modification of PCNA by ubiquitin and SUMO. Nature *419*, 135-141.
Hofmann, K., and Falquet, L. (2001). A ubiquitin-interacting motif conserved in components of the proteasomal and lysosomal protein degradation systems. Trends Biochem Sci *26*, 347-350.
Hofmann, R. M., and Pickart, C. M. (1999). Noncanonical MMS2-encoded ubiquitin-conjugating enzyme functions in assembly of novel polyubiquitin chains for DNA repair. Cell *96*, 645-653.
Hofmann, T. G., and Will, H. (2003). Body language: the function of PML nuclear bodies in apoptosis regulation. Cell Death Differ *10*, 1290-1299.
Hongtao, Y. (2002). Regulation of APC-Cdc20 by the spindle checkpoint. Curr Opin Cell Biol *14*, 706-714.
Hoyt, M. A. (2001). A new view of the spindle checkpoint. J Cell Biol *154*, 909-911.

Hu, M., Li, P., Li, M., Li, W., Yao, T., Wu, J. W., Gu, W., Cohen, R. E., and Shi, Y. (2002). Crystal structure of a UBP-family deubiquitinating enzyme in isolation and in complex with ubiquitin aldehyde. Cell *111*, 1041-1054.
Huang, H., Joazeiro, C. A., Bonfoco, E., Kamada, S., Leverson, J. D., and Hunter, T. (2000). The inhibitor of apoptosis, cIAP2, functions as a ubiquitin-protein ligase and promotes in vitro monoubiquitination of caspases 3 and 7. J Biol Chem *275*, 26661-26664.
Huang, L., Kinnucan, E., Wang, G., Beaudenon, S., Howley, P. M., Huibregtse, J. M., and Pavletich, N. P. (1999). Structure of an E6AP-UbcH7 complex: insights into ubiquitination by the E2-E3 enzyme cascade. Science *286*, 1321-1326.
Huang, Y., Baker, R. T., and Fischer-Vize, J. A. (1995). Control of cell fate by a deubiquitinating enzyme encoded by the fat facets gene. Science *270*, 1828-1831.
Huibregtse, J. M., Scheffner, M., Beaudenon, S., and Howley, P. M. (1995). A family of proteins structurally and functionally related to the E6-AP ubiquitin-protein ligase. Proc Natl Acad Sci U S A *92*, 5249.
Hunt, L. T., and Dayhoff, M. O. (1977). Amino-terminal sequence identity of ubiquitin and the nonhistone component of nuclear protein A24. Biochem Biophys Res Commun *74*, 650-655.
Hyun, T. S., and Ross, T. S. (2004). HIP1: trafficking roles and regulation of tumorigenesis. TRENDS Mol Med *10*, 194-199.
Ishov, A. M., G., S. A., Negorev, D., Vladimirova, O. V., Neff, N., Kamitani, T., Yeh, E. T., Strauss, J. J. F., and Maul, G. G. (1999). PML is critical for ND10 formation and recruits the PML-interacting protein Daxx to this nuclear structure when modified by SUMO-1. J Cell Biol *147*, 221-234.
Ito, K., Adachi, S., Iwakami, R., Yasuda, H., Muto, Y., Seki, N., and Okano, Y. (2001). N-Terminally extended human ubiquitin-conjugating enzymes (E2s) mediate the ubiquitination of RING-finger proteins, ARA54 and RNF8. Eur J Biochem *268*, 2725-2732.
Jackman, M., Lindon, C., Nigg, E. A., and Pines, J. (2003). Active cyclin B1-Cdk1 first appears on centrosomes in prophase. Nat Cell Biol *5*, 143-148.
Jackson, P. K., Eldridge, A. G., Freed, E., Furstenthal, L., Hsu, J. Y., Kaiser, B. K., and Reimann, J. D. (2000). The Lore of the RINGs: substrate recognition and catalysis by ubiquitin ligases. Trends Cell Biol *10*, 429-439.
Jang, M. S., Ryu, S. W., and Kim, E. (2002). Modification of Daxx by small ubiquitin-related modifier-1. Biochem Biophys Res Commun *295*, 495-500.
Jensen, D. E., Proctor, M., Marquis, S. T., Gardner, H. P., Ha, S. I., Chodosh, L. A., Ishov, A. M., Tommerup, N., Vissing, H., Sekido, Y.*, et al.* (1998). BAP1: a novel ubiquitin hydrolase which binds to the BRCA1 RING finger and enhances BRCA1-mediated cell growth suppression. Oncogene *16*, 1097-1112.
Jensen, J. P., Bates, P. W., Yang, M., Vierstra, R. D., and Weissman, A. M. (1995). Identification of a family of closely related human ubiquitin conjugating enzymes. J Biol Chem *270*, 30408-30414.
Jentsch, S. (1992). Ubiquitin-dependent protein degradation: a cellular perspective. Trends Cell Biol *2*, 98-103.
Jesenberger, V., and Jentsch, S. (2002). Deadly encounter: ubiquitin meets apoptosis. Nat Rev Mol Cell Biol *3*, 112-121.
Jin, P., Hardy, S., and Morgan, D. O. (1998). Nuclear localization of cyclin B1 controls mitotic entry after DNA damage. J Cell Biol *141*, 875-885.

Joazeiro, C. A., and Weissman, A. M. (2000). RING finger proteins: mediators of
ubiquitin ligase activity. Cell *102*, 549-552.
Joazeiro, C. A., Wing, S. S., Huang, H., Leverson, J. D., Hunter, T., and Liu, Y. C. (1999). The tyrosine kinase negative regulator c-Cbl as a RING-type, E2-dependent ubiquitin-protein ligase. Science *286*, 309-312.
Johnson, E. S., and Blobel, G. (1999). Cell cycle regulated attachment of the ubiquitin-related protein SUMO to the yeast septins. J Cell Biol *147*, 981-994.
Johnson, E. S., Ma, P. C. M., Ota, I. M., and Varshavsky, A. (1995). A Proteolytic Pathway That Recognizes Ubiquitin as a Degradation Signal. J Biol Chem *270*, 17442-17456.
Johnson, L. N., and Lewis, R. J. (2001). Structural basis for control by phosphorylation. Chem Rev *101*, 2209-2242.
Joseph, J., Tan, S. H., Karpova, T. S., McNally, J. G., and Dasso, M. (2002). SUMO-1 targets RanGAP1 to kinetochores and mitotic spindles. J Cell Biol *156*, 595-602.
Kahana, J. A., and Cleveland, D. W. (2001). Some Importin News About Spindle Assembly. Science *291*, 1718-1719.
Kaksonen, M., Sun, Y., and Drubin, D. G. (2003). A pathway for association of receptors, adaptors, and actin during endocytic internalization. Cell *115*, 475-487.
Kanayama, A., Seth, R. B., Sun, L., Ea, C.-K., Hong, M., Shaito, A., Chiu, Y.-H., Deng, L., and Chen, Z. J. (2004). TAB2 and TAB3 Activate the NFkappaB Pathway through Binding to Polyubiquitin Chains. Cell *15*, 535-548.
Kang, D., Chen, J., Wong, J., and Fang, G. (2002). The checkpoint protein Chfr is a ligase that ubiquitinates Plk1 and inhibits Cdc2 at the G2 to M transition. J Cell Biol *156*, 249-259.
Katzmann, D. J., Odorizzi, G., and Emr, S. D. (2002). Receptor downregulation and multivesicular-body sorting. Nat Rev Mol Cell Biol *3*, 893-905.
Kleijnen, M., Shih, A. H., Zhou, P., Kumar, S., Soccio, R. E., Kedersha, N. L., Gill, G., and Howley, P. M. (2000). The hPLIC proteins may provide a link between the ubiquitination machinery and the proteasome. MolCell *6*, 409-419.
Kloetzel, P. M. (2001). Antigen processing by the proteasome. Nat Rev Mol Cell Biol *2*, 179-187.
Koegl, M., Hoppe, T., Schlenker, S., Ulrich, H. D., Mayer, T. U., and Jentsch, S. (1999). A novel ubiquitination factor, E4, is involved in multiubiquitin chain assembly. Cell *96*, 635-644.
Kong, M., Barnes, E. A., Ollendorff, V., and Donoghue, D. J. (2000). Cyclin F regulates the nuclear localization of cyclin B1 through a cyclin-cyclin interaction. Embo J *19*, 1378-1388.
Kotani, S., Tanaka, H., Yasuda, H., and Todokoro, K. (1999). Regulation of APC activity by phosphorylation and regulatory factors. J Cell Biol *146*, 791-800.
Kovalenko, A., Chable-Bessia, C., Cantarella, G., Israel, A., Wallach, D., and Courtois, G. (2003). The tumour suppressor CYLD negatively regulates NF-kappaB signalling by deubiquitination. Nature *424*, 801-805.
Kreft, S. G., and Nassal, M. (2003). hRUL138, a novel human RNA-binding RING-H2 ubiquitin-protein ligase. J Cell Sci *116*, 605-616.

Kwek, S. S., Derry, J., Tyner, A. L., Shen, Z., and Gudkov, A. V. (2001). Functional analysis and intracellular localization of p53 modified by SUMO-1. Oncogene *20*, 2587-2599.
Lake, M. W., Wuebbens, M. M., Rajagopalan, K. V., and Schindelin, H. (2001). Mechanism of ubiquitin activation revealed by the structure of a bacterial MoeB-MoaD complex. Nature *414*, 325-329.
Lam, Y. A., DeMartino, G. N., Pickart, C. M., and Cohen, R. E. (1997). Specificity of the ubiquitin isopeptidase in the PA700 regulatory complex of the 26 S proteasomes. J Biol Chem *272*, 28438-28446.
Lam, Y. A., and Pickart, C. M. (2000). Inhibition of the ubiquitin-proteasome system in Alzheimer's disease. Proc Natl Acad Sci U S A *97*, 9902-9906.
Lamb, J. R., Tugendreich, S., and Hieter, P. (1995). Tetratrico peptide repeat interactions: to TPR or not to TPR? Trends Biochem Sci *20*, 257-259.
Lander, E. S., Linton, L. M., Birren, B., Nusbaum, C., Zody, M. C., Baldwin, J., Devon, K., Dewar, K., Doyle, M., FitzHugh, W.*, et al.* (2001). Initial sequencing and analysis of the human genome. Nature *409*, 860-921.
Lane, H. A., and Nigg, E. A. (1996). Antibody microinjection reveals an essential role for human polo-like kinase 1 (Plk1) in the functional maturation of mitotic centrosomes. J Cell Biol *135*, 1701-1713.
Layfield, R., Alban, A., Mayer, R. J., and Lowe, J. (2001). The ubiquitin protein catabolic disorders. Neuropathology and Applied Neurobiology *27*, 171-179.
Lehman, A. L., Nakatsu, Y., Ching, A., Bronson, R. T., Oakey, R. J., Keiper-Hrynko, N., Finger, J. N., Durham-Pierre, D., Horton, D. B., Newton, J. M.*, et al.* (1998). A very large protein with diverse functional motifs is deficient in *rjs* (runty, jerky, sterile) mice. Proc Natl Acad Sci U S A *95*, 9436-9441.
Leroy, E., Boyer, R., Auburger, G., Leube, B., Ulm, G., Mezey, E., Harta, G., Brownstein, M. J., Jonnalagada, S., Chernova, T.*, et al.* (1998). The ubiquitin pathway in Parkinson's disease. Nature *395*, 451-452.
Li, F., Ambrosini, G., Chu, E. Y., Plescia, J., Tognin, S., Marchisio, P. C., and Altieri, D. C. (1998). Control of apoptosis and mitotic spindle checkpoint by survivin. Nature *396*, 580-584.
Li, H., Leo, C., Zhu, J., Wu, X., O'Neil, J., Park, E., and Chen, J. D. (2000a). Sequestration and inhibition of Daxx-mediated transcriptional repression by PML. Mol Cell Biol *20*, 1784-1796.
Liakopoulos, D., Doenges, G., Matuschewski, K., and Jentsch, S. (1998). A novel ubiquitin protein modification pathway related to ubiquitin system. Embo J *17*, 2208-2214.
Liao, H., Byeon, I. J., and Tsai, M. D. (1999). Structure and function of a new phosphopeptide-binding domain containing the FHA2 of Rad53. J Mol Biol *294*, 1041-1049.
Lin, J. H., Deng, G., Huang, Q., and Morser, J. (2000). KIAP, a novel member of the inhibitor of apoptosis protein family. Biochem Biophys Res Commun *279*, 820-831.
Lindon, C., and Pines, J. (2004). Ordered proteolysis in anaphase inactivates Plk1 to contribute to proper mitotic exit in human cells. J Cell Biol *164*, 233-241.
Liston, P., Fong, W. G., Kelly, N. L., Toji, S., Miyazaki, T., Conte, D., Tamai, K., Craig, C. G., McBurney, M. W., and Korneluk, R. G. (2001). Identification of XAF1 as an antagonist of XIAP anti-Caspase activity. Nat Cell Biol *3*, 128-133.
Liston, P., Fong, W. G., and Korneluk, R. G. (2003). The inhibitors of apoptosis: there is more to life than Bcl2. Oncogene *22*, 8568-8580.

Liston, P., Roy, N., Tamai, K., Lefebvre, C., Baird, S., Cherton-Horvat, G., Farahani, R., McLean, M., Ikeda, J. E., MacKenzie, A., and Korneluk, R. G. (1996). Suppression of apoptosis in mammalian cells by NAIP and a related family of IAP genes. Nature *379*, 349-353.
Liu, X., and Erikson, R. L. (2002). Activation of Cdc2/cyclin B and inhibition of centrosome amplification in cells depleted of Plk1 by siRNA. Proc Natl Acad Sci U S A *99*, 8672-8676.
Liu, Z., Haas, A. L., Diaz, L. A., Conrad, C. A., and Giudice, G. J. (1996). Characterization of a Novel Keratinocyte Ubiquitin Carrier Protein. J Biol Chem *271*, 2817-2822.
Loeb, K. R., and Haas, A. L. (1994). Conjugates of ubiquitin cross reactive protein distribute in a cytoskeletal pattern. Mol Cell Biol *14*, 8408-8419.
Lorick, K. L., Jensen, J. P., Fang, S., Ong, A. M., Hatakeyama, S., and Weissman, A. M. (1999). RING fingers mediate ubiquitin-conjugating enzyme (E2)-dependent ubiquitination. Proc Natl Acad Sci U S A *96*, 11364-11369.
Mahajan, R., Delphin, C., Guan, T., Gerace, L., and Melchior, F. (1997). A small ubiquitin-related polypeptide involved in targeting RanGAP1 to nuclear pore complex protein RanBP2. Cell *88*, 97-107.
Margolis, R. L., Lohez, O. D., and Andreassen, P. R. (2003). G1 tetraploidy checkpoint and the suppression of tumorigenesis. J Cell Biochem *88*, 673-683.
Margottin, F., Bour, S. P., Durand, H., Selig, L., Benichou, S., Richard, V., Thomas, D., Strebel, K., and Benarous, R. (1998). A novel human WD protein, h-beta TrCp, that interacts with HIV-1 Vpu connects CD4 to the ER degradation pathway through an F-box motif. Mol Cell *1*, 565-574.
Martinez-Noel, G., Muller, U., and Harbers, K. (2001). Identification of molecular determinants required for interaction of ubiquitin-conjugating enzymes and RING finger proteins. Eur J Biochem *268*, 5912-5919.
Matunis, M. J., Coutavas, E., and Blobel, G. (1996). A novel ubiquitin-like modification modulates the partitioning of the Ran-GTPase-activating protein RanGAP1 between the cytosol and the nuclear pore complex. J Cell Biol *135*, 1457-1470.
McGrath, J. P., Jentsch, S., and Varshavsky, A. (1991). UBA 1: an essential yeast gene encoding ubiquitin-activating enzyme. Embo J *10*, 227-236.
Meresse, P., Dechaux, E., Monneret, C., and Bertounesque, E. (2004). Etoposide: discovery and medicinal chemistry. Curr Med Chem *11*, 2443-2466.
Metzler, M., Li, B., Gan, L., Georgiou, J., Gutekunst, C. A., Wang, Y., Torre, E., Devon, R. S., Oh, R., Legendre-Guillemin, V.*, et al.* (2003). Disruption of the endocytic protein HIP1 results in neurological deficits and decreased AMPA receptor trafficking. Embo J *22*, 3254-3266.
Meyers, M., Hwang, A., Wagner, M. W., and Boothman, D. A. (2004). Role of DNA mismatch repair in apoptotic responses to therapeutic agents. Environ Mol Mutagen *44*, 249-264.
Millband, D. N., Campbell, L., and Hardwick, K. G. (2002). The awesome power of multiple model systems: interpreting the complex nature of the spindle checkpoint signaling. Trends Cell Biol *12*, 205-209.
Miura, T., Klaus, W., Gsell, B., Miyamoto, C., and Senn, H. (1999). Characterization of the binding interface between ubiquitin and class I human ubiquitin-conjugating enzyme 2b by multidimensional heteronuclear NMR spectroscopy in solution. J Mol Biol *290*, 213-228.

Mizushima, M., Noda, T., Yoshimori, T., Tanaka, Y., Ishii, T., George, M. D., Klionsky, D. J., Ohsumi, M., and Ohsumi, Y. (1998). A protein conjugation system essential for autophagy. Nature *395*, 395-398.
Moore, F. L., Jaruzelska, J., Fox, M. S., Urano, J., Firpo, M. T., Turek, P. J., Dorfman, D. M., and Pera, R. A. (2003). Human Pumilio-2 is expressed in embryonic stem cells and germ cells and interacts with DAZ (Deleted in AZoospermia) and DAZ-like proteins. Proc Natl Acad Sci U S A *100*, 538-543.
Mosesson, Y., Shtiegman, K., Katz, M., Zwang, Y., Vereb, G., Szollosi, J., and Yarden, Y. (2003). Endocytosis of receptor tyrosine kinases is driven by monoubiquitylation, not polyubiquitylation. J Biol Chem *278*, 21323-21326.
Muller, S., Matunis, M. J., and Dejean, A. (1998). Conjugation with the ubiquitin-related modifier SUMO-1 regulates the partitioning of PML within the nucleus. Embo J *17*, 61-70.
Murata, S., Minami, Y., Minami, M., Chiba, T., and Tanaka, K. (2001). CHIP is a chaperone-dependent E3 ligase that ubiquitylates unfolded protein. EMBO Rep *2*, 1133-1138.
Muratani, M., and Tansey, W. P. (2003). How the ubiquitin-proteasome system controls transcription. Nat Rev Mol Cell Biol *4*, 192-201.
Murone, M., and Simanis, V. (1996). The fission yeast dma1 gene is a component of the spindle assembly checkpoint, required to prevent septum formation and premature exit from mitosis if spindle function is compromised. Embo J *15*, 6605-6616.
Nakamura, S., Roth, J. A., and Mukhopadhyay, T. (1994). Regulated degradation of the transcription factor Gcn4. Embo J *13*, 6021-6030.
Nakayama, K., Nagahama, H., Minamishima, Y. A., Matsumoto, M., Nakamichi, I., Kitagawa, K., Shirane, M., Tsunematsu, R., Tsukiyama, T., Ishida, N*., et al.* (2000). Targeted disruption of Skp2 results in accumulation of cyclin E and p27(Kip1), polyploidy and centrosome overduplication. Embo J *19*, 2069-2081.
Nishikawa, H., Ooka, S., Sato, K., Arima, K., Okamoto, J., Klevit, R. E., Fukuda, M., and Ohta, T. (2004). Mass spectrometric and mutational analyses reveal Lys-6-linked polyubiquitin chains catalyzed by BRCA1-BARD1 ubiquitin ligase. J Biol Chem *279*, 3916-3924.
Nocker, S. V., and Vierstra, R. D. (1993). Multiubiquitin chains linked through lysine 48 are abundant in vivo and are competent intermediates in the ubiquitin proteolytic pathway. J Biol Chem *268*, 24766-24773.
Nourry, C., Maksumova, L., Pang, M., Liu, X., and Wang, T. (2004). Direct interaction between Smad3, APC10, CDH1 and HEF1 in proteasomal degradation of HEF1. BMC Cell Biol *5*, 20.
Ohi, M. D., Vander Kooi, C. W., Rosenberg, J. A., Chazin, W. J., and Gould, K. L. (2003). Structural insights into the U-box, a domain associated with multi-ubiquitination. Nat Struct Biol *10*, 250-255.
Ohkura, H., Hagan, I. M., and Glover, D. M. (1995). The conserved Schizosaccharomyces pombe kinase plo1, required to form a bipolar spindle, the actin ring, and septum, can drive septum formation in G1 and G2 cells. Genes Dev *9*, 1059-1073.
Osaka, F., Kawasaki, H., Aida, N., Saeki, M., Chiba, T., Kawashima, S., Tanaka, K., and Kato, S. (1998). A new NEDD8-ligating system for cullin-4A. Genes Dev *12*, 2263-2268.

Ouyang, B., Li, W., Pan, H., Meadows, J., Hoffmann, I., and Dai, W. (1999). The physical association and phosphorylation of Cdc25C protein phosphatase by Prk. Oncogene *18*, 6029-6036.
Ozkaynak, E., Finley, D., and Varshavsky, A. (1984). The yeast ubiquitin gene: head-to-tail repeats encoding a polyubiquitin precursor protein. Nature *312*, 663-666.
Passmore, L. A., and Barford, D. (2004). Getting into position: the catalytic mechanisms of protein ubiquitylation. Biochem J *379*, 513-525.
Patnaik, A., Chau, V., and Wills, J. W. (2000). Ubiquitin is part of the retrovirus budding machinery. Proc Natl Acad Sci U S A *97*, 13069-13074.
Patra, D., and Dunphy, W. G. (1998). Xe-p9, a Xenopus Suc1/Cks protein, is essential for the Cdc2-dependent phosphorylation of the anaphase- promoting complex at mitosis. Genes Dev *12*, 2549-2559.
Peng, J., Schwarts, D., Elias, S., Thoreen, C. C., Cheng, D., Marsischky, G., Roelofs, J., Finley, D., and Gygi, S. P. (2003). A proteomics approach to understanding protein ubiquitination. Nat Biotechnol *21*, 921-926.
Pereira, G., Hofken, T., Grindlay, J., Manson, C., and Schiebel, E. (2000). The Bub2p spindle checkpoint links nuclear migration with mitotic exit. Mol Cell *6*, 1-10.
Peters, J. M. (2002). The anaphase-promoting complex: proteolysis in mitosis and beyond. Mol Cell *9*, 931-943.
Petroski, M. D., and Deshaies, R. J. (2003). Context of multiubiquitin chain attachment influences the rate of Sci1 degradation. MolCell *11*, 6021-6030.
Pfleger, C. M., and Kirschner, M. W. (2000). The KEN box: an APC recognition signal distinct from the D box targeted by Cdh1. Genes Dev *14*, 655-665.
Pickart, C. M. (2001). Mechanisms underlying ubiquitination. Annu Rev Biochem *70*, 503-533.
Pines, J., and Hunter, T. (1991). Human cyclins A and B1 are differentially located in the cell and undergo cell cycle-dependent nuclear transport. J Cell Biol *115*, 1-17.
Pray, T. R., Parlati, F., Huang, J., Wong, B. R., Payan, D. G., Bennett, M. K., Issakani, S. D., Molineaux, S., and Demo, S. D. (2002). Cell cycle regulatory E3 ubiquitin ligases as anticancer targets. Drug Resistance Updates *5*, 249-258.
Raiborg, C., Bache, K. G., Gillooly, D. J., Madshus, I. H., Stang, E., and Stenmark, H. (2002). Hrs sorts ubiquitinated proteins into clathrin-coated microdomains of early endosomes. Nat Cell Biol *4*, 394-398.
Rajagopalan, K. V. (1997). Biosynthesis and processing of the molybdenum cofactors. Biochem Soc Trans *25*, 757-761.
Rao, D. S., Bradley, S. V., Kumar, P. D., Hyun, T. S., Saint-Dic, D., Oravecz-Wilson, K., Kleer, C. G., and Ross, T. S. (2003). Altered receptor trafficking in Huntingtin Interacting Protein 1-transformed cells. Cancer Cell *3*, 471-482.
Rao, D. S., Chang, J. C., Kumar, P. D., Mizukami, I., Smithson, G. M., Bradley, S. V., Parlow, A. F., and Ross, T. S. (2001). Huntingtin interacting protein 1 Is a clathrin coat binding protein required for differentiation of late spermatogenic progenitors. Mol Cell Biol *21*, 7796-7806.
Rao, D. S., Hyun, T. S., Kumar, P. D., Mizukami, I. F., Rubin, M. A., Lucas, P. C., Sanda, M. G., and Ross, T. S. (2002). Huntingtin-interacting protein 1 is overexpressed in prostate and colon cancer and is critical for cellular survival. J Clin Invest *110*, 351-360.

Redman, K. L., and Burris, G. W. (1996). The cDNA for the ubiquitin-52-amino-acid fusion protein from rat encodes a previously unidentified 60 S ribosomal subunit protein. Biochem J *315 (Pt 1)*, 315-321.
Reed, S. I. (2003). Ratchets and clocks: the cell cycle, ubiquitylation and protein turnover. Nat Rev Mol Cell Biol *4*, 855-864.
Rocca, A., Lamaze, C., Subtil, A., and Dautry-Varsat, A. (2001). Involvement of the ubiquitin/proteasome system in sorting of the interleukin 2 receptor beta chain to late endocytic compartments. Mol Biol Cell *12*, 1293-1301.
Rodriguez, M. S., Desterro, J. M., Lain, S., Midgley, C. A., Lane, D. P., and Hay, R. T. (1999). SUMO-1 modification activates the transcriptional response of p53. Embo J *18*, 6455-6461.
Rokudai, S., Fujita, N., Kitahara, O., Nakamura, Y., and Tsuruo, T. (2002). Involvement of FKHR-dependent TRADD expression in chemotherapeutic drug-induced apoptosis. Mol Cell Biol *22*, 8695-8708.
Rosa, J. L., Casaroli-Marano, R. P., Buckler, A. J., Vilaro, S., and Barbacid, M. (1996). p619, a giant protein related to the chromosome condensation regulator RCC1, stimulates guanine nucleotide exchange on ARF1 and Rab proteins. Embo J *15*, 4262-4273.
Rothe, M., Pan, M. G., Henzel, W. J., Ayres, T. M., and Goeddel, D. V. (1995). The TNFR2-TRAF signaling complex contains two novel proteins related to baculoviral inhibitor of apoptosis proteins. Cell *83*, 1243-1252.
Salomoni, P., and Pandolfi, P. P. (2002). The role of PML in tumor suppression. Cell *108*, 165-170.
Samuel, T., Okada, K., Hyer, M., Welsh, K., Zapata, J. M., and Reed, J. C. (2005). cIAP1 Localizes to the Nuclear Compartment and Modulates the Cell Cycle. Cancer Res *65*, 210-218.
Sancho, E., Vila, M. R., Sanchez-Pulido, L., Lozano, J. J., Paciucci, R., Nadal, M., Fox, M., Harvey, C., Bercovich, B., Loukili, N.*, et al.* (1998a). Role of UEV-1, an inactive variant of the E2 ubiquitin-conjugating enzymes, in in vitro differentiation and cell cycle behavior of HT-29-M6 intestinal mucosecretory cells. Mol Cell Biol *18*, 576-589.
Sancho, E., Vilà, M. R., Sánchez-Pulido, L., Lozano, J. J., Paciucci, R., Nadal, M., Fox, M., Harvey, C., Bercovich, B., Loukili, N.*, et al.* (1998b). Role of UEV-1, an Inactive Variant of the E2 Ubiquitin-Conjugating Enzymes, in In Vitro Differentiation and Cell Cycle Behavior of HT-29-M6 Intestinal Mucosecretory Cells. Mol Cell Biol *18*, 576-589.
Sax, J. K., Fei, P., Murphy, M. E., Bernhard, E., Korsmeyer, S. J., and El-Deiry, W. S. (2002). BID regulation by p53 contributes to chemosensitivity. Nat Cell Biol *4*, 842-849.
Scheffner, M., Nuber, U., and Huibregtse, J. M. (1995). Protein ubiquitination involving an E1-E2-E3 enzyme ubiquitin thioester cascade. Nature *373*, 81-83.
Schmidt, A., Duncan, P. I., Rauh, N. R., Sauer, G., Fry, A. M., Nigg, E. A., and Mayer, T. U. (2005). Xenopus polo-like kinase Plx1 regulates XErp1, a novel inhibitor of APC/C activity. Genes Dev *19*, 502-513.
Schwarz, S. E., Matusschewski, K., Liakopoulos, D., Scheffner, M., and Jentsch, S. (1998). The ubiquitin-like proteins SMT3 and SUMO-1 are conjugated by the UBC9 E2 enzyme. Proc Natl Acad Sci U S A *95*, 560-564.
Scolnick, D. M., and Halazonetis, T. D. (2000). Chfr defines a mitotic stress checkpoint that delays entry into metaphase. Nature *406*, 430-435.

Seeger, M., Hartmann-Petersen, R., Wilkinson, C. R., Wallace, M., Samejima, I., Taylor, M. S., and Gordon, C. (2003). Interaction of the APC/Cyclosome and 26S proteasome protein complexes with multiubiquitin chain binding proteins. J Biol Chem *278*, 16791-16796.
Seol, J. H., Feldman, R. M., Zachariae, W., Shevchenko, A., Correll, C. C., Lyapina, S., Chi, Y., Galova, M., Claypool, J., Sandmeyer, S.*, et al.* (1999). Cdc53/cullin and the essential Hrt1 RING-H2 subunit of SCF define a ubiquitin ligase module that activates the E2 enzyme Cdc34. Genes Dev *13*, 1614-1626.
Seong, Y. S., Kamijo, K., Lee, J. S., Fernandez, E., Kuriyama, R., Miki, T., and Lee, K. S. (2002). A spindle checkpoint arrest and a cytokinesis failure by the dominant-negative polo-box domain of Plk1 in U-2 OS cells. J Biol Chem *277*, 32282-32293.
Shah, J. V., and Cleveland, D. W. (2000). Waiting for anaphase: Mad2 and the spindle assembly checkpoint. Cell *103*, 997-1000.
Shekhtman, A., and Cowburn, D. (2002). A ubiquitin-interacting motif from Hrs binds to and occludes the ubiquitin surface necessary for polyubiquitination in monoubiquitinated proteins. Biochem Biophys Res Commun *296*, 1222-1227.
Shi, C. S., and Kehrl, J. H. (2003). Tumor necrosis factor (TNF)-induced germinal center kinase-related (GCKR) and stress-activated protein kinase (SAPK) activation depends upon the E2/E3 complex Ubc13-Uev1A/TNF receptor-associated factor 2 (TRAF2). J Biol Chem *278*, 15429-15434.
Shih, S. C., Sloper-Mould, K. E., and Hicke, L. (2000). Monoubiquitin carries a novel internalization signal that is appended to activated receptors. Embo J *19*, 187-198.
Shiio, Y., and Eisenman, R. N. (2003). Histone sumoylation is associated with transcriptional repression. Proc Natl Acad Sci U S A *100*, 13225-13230.
Shirayama, M., Zachariae, W., Ciosk, R., and Nasmyth, K. (1998). The Polo-like kinase Cdc5p and the WD-repeat protein Cdc20p/fizzy are regulators and substrates of the anaphase promoting complex in Saccharomyces cerevisiae. Embo J *17*, 1336-1349.
Shtiegman, K., and Yarden, Y. (2003). The role of ubiquitylation in signaling by growth factors: implications to cancer. Semin Cancer Biol *13*, 29-40.
Simanis, V. (2003). Events at the end of mitosis in the budding and fission yeasts. J Cell Sci *116*, 4263-4275.
Sloper-Mould, K. E., J.C., J., Pickart, C. M., and Hicke, L. (2001). Distinct functional surface regions on ubiquitin. J Biol Chem *276*, 30483-30489.
Sonneveld, E., Vrieling, H., Mullenders, L. H., and van Hoffen, A. (2001). Mouse mismatch repair gene Msh2 is not essential for transcription-coupled repair of UV-induced cyclobutane pyrimidine dimers. Oncogene *20*, 538-541.
Spence, J., Gali, R. R., Dittmar, G., Sherman, F., Karin, M., and Finley, D. (2000a). Cell cycle-regulated modification at the endoplasmatic reticulum. Nature *365*, 176-179.
Spence, J., Gali, R. R., Dittmar, G., Sherman, F., Karin, M., and Finley, D. (2000b). Cell cycle-regulated modification of the ribosome by a variant multiubiquitin chain. Cell *102*, 67-76.
Steffan, J. S., Agrawal, N., Pallos, J., Rockabrand, E., Trotman, L. C., Slepko, N., Illes, K., Lukacsovich, T., Zhu, Y., Cattaneo, E.*, et al.* (2004a). SUMO Modification of Huntingtin and Huntington's Disease Pathology. Science *304*, 100-103.

Steffan, J. S., Agrawal, N., Pallos, J., Rockabrand, E., Trotman, L. C., Slepko, N., Illes, K., Lukacsovich, T., Zhu, Y. Z., Cattaneo, E.*, et al.* (2004b). SUMO modification of Huntingtin and Huntington's disease pathology. Science *304*, 100-104.
Stern, B. M. (2002). Mitosis: aurora gives chromosomes a healthy stretch. Curr Biol *12*, R316-318.
Stern, B. M., and Murray, A. W. (2001). Lack of tension at kinetochores activates the spindle checkpoint in budding yeast. Curr Biol *11*, 1462-1467.
Sternsdorf, T., Jensen, K., and Will, H. (1997). Evidence for covalent modification of the nuclear dot-associated proteins PML and Sp100 by PIC1/SUMO-1. J Cell Biol *139*, 1621-1634.
Strack, B., Calistri, A., Accola, M. A., Palu, G., and Gottlinger, H. G. (2000). A role for ubiquitin ligase recruitment in retrovirus release. Proc Natl Acad Sci U S A *97*, 13063-13068.
Sun, L., Deng, L., Ea, C.-K., Xia, Z.-P., and Chen, Z. J. (2004). The TRAF6 Ubiquitin Ligase and TAK1 Kinase Mediate IKK Activation by BCL10 and MALT1 in T Lymphocytes. Cell *14*, 289-301.
Sunkel, C. E., and Glover, D. M. (1988). polo, a mitotic mutant of Drosophila displaying abnormal spindle poles. J Cell Sci *89 (Pt 1)*, 25-38.
Suzuki, Y., Imai, Y., Nakayama, H., Takahashi, K., Takio, K., and Takahashi, R. (2001a). A serine protease, HtrA2, is released from the mitochondria and interacts with XIAP, inducing cell death. Mol Cell *8*, 613-621.
Suzuki, Y., Nakabayashi, Y., and Takahashi, R. (2001b). Ubiquitin-protein ligase activity of X-linked inhibitor of apoptosis protein promotes proteasomal degradation of caspase-3 and enhances its anti-apoptotic effect in Fas-induced cell death. Proc Natl Acad Sci U S A *98*, 8662-8667.
Swaminathan, S., Amerik, A. Y., and Hochstrasser, M. (1999). The Doa4 deubiquitinating enzyme is required for ubiquitin homeostasis in yeast. Mol Biol Cell *10*, 2583-2594.
Takano, Y., Adachi, S., Okuno, M., Muto, Y., Yoshioka, T., Matsushima-Nishiwaki, R., Tsurumi, H., Ito, K., Friedman, S. L., Moriwaki, H.*, et al.* (2004). The RING finger protein, RNF8, interacts with retinoid X receptor alpha and enhances its transcription-stimulating activity. J Biol Chem *279*, 18926-18934.
Tanaka, T. U. (2002). Bi-orienting chromosomes on the mitotic spindle. Curr Opin Cell Biol *14*, 365-371.
Tanaka, T. U., Rachidi, N., Janke, C., Pereira, G., Galova, M., Schiebel, E., Stark, M. J., and Nasmyth, K. (2002). Evidence that the Ipl1-Sli15 (Aurora kinase-INCENP) complex promotes chromosome bi-orientation by altering kinetochore-spindle pole connections. Cell *108*, 317-329.
Tang, Z., Li, B., Bharadwaj, R., Zhu, H., Ozkan, E., Hakala, K., Deisenhofer, J., and Yu, H. (2001). APC2 Cullin protein and APC11 RING protein comprise the minimal ubiquitin ligase module of the anaphase-promoting complex. Mol Biol Cell *12*, 3839-3851.
Terrell, J., Shih, S., Dunn, R., and Hicke, L. (1998). A function for monoubiquitination in the internalization of a G protein-coupled receptor. Mol Cell *1*, 193-202.
Thomson, T. M., Lozano, J. J., Loukili, N., Carrio, R., Serras, F., Cormand, B., Valeri, M., Diaz, V. M., Abril, J., Burset, M.*, et al.* (2000). Fusion of the human gene for the polyubiquitination coeffector UEV1 with Kua, a newly identified gene. Genome Res *10*, 1743-1756.

Thrower, J. S., Hoffman, L., Rechsteiner, M., and Pickart, C. M. (2000). Recognition of the polyubiquitin proteolytic signal. Embo J *19*, 94-102.
Toyoshima, F., Moriguchi, T., Wada, A., Fukuda, M., and Nishida, E. (1998). Nuclear export of cyclin B1 and its possible role in the DNA damage-induced G2 checkpoint. Embo J *17*, 2728-2735.
Trompouki, E., Hatzivassiliou, E., Tsichritzis, T., Farmer, H., Ashworth, A., and Mosialos, G. (2003). CYLD is a deubiquitinating enzyme that negatively regulates NF-kappaB activation by TNFR family members. Nature *424*, 793-796.
Tsukahara, F., Hattori, M., Muraki, T., and Sakaki, Y. (1996). Identification and cloning of a novel cDNA belonging to tetratricopeptide repeat gene family from Down syndrome-critical region 21q22.2. J Biochem *120*, 820-827.
Ulrich, H. D. (2003). Protein-protein interactions within an E2-RING finger complex. Implications for ubiquitin-dependent DNA damage repair. J Biol Chem *278*, 7051-7058.
Ulrich, H. D., and Jentsch, S. (2000). Two RING finger proteins mediate cooperation between ubiquitin-conjugating enzymes in DNA repair. Embo J *19*, 3388-3397.
Uren, A. G., Pakusch, M., Hawkins, C. J., Puls, K. L., and Vaux, D. L. (1996). Cloning and expression of apoptosis inhibitory protein homologs that function to inhibit apoptosis and/or bind tumor necrosis factor receptor-associated factors. Proc Natl Acad Sci U S A *93*, 4974-4978.
VanDemark, A. P., and Hill, C. P. (2002). Structural basis of ubiquitylation. Curr Opin Struct Biol *12*, 822-830.
VanDemark, A. P., Hofmann, R. M., Tsui, C., Pickart, C. M., and Wolberger, C. (2001). Molecular insights into polyubiquitin chain assembly: crystal structure of the Mms2/Ubc13 heterodimer. Cell *105*, 711-720.
Varadan, R., Assfalg, M., Haririnia, A., Raasi, S., Pickart, C. M., and Fushman, D. (2003). Solution conformation of Lys63-linked di-ubiquitin chain provides clues to functional diversity of polyubiquitin signaling. J Biol Chem *25*.
Varadan, R., Walker, O., Pickart, C., and Fushman, D. (2002a). Structural properties of polyubiquitin chains in solution. J Mol Biol *324*, 637-647.
Varadan, R., Walker, O., Pickart, C. M., and Fushman, D. (2002b). Structural properties of polyubiquitin chains in solution. J Mol Biol *324*, 637-647.
Varelas, X., Ptak, C., and Ellison, M. J. (2003). Cdc34 self-association is facilitated by ubiquitin thiolester formation and is required for its catalytic activity. Mol Cell Biol *23*, 5388-5400.
Verdecia, M. A., Joazeiro, C. A., Wells, N. J., Ferrer, J. L., Bowman, M. E., Hunter, T., and Noel, J. P. (2003a). Conformational flexibility underlies ubiquitin ligation mediated by the WWP1 HECT domain E3 ligase. Mol Cell *11*, 249-259.
Verdecia, M. A., Joazeiro, C. A. P., Wells, N. J., Ferrer, J.-L., Bowman, M. E., Hunter, T., and Noel, J. P. (2003b). Conformational Flexibility Underlies Ubiquitin Ligation Mediated by the WWP1 HECT Domain E3 Ligase. Molecular Cell *11*, 249-259.
Visintin, R., Craig, K., Hwang, E. S., Prinz, S., Tyers, M., and Amon, A. (1998). The phosphatase Cdc14 triggers mitotic exit by reversal of Cdk-dependent phosphorylation. Mol Cell *2*, 709-718.
Visintin, R., Prinz, S., and Amon, A. (1997). CDC20 and CDH1: a family of substrate-specific activators of APC-dependent proteolysis. Science *278*, 460-463.

Vogelstein, B., Lane, D., and Levine, A. J. (2000a). Surfing the p53 network. Nature *408*, 307-310.
Vogelstein, B., Lane, D., and Levine, A. J. (2000b). Surfing the p53 network. Nature *408*, 307-310.
Walden, H., Podgorski, M. S., Huang, D. T., Miller, D. W., Howard, R. J., Minor, D. L., Jr., Holton, J. M., and Schulman, B. A. (2003a). The structure of the APPBP1-UBA3-NEDD8-ATP complex reveals the basis for selective ubiquitin-like protein activation by an E1. Mol Cell *12*, 1427-1437.
Walden, H., Podgorski, M. S., and Schulman, B. A. (2003b). Insights into the ubiquitin transfer cascade from the structure of the activating enzyme for NEDD8. Nature *422*, 330-334.
Wang, C., Deng, L., Hong, M., Akkaraju, G. R., Inoue, J., and Chen, Z. J. (2001a). TAK1 is a ubiquitin-dependent kinase of MKK and IKK. Nature *412*, 346-351.
Wang, C., Deng, L., Hong, M., Akkaraju, G. R., Inoue, J., and Chen, Z. J. (2001b). TAK1 is a ubiquitin-dependent kinase of MKK and IKK. Nature *412*, 346-351.
Wang, R. H., Yu, H., and Deng, C. X. (2004). A requirement for breast-cancer-associated gene 1 (BRCA1) in the spindle checkpoint. Proc Natl Acad Sci U S A *101*, 17108-17113.
Wilkinson, K. D. (1997). Regulation of ubiquitin-dependent processes by deubiquitinating enzymes. Faseb J *11*, 1245-1256.
Wilkinson, K. D. (2000). Ubiquitination and deubiquitination: targeting of proteins for degradation by the proteasome. Semin Cell Dev Biol *11*, 141-148.
Wilkinson, K. D., and Hochstrasser, M. (1998). The Deubiquitinating Enzymes in Ubiquitin. Plenum, New York, 99-125.
Wilkinson, K. D., Urban, M. K., and Haas, A. L. (1980). Ubiquitin is the ATP-dependent proteolysis factor I of rabbit reticulocytes. J Biol Chem *255*, 7529-7532.
Winkler, G. S., Albert, T. K., Dominguez, C., Legtenberg, Y. I., Boelens, R., and Timmers, H. T. (2004). An altered-specificity ubiquitin-conjugating enzyme/ubiquitin-protein ligase pair. J Mol Biol *337*, 157-165.
Wu, P. Y., Hanlon, M., Eddins, M., Tsui, C., Rogers, R. S., Jensen, J. P., Matunis, M. J., Weisman, A. M., Wolberger, C. P., and Pickart, C. M. (2003). A conserved catalytic residue in the ubiquitin-conjugating enzyme family. Embo J *22*, 5241-5250.
Wu, Z., Li, Q., Fortini, M. E., and Fischer, J. A. (1999). Genetic analysis of the role of the drosophila fat facets gene in the ubiquitin pathway. Dev Genet *25*, 312-320.
Wu-Baer, F., Lagrazon, K., Yuan, W., and Baer, R. (2003). The BRCA1/BARD1 Heterodimer Assembles Polyubiquitin Chains through an Unconventional Linkage Involving Lysine Residue K6 of Ubiquitin. J Biol Chem *278*, 34743-34746.
Xiao, W., Chow, B. L., Broomfield, S., and Hanna, M. (2000). The Saccharomyces cerevisiae RAD6 group is composed of an error-prone and two error-free postreplication repair pathways. Genetics *155*, 1633-1641.
Yang, X., Khosravi-Far, R., Chang, H. Y., and Baltimore, D. (1997). Daxx, a novel Fas-binding protein that activates JNK and apoptosis. Cell *89*, 1067-1076.

Yang, Y., Fang, S., Jensen, J. P., Weissman, A. M., and Ashwell, J. D. (2000). Ubiquitin protein ligase activity of IAPs and their degradation in proteasomes in response to apoptotic stimuli. Science *288*, 874-877.
You, J., and Pickart, C. M. (2001). A HECT domain E3 enzyme assembles novel polyubiquitin chains. J Biol Chem *276*, 19871-19878.
Zachariae, W., and Nasmyth, K. (1999). Whose end is destruction: cell division and the anaphase-promoting complex. Genes Dev *13*, 2039-2058.
Zacksenhaus, E., and Sheinin, R. (1990). Molecular cloning, primary structure and expression of the human X linked A1S9 gene cDNA which complements the ts A1S9 mouse L cell defect in DNA replication. Embo J *9*, 2923-2929.
Zhang, B., Zhang, Y., Wang, Z., and Zheng, Y. (2000). The role of Mg2+ cofactor in the guanine nucleotide exchange and GTP hydrolysis reactions of Rho family GTP-binding proteins. J Biol Chem *275*, 25299-25307.
Zheng, N., Schulman, B. A., Song, L., Miller, J. J., Jeffrey, P. D., Wang, P., Chu, C., Koepp, D. M., Elledge, S. J., Pagano, M.*, et al.* (2002). Structure of the Cul1-Rbx1-Skp1-F boxSkp2 SCF ubiquitin ligase complex. Nature *416*, 703-709.
Zheng, N., Wang, P., Jeffrey, P. D., and Pavletich, N. P. (2000). Structure of a c-Cbl-UbcH7 complex: RING domain function in ubiquitin-protein ligases. Cell *102*, 533-539.
Zhong, S., Muller, S., Ronchetti, S., Freemont, P. S., Dejean, A., and Pandolfi, P. P. (2000). Role of SUMO-1-modified PML in nuclear body formation. Blood *95*, 2748-2752.
Zohong, S., Müller, S., Ronchetti, S., Freemont, P. S., Dejean, A., and Pandolfi, P. P. (2000). Role of SUMO-1 modified PML in nuclear body formation. Blood *95*, 2748-2752.